



**FINITE ELEMENT SOLUTION: NONLINEAR FLAPPING BEAMS FOR USE
WITH MICRO AIR VEHICLE DESIGN**

Robert L. Walker, 1st Lieutenant, USAF

AFIT/GAE/ENY/07-M26

DEPARTMENT OF THE AIR FORCE

AIR UNIVERSITY

AIR FORCE INSTITUTE OF TECHNOLOGY

Wright-Patterson Air Force Base, Ohio

APPROVED FOR PUBLIC RELEASE; DISTRIBUTION UNLIMITED

The views expressed in this thesis are those of the author and do not reflect the official policy or position of the United States Air Force, Department of Defense, or the U.S. Government.

AFIT/GAE/ENY/07-M26

**FINITE ELEMENT SOLUTION: NONLINEAR FLAPPING BEAMS FOR USE
WITH MICRO AIR VEHICLE DESIGN**

THESIS

Presented to the Faculty

Department of Aeronautical and Astronautical Engineering

Graduate School of Engineering and Management

Air Force Institute of Technology

Air University

Air Education and Training Command

In Partial Fulfillment of the Requirements for the
Degree of Master of Science in Aeronautical Engineering

Robert L. Walker, B.S.

1st Lieutenant, USAF

March 2007

APPROVED FOR PUBLIC RELEASE; DISTRIBUTION UNLIMITED

AFIT/GAE/ENY/07-M26

**FINITE ELEMENT SOLUTION: NONLINEAR FLAPPING BEAMS FOR USE
WITH MICRO AIR VEHICLE DESIGN**

Robert L. Walker, BS

1st Lieutenant, USAF

Approved:

Dr. Anthony N. Palazotto (Thesis Advisor)

Date

Dr. Philip Beran (Member)

Date

Dr. Richard Cobb (Member)

Date

Acknowledgments

I would like to express my sincere appreciation to my faculty advisor, Dr Anthony Palazotto, for his direction, help, and support throughout the course of this thesis effort. The knowledge and experience is definitely appreciated. I would, also, like to thank my sponsor, Dr Phil Beran, from the Air Force Research Laboratory for both the support and latitude provided to me in this endeavor. Finally I'd like to express my thanks to Dr Richard Cobb for all of his assistance.

Robert L. Walker

Table of Contents

	Page
Acknowledgments.....	iv
Table of Contents.....	v
List of Figures.....	vii
List of Tables	xi
List of Symbols.....	xii
Abstract.....	xiii
I. Introduction / Literature Review	1
Chapter Overview.....	1
Background.....	1
Relevant Research	3
Summary.....	6
II. Theory	7
Linear Systems	7
Nonlinear Systems.....	8
ABAQUS.....	10
Frequency Step	11
Frequency Response Function.....	12
Rayleigh Damping.....	15
Free Vibration / Log Decrement Step	16
Backbone Curve	16
Hilbert Transform.....	19
Duffing Equation.....	23

	Page
MATLAB	24
Research Focus	24
III. Results and Discussion	26
Chapter Overview.....	26
Test Subjects.....	26
Clamped-Clamped Steel Beam – Beam 1	26
Clamped-Clamped Aluminum Beam – Beam 2	40
Clamped- Aluminum Beam – Beam 3	49
Clamped Steel Beam – Beam 4	59
Clamped Composite Beam – Beam 5.....	68
Chapter Summary:.....	83
IV. Conclusions and Recommendations	86
Chapter Overview.....	86
Methods Verified.....	86
Nonlinear Characteristics Summarized	87
Thoughts on Future Research.....	89
Appendix.....	90
Convergence: Number of Elements in each FEM.....	90
MATLAB CODE for Backbone Curve Estimation.....	101
Bibliography	104
Vita	107

List of Figures

	Page
Figure 1. Fly Tech Remote Control Dragonfly.....	3
Figure 2. University of Arizona's Ornithopter	4
Figure 3. Beam Loading Condition	8
Figure 4. Common damped FRF	12
Figure 5. Undamped Linear FRF	13
Figure 6. Undamped Nonlinear FRF	14
Figure 7. Backbone Curve: Linear and Nonlinear	17
Figure 8. Damped FRF: Nonlinear Hardening	18
Figure 9. Backbone Curve: Unstable Region	19
Figure 10. Signal and Hilbert transform in Envelope	20
Figure 11: Amplitude Envelope.....	20
Figure 12: Damped Amplitude Envelope	22
Figure 13: Finding Linear Natural Frequency	24
Figure 14. Section Dimensions: Clamped-Clamped.....	27
Figure 15. C-C Steel beam.....	28
Figure 16. Frequency step picture.....	29
Figure 17. First Mode Eigenvector; $w_1 = 79.02$ Hz	29
Figure 18. Second Mode Eigenvector; $w_2 = 217.70$ Hz.....	30
Figure 19. Third Mode Eigenvector; $w_3 = 426.91$	30
Figure 20. Rayleigh Damping for a Section	31

	Page
Figure 21. Smooth Step Function	32
Figure 22. Free Vibration: Fixed-Fixed Steel Beam.....	33
Figure 23. Amplitude Envelope: Fixed-Fixed Steel Beam.....	34
Figure 24. Instantaneous Frequency: Fixed-Fixed Steel Beam	35
Figure 25. Amplitude vs Nonlinear Frequency: Fixed-Fixed Steel.....	36
Figure 26. Duffing Equation Plot: Fixed-Fixed Steel Beam.....	37
Figure 27. Backbone Curve: Fixed-Fixed Steel.....	38
Figure 28. Steady State: Fixed-Fixed Steel.....	39
Figure 29. Frequency Response Function Data: Fixed-Fixed Steel	40
Figure 30. Free Vibration: Fixed-Fixed Aluminum Beam	43
Figure 31. Amplitude Envelope: Fixed-Fixed Aluminum Beam.....	44
Figure 32. Instantaneous Frequency: Fixed-Fixed Aluminum Beam.....	45
Figure 33. Amplitude vs Nonlinear Frequency: Fixed-Fixed Aluminum.....	46
Figure 34. Duffing Equation Plot: Fixed-Fixed Aluminum Beam	47
Figure 35. Backbone Curve: Fixed-Fixed Aluminum	48
Figure 36. Backbone Comparison: Fixed-Fixed.....	49
Figure 37. Section Dimensions: Clamped Aluminum	50
Figure 38. C Aluminum Beam setup	51
Figure 39. First Mode Eigenvector; $w_1 = 19.911$ Hz	51
Figure 40. Second Mode Eigenvector; $w_2 = 124.49$ Hz.....	51
Figure 41. Free Vibration: Fixed-Free Aluminum Beam	53

	Page
Figure 42. Amplitude Envelope: Fixed-Free Aluminum.....	54
Figure 43. Instantaneous Frequency: Fixed-Free Aluminum	55
Figure 44. Amplitude vs Nonlinear Frequency: Fixed-Free Aluminum.....	56
Figure 45. Duffing Equation Plot: Fixed-Free Aluminum.....	57
Figure 46. Backbone Curve: Fixed-Free Aluminum	58
Figure 47. Fixed-Fixed beam setup: Membrane Strain	59
Figure 48. Free Vibration: Fixed-Free Steel Beam.....	62
Figure 49. Amplitude Envelope: Fixed-Free Steel	63
Figure 50. Instantaneous Frequency: Fixed-Free Steel.....	64
Figure 51. Amplitude vs Nonlinear Frequency: Fixed-Free Steel.....	65
Figure 52. Duffing Equation Plot: Fixed-Free Steel.....	66
Figure 53. Backbone Curve: Fixed-Free Steel.....	67
Figure 54. Backbone Comparison: Fixed-Free: Steel vs Aluminum.....	68
Figure 55. Composite Beam Ply Layup.....	69
Figure 56. Composite Beam Load	70
Figure 57. First Mode Eigenvector; $w_1 = 30.009$ Hz	71
Figure 58. First Mode Eigenvector; $w_1 = 188.48$ Hz	71
Figure 59. Free Vibration: Fixed-Free Composite Beam	73
Figure 60. Amplitude Envelope: Fixed-Free Composite.....	74
Figure 61. Instantaneous Frequency vs Time: Fixed-Free Composite	75
Figure 62. Amplitude vs Nonlinear Frequency: Fixed-Free Composite.....	76

	Page
Figure 63. Duffing Equation Plot: Fixed-Free Composite.....	77
Figure 64. Backbone Curve: Fixed-Free Composite	78
Figure 65. Backbone Comparison: Fixed-Free: Isotropic vs Composite.....	79
Figure 66. Backbone Comparison: Fixed-Free: All.....	80
Figure 67. Backbone Comparison: Fixed-Free Composite Beams.....	81
Figure 68. Backbone Comparison: Fixed-Free Composite: 3 Nodes	82
Figure 69. Node Placement on Composite Beam: 1”, 3” and 6.08” from fixed end	83
Figure 70. Convergence plots C-C Steel.....	91
Figure 71. Convergence plots C-C Steel.....	92
Figure 72. Convergence plots C-C Aluminum	93
Figure 73. Convergence plots C Aluminum	94
Figure 74. Convergence plots C Composite	95
Figure 75. Convergence plots C Composite	96
Figure 76. Convergence plots C C Aluminum.....	97
Figure 77. Convergence plots C-C Aluminum	98
Figure 78. Convergence plots C Steel.....	99
Figure 79. Convergence plots C Steel.....	100

List of Tables

	Page
Table 1. Section Properties: C-C Steel Beam	27
Table 2. Natural Frequencies: Clamped-Clamped Steel Beam	30
Table 3. Duffing Equation Results Comparison	38
Table 4. Section Properties: C-C Aluminum Beam.....	41
Table 5. Natural Frequencies: Fixed-Fixed Aluminum Beam.....	41
Table 6. Section Properties: C Aluminum	50
Table 7. Section Properties: Fixed Aluminum Beam	52
Table 8. Section Properties: C Steel Beam	60
Table 9. Section Properties: Fixed Steel Beam.....	61
Table 10. Section Properties: C Composite Beam.....	70
Table 11. Section Properties: Fixed Composite Beam	71
Table 12. Estimated Backbone Curve Values.....	84
Table 13. Past and present Backbone Curve parameter comparison	87

List of Symbols

A	Amplitude	(inches)
α_1	Rayleigh Mass Coefficient	(s ⁻¹)
α_2	Rayleigh Stiffness Coefficient	(s)
β	Cubic Stiffness Coefficient	(in ⁻² s ⁻²)
d	Displacement	(inches)
E	Modulus of Elasticity	(psi)
G	Shear Modulus	(psi)
h	height	(inches)
l	length	(inch)
P	transverse load force	(lb _f)
ρ	mass density	(lb s ² /inch ⁴)
t	thickness	(inches)
ν	poisons ratio	(-)
w	width	(inches)
ω	frequency	(Hz)
ω_n	n th natural frequency at zero amplitude	(Hz)
Ω	Nonlinear Frequency	(Hz)
ξ_n	n th Modal damping ratio	(-)

Abstract

The development and use of Micro Air Vehicles is becoming more and more important to the military. Size, weight, maneuverability, stealth, and fuel consumption are just some of the constraints on a future Micro Air Vehicle. Perfect blueprints for a small scale flying machine are both insects and humming birds. Medium sized hummingbirds are found to have wings-beats at a frequency of 18-28 Hz. There is a vast amount of complexity to just how these creatures can create lift; however, this study looks at different beams made of common materials with 1st natural bending frequencies in this range. This study documents and evaluates the use of analytical tools to solve for nonlinear characteristics of a system. A function called the backbone curve is incorporated into a MATLAB program. The Hilbert transform characterized by the nonlinear decrement approach captures all of the necessary coefficients for this function. ABAQUS/CAE is relied upon. The numerical finite element results are compared to experiments. This work gives a better understanding of how materials and geometry perform when used in Micro Air Vehicle design considering large displacements.

FINITE ELEMENT SOLUTION: NONLINEAR FLAPPING BEAMS FOR USE WITH MICRO AIR VEHICLE DESIGN

I. Introduction / Literature Review

Chapter Overview

The purpose of this chapter is to introduce the need for a Micro Air Vehicle, its possible solutions, similar projects underway, and past relevant research.

Background

Micro Air Vehicle (MAV) refers to a relatively new unmanned type of aircraft that are generally an order of magnitude smaller than typical aircraft of today. A Micro Air Vehicle was defined by the Defense Advanced Research Project Agency (DARPA) MAV program in 1997 as “vehicles no larger than six inches in either length, width or height and perform a useful military mission at an affordable cost.” [17] These MAV(s) are foreseen to be expendable and available to individual soldiers or units for requirements in reconnaissance, surveillance, battle damage assessment, targeting, sensor placement, communication relays, or for sensing chemical, nuclear or biological substances and be able to sustain missions of up to 2 hours long [17]. There are three main types of Micro Air Vehicles that could offer a solution to these needs: fixed wing vehicles, rotorcraft vehicles and flapping wing vehicles or ‘ornithopters’. Though all are

feasible solutions, a flapping wing design is of interest because it allows best for loitering in small areas while also having a small acoustic signature.

The most useful flapping wing Micro Air Vehicle design would be one that resembles the flight of a hummingbird for its sustained hovering capabilities along with vertical and horizontal movements that are produced by the flapping of its wings. This same flight pattern can be found in certain bats and insects as well. This would allow a MAV access to areas not reachable at present times. The Giant Hummingbird with a length of 8.5 inches and weight of 20 grams closely resembles the size of an MAV and has a wing frequency of approximately 18-30 Hz [15]. Smaller hummingbirds have wing frequencies of 60-80 Hz while insect wing frequencies are even higher such as a bee wing of 200 Hz. A MAV or ornithopter with similar flapping frequencies is eventually desired.

Ornithopter:

The term ornithopter comes from the Greek word *ornithos* "bird" and *pteron* "wing". Ornithopters are defined as mechanical aircraft which mimic the flight of birds, bats or insects. The flapping wing motion is used for most flight characteristics including lift, propulsion and control. While mimicking the flapping wing motion of birds, bats or insects, ornithopters are usually built to the same scale as these creatures as well, but don't have to be [19]. Inspired by Leonardo Da Vinci, many successful attempts at manned flight in ornithopters date back to 1870. With modern technological advances, smaller scaled ornithopters are being developed all over the world.

Relevant Research

‘Fly Tech’ recently developed a widely commercialized remote controlled dragonfly with two sets of 18” wings as seen in Figure 1 [20].



Figure 1. Fly Tech Remote Control Dragonfly

This vehicle shows that a battery powered remote control ornithopter can be produced at an affordable cost; however, dragonfly is three times as large as a defined Micro Air Vehicle. There is also no advanced control with this model. The wings can flap faster to produce more lift and propulsion while turning is accomplished using a small tail rotor. Hovering, vertical and backwards flight movements are not replicable on a regular basis. The battery has only a 10 minute lifespan before recharge is necessary.

In July 2006 the University of Arizona placed first in the Ornithopter portion of the 10th Annual Micro Air Vehicle Competition in Provo, Utah with their vehicle shown in Figure 2 [14]. The University of Florida continues to dominate in the other three portions of the MAV competition [1].



Figure 2. University of Arizona's Ornithopter

The ornithopter competition is judged on both size and laps the aircraft can complete in 2 minutes. The University of Arizona's ornithopter's wingspan measures less than 6 inches and is the world's smallest radio controlled ornithopter [14]. The wings are made of carbon fiber struts covered with Mylar and flap similar to a hummingbird at a frequency of 50 Hz. This aircraft is one of the closest developments to date of what a future flapping wing MAV will be; however, this ornithopter only has a flight time of 3 minutes and while it flies like a bird it too does not have the hovering, vertical, and backward flight characteristics of a hummingbird.

A Micro Air Vehicle and wing capable of replicating the intricacies of a hummingbird in flight is still years away. There are many different size, shape, material, and design possibilities to list. A fundamental element of an engineering structure is a beam and to simplify things, most structures can be modeled as such, including bridges, antenna towers, helicopter rotors, and wings. Even a complex wing structure is made up

of multiple beam elements and the understanding of a beam structure will benefit the understanding of the more complex structure [13]. Pramod Malatkar understood this and in July of 2003 put in print an extensive study on nonlinear vibrations in metallic cantilever beams and plates subject to transverse harmonic excitations. This study includes parametric system identification, and jump frequency determination, but concentrated on energy transfer between widely spaced modes. He states that interesting phenomenon occurs in structures that exhibit nonlinearity that cannot be explained by linear models [13]. Most structures experience nonlinear characteristics although some are weaker than others. Linear models are only accurate when displacements are kept small or when the nonlinearity is weak.

In 2003, a combined effort of Robert Gordon, Joseph Holikamp, and Michael Spottswood did a study on sonic fatigue problems in military aircraft. “Sonic fatigue is characterized by large amplitude, nonlinear response of thin skins to intense aeroacoustic loads” [9]. The main purpose of their research was to set up well characterized experiments that could be replicated with Finite Element methods for validation of the FEMs themselves. These experiments were for a 9.00” clamped-clamped steel beam. One experiment recorded simple harmonic response data for the beam to acquire linear frequencies (ω_0), and the cubic stiffness coefficient (β) for the beam using both the Hilbert transform and the Estimated Backbone equation [9].

Also in 2003, Matthew Ernst and Anthony Palazotto conducted a study of the same clamped-clamped Steel beam using ABAQUS/CAE for the simulation of their simple harmonic response data [6]. They applied both the Hilbert transform and the

estimated Backbone Curve equation to their results and found the natural frequencies and the values of linear ω_0 and the cubic stiffness coefficient (β) for various values of the estimated damping ratio (ξ). The results were compared to those in [9] for accuracy.

Yamaki and Mora conducted an experimental investigation in 1980 of a Clamped-Clamped beam with harmonic base excitation on an electrodynamic shaker. FRF curves were generated with swept sine excitation for several input forces [16].

Capt Adam Tobias conducted a study of both Aluminum and Composite clamped-free beams from 2006-2007, concentrating on visual methods to capture the beams vibrations. These methods include high speed photography, and multiple laser vibrometers. The beams in the study included a clamped-free 10.125” Aluminum beam and a clamped-free 6.08” Composite beam [15].

Summary

This study will look at a finite element analysis using ABAQUS for five beams, its ability to show and provide data for the nonlinear characteristics of the beams.

II. Theory

Linear Systems

One of the most widely used simplifications in beam theory is the assumption that a system is linear. Linear systems are systems that are subject to superposition where their input and outputs can be added together yielding another set of correct results for that system. Likewise, the inputs and outputs can be multiplied by constants as well. This assumption not only makes calculations much easier, but it is also very accurate for small deflections. The strain for an Euler-Bernoulli beam is shown by the following equation [3].

$$\epsilon_x = \epsilon_{\text{axial}} + \epsilon_{\text{bending}} \quad (1)$$

$$\epsilon_{\text{axial}} = du/dx$$

$$\epsilon_{\text{bending}} = z (d^2w/dx^2)$$

where

u = displacement in the axial direction

w = displacement in the direction of the force P

z = distance from the midsurface of the beam

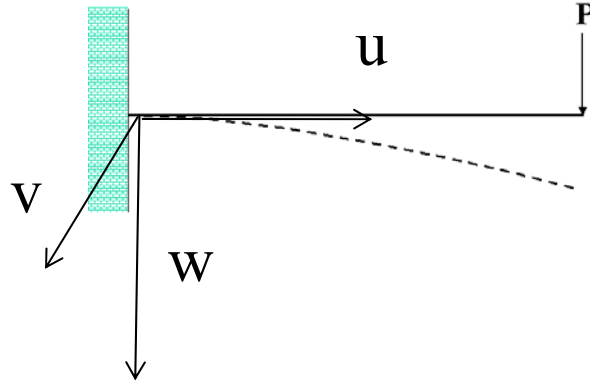


Figure 3. Beam Loading Condition

For a beam under loading conditions shown above in Figure 3, the axial strain term du/dx in linear theory will be equal to zero as the rotation of the beam is not great enough to add a component of force in the axial direction on the beam. For a beam of small deflections, these equations work well in approximating the strain, however, in everyday life, no physical system is strictly linear [13]. The flapping motions of the beams in this study well surpass the small deflections for a linear system. With deflections much greater than the thickness of the beam, the beams will be better suited for nonlinear analysis.

Nonlinear Systems

The term nonlinearity means that the inputs and outputs of a system are not additive as they are in a linear system. The response is not directly proportional to the inputs that produced it [13]. There are three main types of nonlinearities in a system, material nonlinearity, contact nonlinearity, and geometric nonlinearity. One example of

geometric nonlinearity stems from deformations large enough where the system develops membrane stretching forces that carry a portion of the load [3]. These new forces bring about membrane strain terms that must be accounted for in our nonlinear beam strain equations. Large rotations are also considered and in turn, the strain due to beam bending will change as well.

$$\epsilon_x = \epsilon_{\text{membrane}} + \epsilon_{\text{bending}} \quad (2)$$

$$\epsilon_{\text{membrane}} = du/dx + \frac{1}{2} (du/dx)^2 + \frac{1}{2} (dw/dx)^2$$

$$\epsilon_{\text{bending}} = z (d^2w/dx^2) / [1 + (dw/dx)^2]^{3/2}$$

This familiar Green Strain beam relationship will help when visualizing what is going on in the beams however, they will not be exactly correct as the program of choice, ABAQUS, uses a different method to calculate its strains. ABAQUS is used heavily by BMW. Therefore, the method approach ABAQUS follows is very useful in the auto industry which deals with models of automobiles crashing where rubber and polymers are considered as materials. ABAQUS used what is called the Green-Naghdi (G-N) rate.

The G-N rate can make use of the usual constitutive relations often used, but stress is related to a rate of deformation gradient matrix. That is what makes it so ideal when we have large movement. In addition, since it is time dependent it can be used when the material is time dependent such as viscoelasticity, viscoplasticity as well as hyperelasticity. It thus has value when the material is rubbery. Therefore, to sum it up, ABAQUS uses a large displacement time dependent theory which allows rate functional expressions without the higher order terms. It removes the rigid body rotations by a corotational system of coordinates which therefore does away with nonlinear

displacement rate gradients. We can use the usual constitutive relationships to help visualize what is happening, but keep in mind that the stress rate is related to the rate deformation tensor, not the natural strain.

Because ABAQUS/CAE/Explicit follows the corotated G-N rate relations, a load acting vertically down at the end of a cantilever beam will translate into a load along the axial direction and in the normal direction. Thus, as the rotation gets larger, the axial membrane and the higher order nonlinear membrane terms increase. These G-N stress rate terms prove that the analysis developed by the code has a large rotation term in it. As the movement gets larger, the axial loading becomes greater. This scenario can be expressed very nicely with the Green Strain terms as shown above.

ABAQUS

ABAQUS/CAE will be used for the all Finite Element analysis in this study. The CAE section of ABAQUS will be used to handle nonlinear analysis through explicit integration.

Geometric Nonlinear effects in ABAQUS can be added into the system by simply turning the NLGEOM choice ON. Explicit direct integration is best suited to wave propagation problems and can handle nonlinearity better than both implicit direct integration and the modal method. Computer storage requirements are kept to a minimum and the computational cost per time step is small. The drawback is the critical time step, t_{crit} . [3].

An explicit step in ABAQUS can be very unstable. If Δt or t_{crit} is too large, explicit integration fails; if Δt is unnecessarily small, the time it takes ABAQUS to

compute a solution can take a very long time. It is necessary to consider both when choosing a t_{crit} [3]. ABAQUS does this for the user when an automatic time step is selected.

Frequency Step

There are many types of natural frequencies of a beam including axial, torsional, and bending directions. This study will concentrate on the bending natural frequencies that correlate to the flapping motion of a beam. The bending natural frequencies will be in-plane with the applied force. These natural frequencies are found using a ‘Frequency Step’ in ABAQUS/CAE. The natural frequencies are matched up with their Eigenvectors to ensure they are the correct modes. The ABAQUS results should match the theoretical bending natural frequency equations. Since this study includes both fixed-free and fixed-fixed beams, both are shown below.

Theoretical values for a fixed-free beam bending modes

$$\omega_1 = \frac{1.875^2}{2\pi} \sqrt{\frac{EI}{\rho AL^4}} \quad \text{and} \quad \omega_2 = \frac{4.690^2}{2\pi} \sqrt{\frac{EI}{\rho AL^4}} \quad (3)$$

Theoretical values for a fixed-fixed beam bending modes

$$\omega_1 = \frac{4.733^2}{2\pi} \sqrt{\frac{EI}{\rho AL^4}} \quad \text{and} \quad \omega_2 = \frac{7.855^2}{2\pi} \sqrt{\frac{EI}{\rho AL^4}} \quad \text{and} \quad \omega_3 = \frac{11.00^2}{2\pi} \sqrt{\frac{EI}{\rho AL^4}} \quad (4)$$

Frequency Response Function

A Frequency Response Function plots a magnitude vs. frequency for a given point in a system. The most common of plotted magnitudes are accelerations, velocities, and displacements. An example of a common damped FRF for one mode is shown in Figure 4.

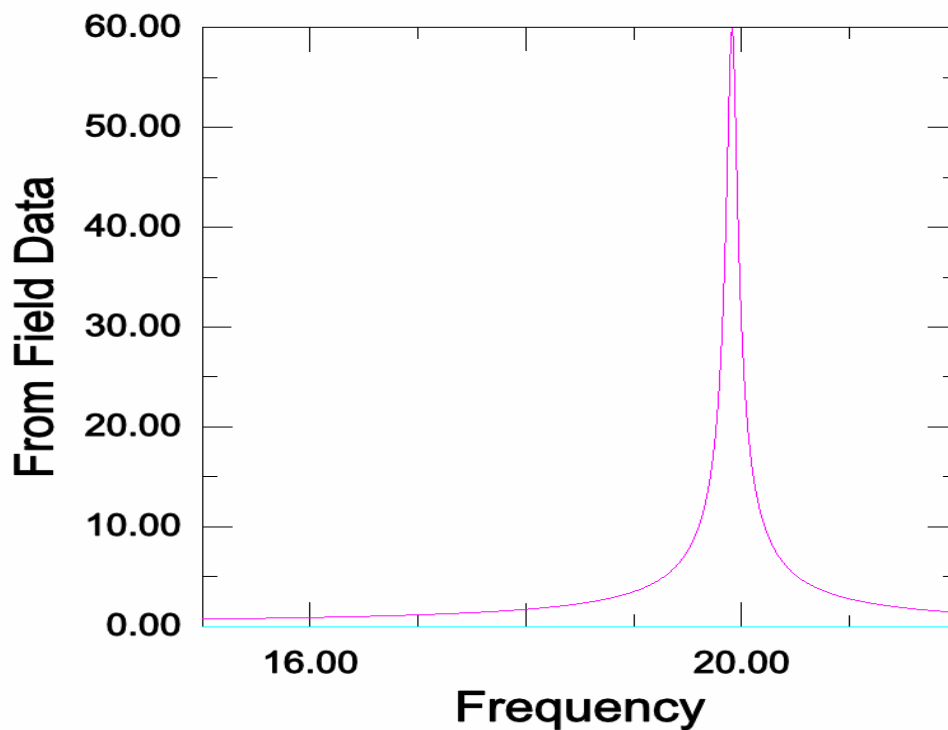


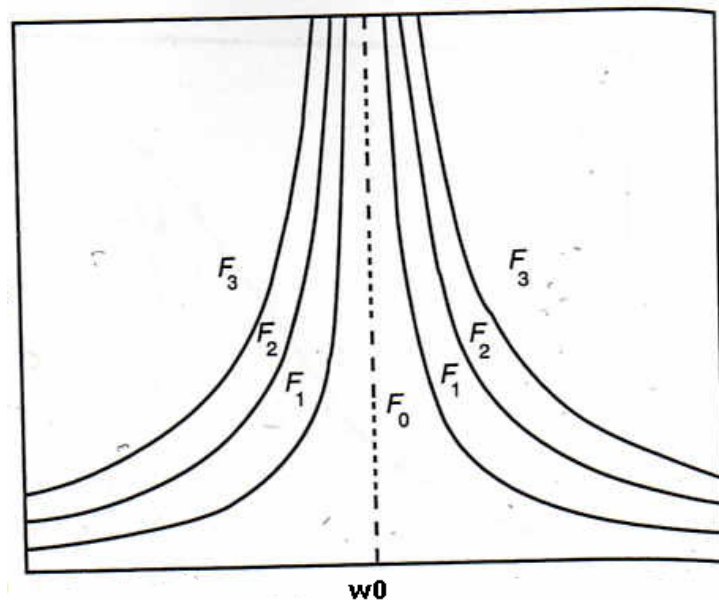
Figure 4. Common damped FRF

Because this Frequency Response Function is slightly damped, its peak Field Data magnitude does not approach ∞ . This FRF line represents a single location on the beam where data was acquired. In a Finite Element simulation this location will be on any node in the FEM mesh. In laboratory data, these locations are anywhere that there is data

taken on the beam, rather it be taken by an accelerometer, laser vibrometer, or high speed photography.

Frequency Response Functions can be attained in various ways via results from experiments in a laboratory or from computer simulations. Frequency sweeps in the frequency domain or random input signals in the time domain are both commonly used. A well developed FRF allows w_n , w_d , w_r and modal damping coefficients ξ_n to be calculated, while multiple FRFs allow Eigenvectors to be computed.

An example of an undamped linear Frequency Response Function at one mode is below in Figure 5. This FRF represents one point on a beam subject to three different increasing loads, F_1 , F_2 and F_3 . F_0 represents the linear natural frequency of the beam. In a linear FRF the peak for any given mode achieves its highest point at the value of the natural frequency, w_n . If the system is undamped, the response will approach ∞ .



(Ref. 1)

Figure 5. Undamped Linear FRF

An example of an undamped nonlinear Frequency Response Function at one mode is below in Figure 6. This FRF once again represents one Finite Element (FE) node on a beam subject to two different loads of increasing magnitude, F_1 and F_2 . F_0 represents the nonlinear curve that curves F_1 and F_2 are following. This curve is called the Backbone Curve and is gone over in more depth later. In a nonlinear FRF, the peak for mode n can attain its highest point at or near ω_n if the structure has weak nonlinearity, but can also attain its highest peak at an ω either less or greater than ω_n itself depending on the structure's properties, setup, and mode. Like the undamped linear FRF, the response of the system will also approach ∞ if the system is truly undamped. If a system is modeled as a nonlinear system, its magnitude of response at a given natural frequency will always be less than or equal to the same system modeled linearly [1].

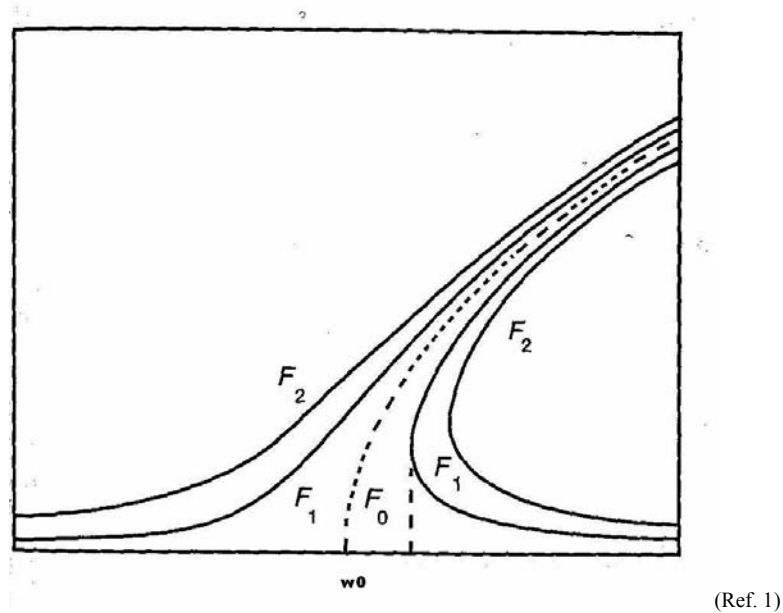


Figure 6. Undamped Nonlinear FRF

To produce a nonlinear FRF using ABAQUS, a separate run is accomplished for each individual point on the FRF curve. For a the forcing function $P \cdot \sin(\omega t)$, P will be held constant while ω is varied. Each runs steady-state displacement at the tip is recorded to produce a particular FRF.

Rayleigh Damping

Damping dissipates energy producing the envelope in which a free vibration problem will decay with time. It also limits the amplitude of a Frequency Response Function and prevents response from going to ∞ . One way to estimate damping is with Rayleigh damping or proportional damping. In Rayleigh damping, the global damping matrix, $[C]$ is proportional to both the mass matrix $[M]$ and the stiffness matrix $[K]$ by the constants α_1 and α_2 . [3].

$$[C] = \alpha_1 [M] + \alpha_2 [K] \quad (5)$$

“The $\alpha_1[M]$ contribution damps the lowest modes most heavily, while the $\alpha_2[K]$ contribution damps the highest modes most heavily.” [3] The mass dampening coefficient α is found by the equation

$$\alpha_1 = 2 \cdot \omega_1 \cdot \omega_2 \cdot (\xi_1 \cdot \omega_2 - \xi_2 \cdot \omega_1) / (\omega_2^2 - \omega_1^2) \quad (6)$$

The stiffness dampening coefficient β is found by the equation

$$\alpha_2 = 2 \cdot (\xi_2 \cdot \omega_2 - \xi_1 \cdot \omega_1) / (\omega_2^2 - \omega_1^2) \quad (7)$$

where ω_n and ξ_n are the n^{th} natural in-plane bending frequencies and n^{th} modal damping ratio respectively. For all experiments in this study, values of ω_1 and ω_2 are found using ABAQUS. The Finite Elements Models are built in ABAQUS and a ‘Frequency Step’

set up to calculate the ω_n values. The ξ_n values are simply damping ratios that can be acquired experimentally using the half power method. The ξ_n values of 0.03, 0.003 and 0.0003 were all assumed in the previous experiment by Ernst and Palazotto and the ξ_n value of 0.003 was found to produce the most accurate results to the Gordon, Holkamp and Spottswood laboratory experiments. For all experiments in this study, ξ_n is assumed to be 0.003.

Free Vibration / Log Decrement Step

In ABAQUS a free vibration of an undamped linear or nonlinear system will oscillate forever without losing any energy. The magnitude of the Amplitude Envelope is the same at time $t = 100$ as it is at $t = 1$. Once damping is introduced into the system, the amplitude of the oscillations will decrease with an exponential decay following the equation

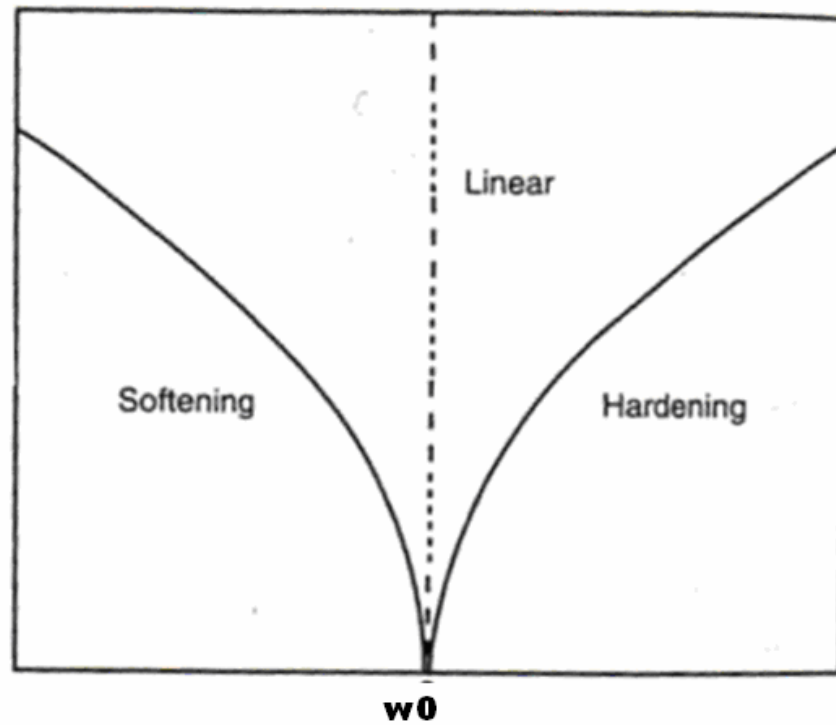
$$\text{Amplitude Envelope} = A_{\text{envelope}} = A_0 \cdot e^{\xi_n \omega_n t} = A(t) \quad (8)$$

The log decrement step will produce data that will supply both the Amplitude Envelope and the Instantaneous Frequency for development of the backbone curve.

Backbone Curve

At mode n , the Backbone Curve represents the nonlinearity of the structure as at a given point. It is the theoretical line that the FRF follows. Figure 7 shows a backbone curve in both a linear and nonlinear system. In a linear system, the backbone curve is a vertical line at ω_n . In a nonlinear system, the backbone curve can be a line or curve that

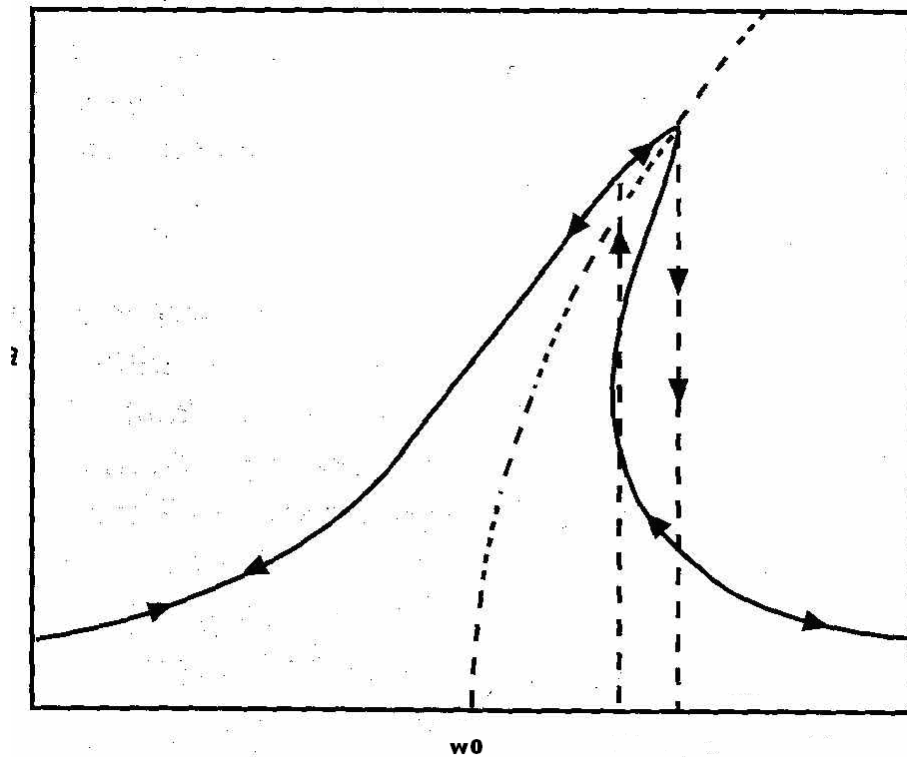
starts at the linear value of ω_n and leans to either the left, softening, or to the right, hardening.



(Ref. 1)

Figure 7. Backbone Curve: Linear and Nonlinear

Figure 8 shows a damped backbone curve experiencing nonlinear hardening. The Frequency Response Function has a definite value at its peak. The peak is at a higher value of ω than the linear natural frequency as the FRF follows the backbone curve asymptotically.

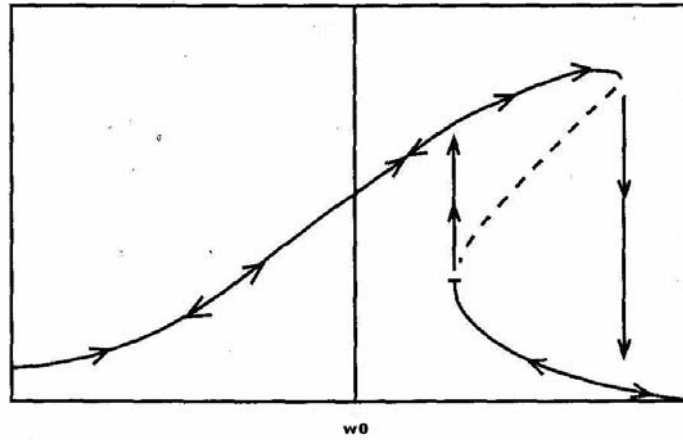


(Ref. 1)

Figure 8. Damped FRF: Nonlinear Hardening

The backbone curve lies between the lower and upper level of stability. The dotted line in Figure 9 represents the unstable region of the nonlinear Frequency Response Function. This region cannot be simulated in a laboratory experiment. For example, if a frequency sweep is done on the beam from the lower frequencies, the response will follow the upper boundary until the peak is reached. The response will then fall off to a stable region at that same frequency. The unstable region along with the stable region under the upper boundary will not be captured. The lower boundary stable region can be captured by doing a frequency sweep from the higher frequencies to lower

frequencies, but will again jump up to the upper boundary, missing the unstable region altogether.



(Ref. 1)

Figure 9. Backbone Curve: Unstable Region

The backbone curve can be found via Schudt's method [9] which includes Sine-sweep testing and jump-down points. However, this is difficult, and not only requires experimental capabilities, but also requires a lot of time. Therefore, all backbone data found in this study will be found using the Hilbert transform and free response decrement data.

Hilbert Transform

The Hilbert transform named after David Hilbert has been used in signal processing for years. It permits a signal in the time domain to be analyzed in the frequency domain. It does this by giving the original signal both real and imaginary parts. It is defined by the integral transform:

$$H[y(t)] = \tilde{y}(t) = \frac{1}{\pi} \int_{-\infty}^{\infty} \frac{y(\tau)}{(t-\tau)} \cdot d\tau \quad (9)$$

where $\tilde{y}(t)$ is the Hilbert transform of the original signal $y(t)$.

The Hilbert transform shifts the phase of the signal by $-\pi/2$ while still keeping the same envelope, amplitudes and other spectral components. An example of a phase shift to a signal is shown below in Figure 10 [7].

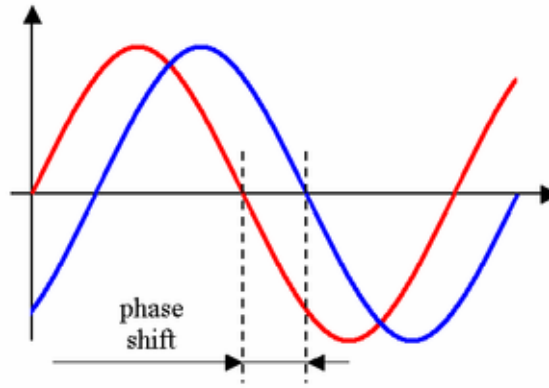


Figure 10. Signal and Hilbert transform in Envelope

Notice the phase shift while the signals both lie in the envelope $A(t)$. The frequencies of the two signals remain the same as well.

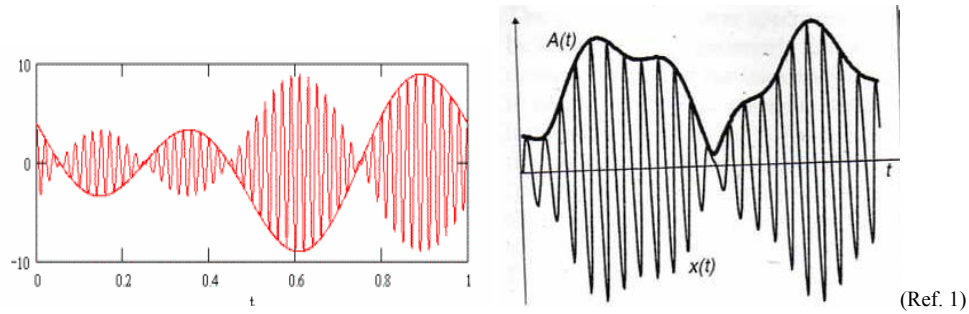


Figure 11: Amplitude Envelope

The peaks of the signal at each oscillation can be plotted, and as a whole produce the envelope of the signal, $A(t)$. The envelope can be as simple as a straight line in an undamped system, or more complicated from an unstable or random signal, as can be seen in Figure 11. In a damped system, $A(t)$ is directly related to the decay rate ξ [7].

The envelope of the signal is very important in the Hilbert transform and the breakdown of the signal attributes. The instantaneous amplitudes and their corresponding instantaneous frequencies are completely dependent on the domain of the Amplitude Envelope. In an undamped system the envelope will be a constant horizontal line and in turn the instantaneous amplitude and frequency are constant values as well. For this reason, a simulation of a damped beam undergoing free vibration is perfect for use with the Hilbert transform to find the backbone curve.

Using the Hilbert transform, what is known as an Analytical Signal, Y , can be produced [7].

$$Y = y(t) + i \cdot \tilde{y}(t) \quad (10)$$

where $\tilde{y}(t)$ is referred to as the quadrature or conjugate function of $y(t)$. This is similar to the Euler formula $e^{iz} = \cos(z) + i \cdot \sin(z)$ where $\sin(z)$ is the Hilbert transform of $\cos(z)$ [7].

$y(t)$ is simplified by separating it into its two parts, $y(t) = A(t) \cdot c(t)$; $A(t)$ for the envelope and $c(t)$ for the oscillations as shown in Figure 12, $\tilde{y}(t)$ then becomes $\tilde{y}(t) = A(t) \cdot \dot{c}(t)$. The analytical signal becomes $Y(t) = A(t)[c(t) + i \cdot \dot{c}(t)]$ [6].

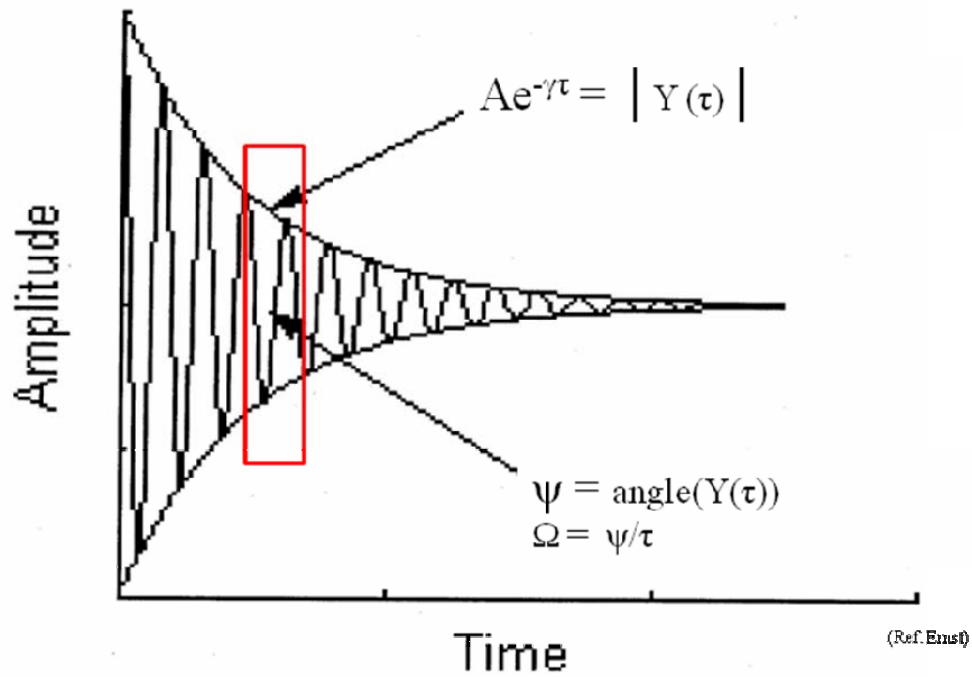


Figure 12: Damped Amplitude Envelope

By breaking up $Y(t)$ into smaller sections the size of $(t-t_0)$, the instantaneous amplitude, instantaneous phase, and instantaneous frequencies can be all be found.

The instantaneous amplitude can be found by the equation $A(t) = |Y(t)|$.

The instantaneous phases are found by using the MATLAB function `Phase = angle[Y(t)]` [6].

The instantaneous frequencies can be found by taking the slope of the instantaneous phase over the same time period $(t-t_0)$ [7].

This transform allows somewhat complex systems to be analyzed in the time domain and allows one to see the instantaneous attributes of frequency, phase, and amplitude [7]. These values will be used in the estimation of the Backbone Curve for all displacements.

Duffing Equation

A simple model used to approximate the nonlinearity in a beam is the SDOF Duffing Oscillator

$$\ddot{y} + C \dot{y} + \omega_0^2 y + \beta y^3 = P \sin(\omega t) \quad (11)$$

The Duffing equation is very useful as it simplifies the backbone curve. The backbone curve is estimated by

$$\Omega^2 = \omega_0^2 + \frac{3}{4} \beta A^2 \quad (12)$$

Ω - instantaneous nonlinear frequency

A - instantaneous displacement amplitude

ω_0 - linear natural frequency is held constant

β - cubic stiffness coefficient

In the equation the value of ω_0 , linear natural frequency is held constant. As seen in Figure 13, this ω_0^2 is the value where the Hilbert transform data curve fit crosses the Ω^2 axis when the instantaneous amplitude is 0 [6]. The Duffing equation is meant to model a 1-D nonlinear spring-mass system. In this study it is applied to the beams at a node which undergoes the largest displacement. Each node on the beams will have its own unique backbone curve. The β value represents the strength of the nonlinear effect on the beam.

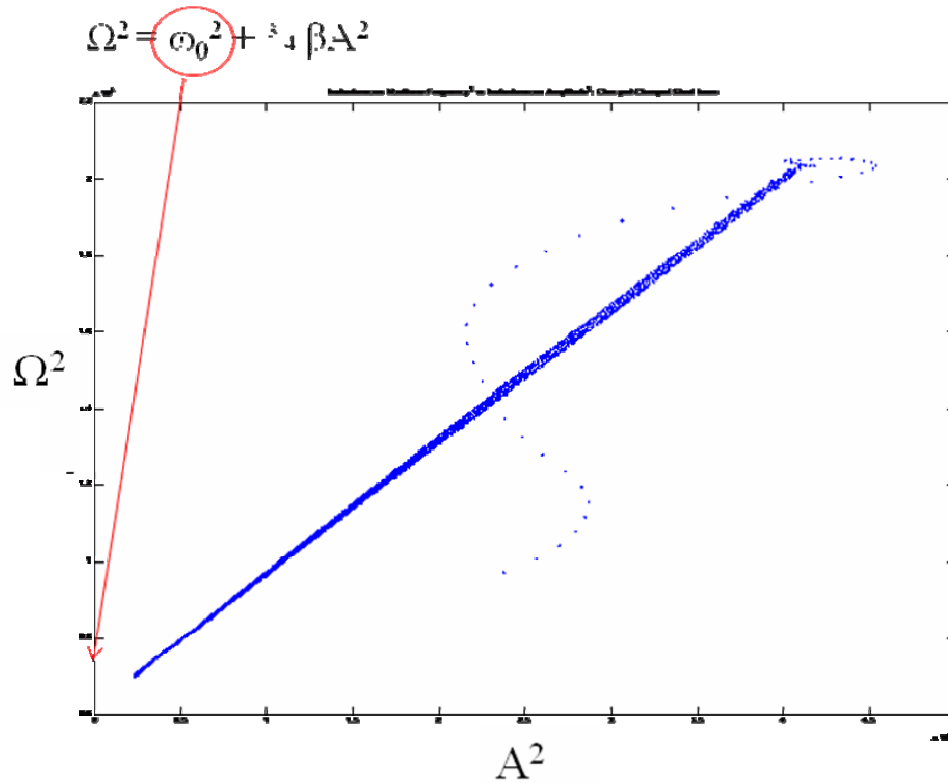


Figure 13: Finding Linear Natural Frequency

MATLAB

MATLAB is used to acquire a backbone curve by utilizing the Hilbert transform and Duffing equation from the results produced by ABAQUS/CAE for each of the five Finite Element Models. The MATLAB code used was provided by Ernst and Palazotto [6].

Research Focus

This research is focused on the evaluation of using ABAQUS/CAE to solve nonlinear problems for a flapping beam and whether or not ABAQUS/CAE results used

with MATLAB via the Hilbert transform correctly characterize the nonlinearity of beams based on previous experiments. Results will also be compared to one another to find trends of nonlinearity in the beams.

III. Results and Discussion

Chapter Overview

The purpose of this chapter is to both characterize and discuss the results of the beam models used in this study. The subsequent paragraphs describe the five beams. The first two models set up beams with clamped-clamped supports to see the affects. The last three models set up beams with clamped-free ends to depict something similar to a Micro Air Vehicle wing. All of the beams are compared in their effects of nonlinearity.

Test Subjects

Clamped-Clamped Steel Beam – Beam 1

To start out the study, there is a desire to develop a method that could represent some nonlinear characteristics in a relatively timely and repeatable process. This had been done before by Gordon, Hollkamp and Spottswood [9] and Ernst [6] for the same 9.00” clamped-clamped Steel beam. The study accomplished in [9] utilized experimental data with the Hilbert transform and Duffing equation. The study in [6] used Finite Element analysis data along with the Hilbert transform and Duffing equation. Using this same beam setup will both verify the methods used in this study as well as give a baseline beam model to compare other results against. This beam setup will be referred to as Beam 1.

Using ABAQUS/CAE, a finite element model was developed for a Clamped-Clamped 9” long Steel beam shown in Figure 15. The beam itself is modeled symmetrically as a 4.5” beam in two-dimensional planar modeling space in ABAQUS as

a deformable wire in the 1-direction. In ABAQUS, a section is a cross sectional area with properties and dimensions that can be applied to wires. A section is applied to the wireframe with the following Steel properties and dimensions:

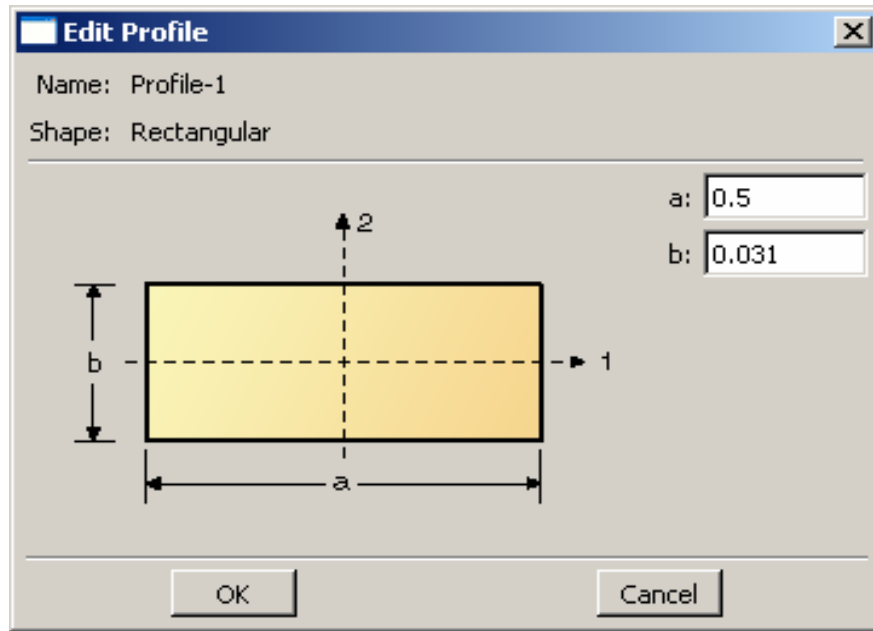


Figure 14. Section Dimensions: Clamped-Clamped

Table 1. Section Properties: C-C Steel Beam

t, thickness in the 2-direction = 0.031"
w, width in the 3-direction = 0.5"
E, Young's Modulus of Elasticity = 29.7 Mpsi
ν , Poisson's ratio = 0.33
G, Shear Modulus = 11.1 Mpsi
ρ , mass density = $7.36 \times 10^{-4} \text{ lb} \cdot \text{s}^2 \cdot \text{in}^{-4}$

A cantilevered or “Encastre” boundary condition is applied to one end of the beam, $x = 0$ ”. A Y-symmetry boundary condition is applied at $x = 4.5$ ”. A load, P , is also applied to the midspan of the beam at $x = 4.5$ ” as shown in Figure 15.

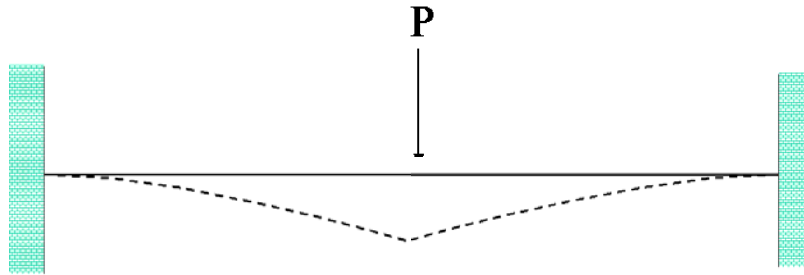


Figure 15. C-C Steel beam

Retrieving the Natural Frequencies

A Frequency Step is applied in ABAQUS to find natural bending frequencies of the beam. ABAQUS shows the Eigenvectors along with the natural frequencies. This makes it easy to separate the bending natural frequencies from the torsional, axial and out of plane bending natural frequencies.

Edit Step [X]

Name: Frequency Step
Type: Frequency

Basic Parallel Lanczos Other

Description: []

NIgeom: Off [Edit...]

Eigensolver: ☒ Lanczos ☐ Subspace ☐ AMS

Number of eigenvalues requested: ☐ All in frequency range
☒ Value: [20]

☐ Frequency shift (cycles/time)**2: []

☐ Minimum frequency of interest (cycles/time): []

☐ Maximum frequency of interest (cycles/time): []

☒ Include acoustic-structural coupling where applicable

Block size: ☒ Default ☐ Value: []

Maximum number of block Lanczos steps: ☒ Default ☐ Value: []

☐ Include residual modes

[OK] [Cancel]

Figure 16. Frequency step picture

The results of the frequency step are shown in Table 2. The Eigenvectors are shown in Figure 17 - Figure 19.



Figure 17. First Mode Eigenvector; $w_1 = 79.02$ Hz

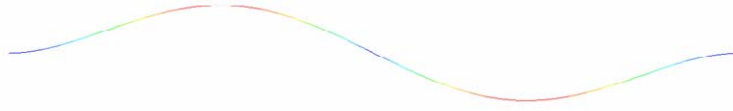


Figure 18. Second Mode Eigenvector; w2 = 217.70 Hz



Figure 19. Third Mode Eigenvector; w3 = 426.91

Table 2. Natural Frequencies: Clamped-Clamped Steel Beam

Theoretical results	$\omega_1 = 79.12$	$\omega_2 = 217.94$	$\omega_3 = 427.40$
ABAQUS results	$\omega_1 = 79.02$	$\omega_2 = 217.70$	$\omega_3 = 426.91$
Relative Error	0.13%	0.11%	0.11%

The Rayleigh Damping coefficients, α_1 and α_2 , are solved for by Equation (6) and (7) and an estimated $\zeta_1 = \zeta_2 = 0.3\%$ along with the ω_1 and ω_2 values above. The coefficients α_1 and α_2 are placed in ABAQUS in the advanced damping section shown in Figure 20.

$$\alpha_1 = 2.51$$

-- note: for all beams, $\alpha_2 \ll \alpha_1$ and is assumed to be 0

Edit Beam Section

Name: BeamSection
Type: Beam

Section integration: ☒ Before analysis ☐ During analysis

Profile name: Steel Beam Create...

Profile shape: Box

Basic **Advanced** **Output Points**

Damping

Alpha: 2.51
Beta: 0
Composite: 0

Transverse Shear Stiffness

☐ Specify transverse shear

Slenderness compensation: ☒ Use analysis product default ☐ Value: 0.25

K23: K13:

Generalized Profile Offset

Centroid: X1: 0 X2: 0

Shear Center: X1: 0 X2: 0

OK Cancel

Figure 20. Rayleigh Damping for a Section

In the next step the Rayleigh damping coefficients will allow for a non constant Amplitude envelope. The damping will produce a log decrement decay of the beams amplitude over time.

Producing the Log Decrement Response

Two steps are necessary to produce a log decrement plot in ABAQUS. Both steps are ‘Explicit, General’ steps with the nonlinearity turned on. The first step applies a load to the beam to cause a deflection in the w or 3-direction. This first deflection will be the

maximum deflection of the beam throughout both time steps. In the first step, load P is set as a 'smooth step' function with an maximum value of 0.5 lbf. This produces a maximum displacement of approximately 0.08 inches, a similar deflection to past experiments of Ernst and Palazotto [6]. The load is applied for 0.0125 seconds. The smooth step allows for the force to be applied with a zero derivative at both the beginning and end of the 0.0125 time step. A generic smooth step function that is applied to this beam as well as the others is shown in Figure 21.

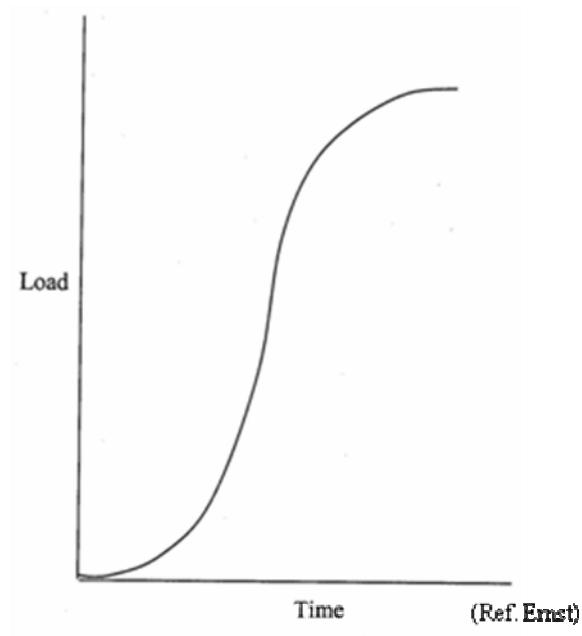


Figure 21. Smooth Step Function

In the second step, the beam is allowed to freely vibrate. The time step must be long enough to produce an adequate amount of data for the production of a backbone curve. The load from step 1 is deactivated. Step two is applied for length of time of 1.4 seconds.

The fixed-fixed Steel beam's free vibration response is below in Figure 22. The beam starts out at a displacement of 0.07 inches and at 1.4 seconds has decayed to a displacement of 0.015 inches. During this decay the frequency of the oscillation is changing. It is clearly seen that the oscillation frequencies at the beginning of the decay are higher than the frequencies towards $t = 1.4$ seconds. This plot holds all of the information necessary to create a backbone curve of the first mode for the Fixed-Fixed Steel beam. This data is saved in a .rpt file and opened in MATLAB.

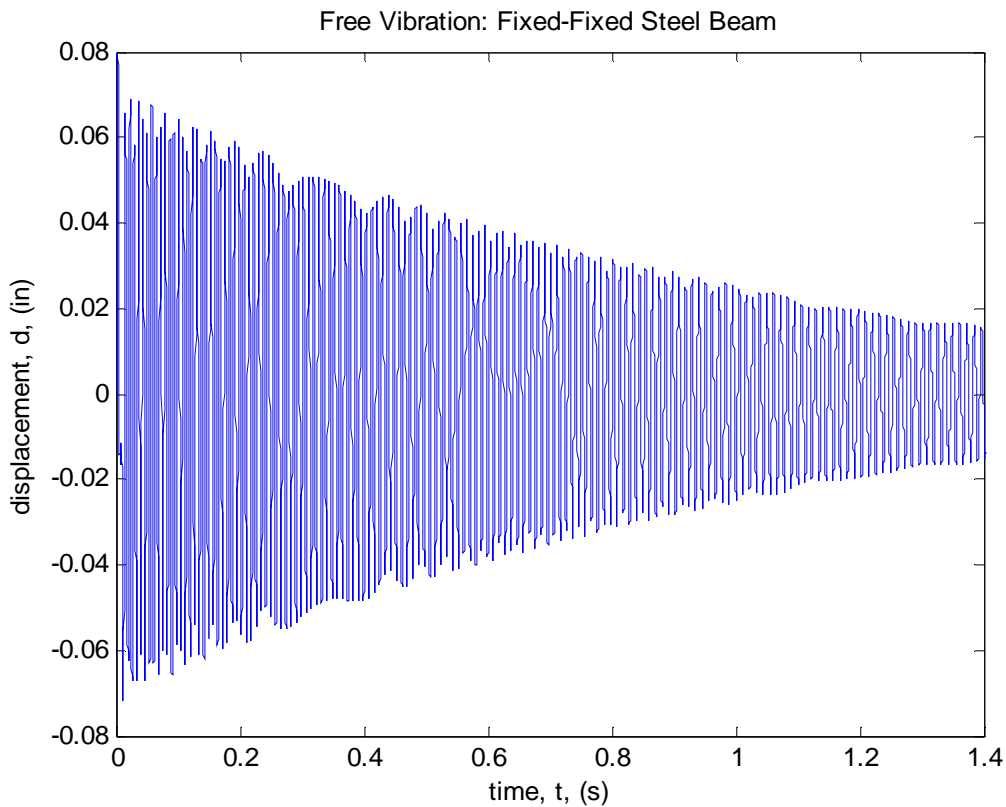


Figure 22. Free Vibration: Fixed-Fixed Steel Beam

After applying the Hilbert transform via MATLAB, the free vibration signal is broken up into two parts. The first part is called the Amplitude Envelope, and is made up

of the signals maximum amplitude against time. The Amplitude Envelope is shown in Figure 23. The second part is the called the Instantaneous Frequency, and is made up of the signals nonlinear frequencies at any given time. This is shown in Figure 24.

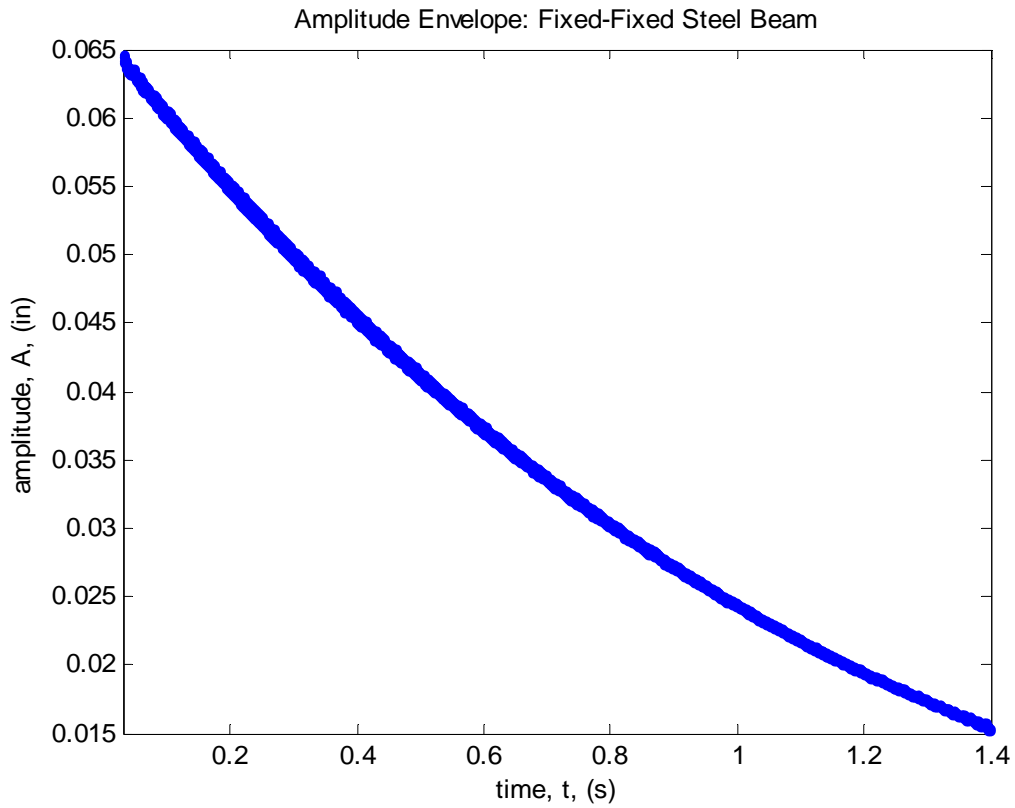


Figure 23. Amplitude Envelope: Fixed-Fixed Steel Beam

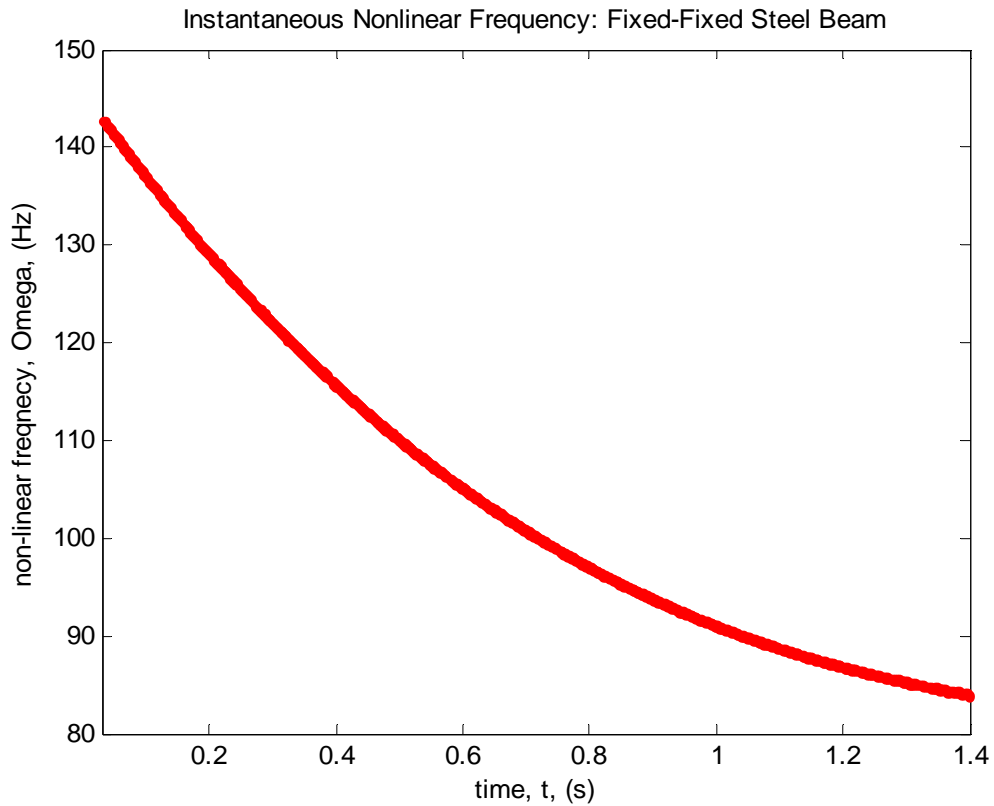


Figure 24. Instantaneous Frequency: Fixed-Fixed Steel Beam

These two parts are plotted against one another in Figure 25 to create a plot of Amplitude versus Nonlinear Frequency in what essentially is the part of the backbone curve. This will not be what is referred to as the Backbone Curve however as it only contains information for amplitudes that fell within the range of the free vibration simulation from ABAQUS. There are also outliers present that are attributed to the beginning and ending portions of the ABAQUS data.

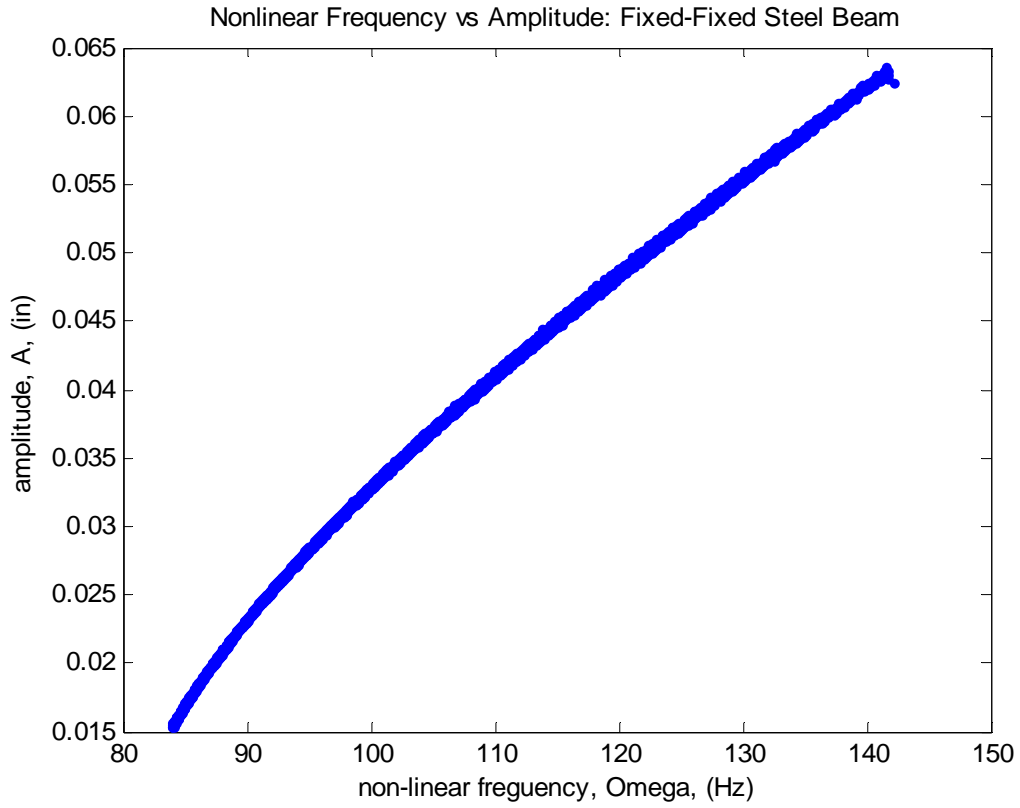


Figure 25. Amplitude vs Nonlinear Frequency: Fixed-Fixed Steel

To create the Backbone Curve for all amplitudes, the Amplitude and Nonlinear Frequency values are squared and are plotted against one another in Figure 26. The Estimated Backbone Curve equation (12) is applied to find the values of ω_0 and β .

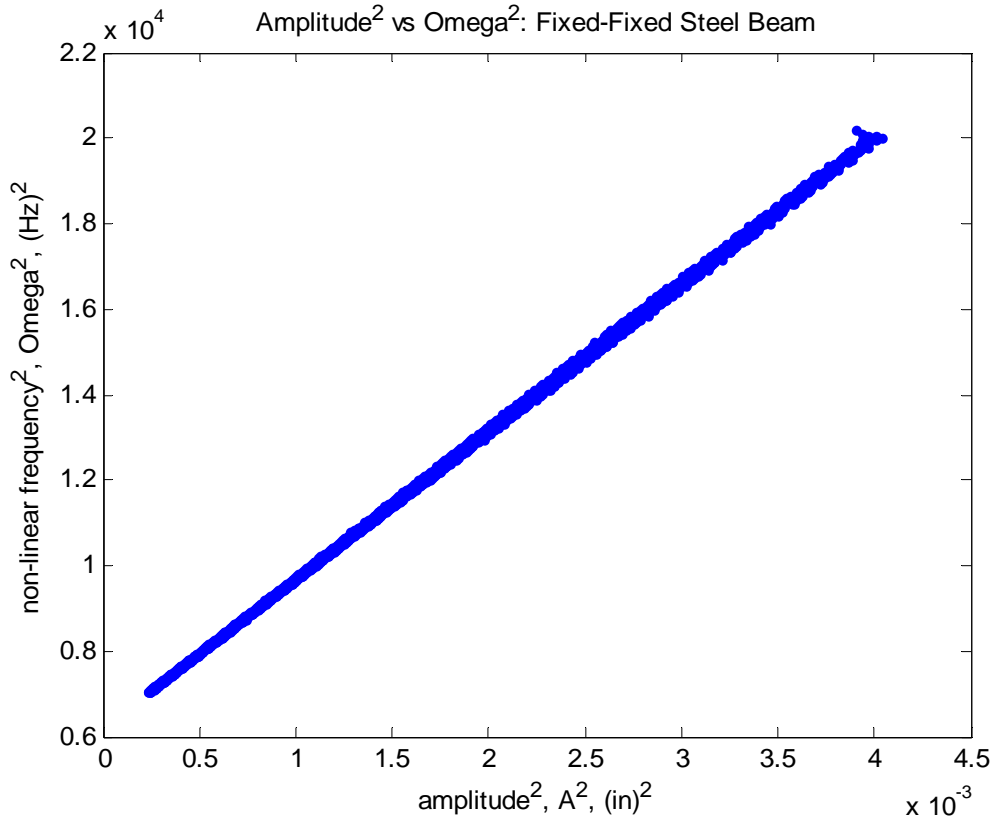


Figure 26. Duffing Equation Plot: Fixed-Fixed Steel Beam

The following information was obtained for the first mode Backbone Curve for the Fixed-Fixed Steel beam. The linear frequency $\omega_0 = 79.02$ Hz and the coefficient $\beta = 1.814\text{e}8 \text{ in}^{-2} \text{ s}^{-2}$. These results are used to show the nonlinearity of the beam compared to a linear backbone curve and form the equation $\Omega^2 = \omega_0^2 + \frac{3}{4} \beta A^2$.

In Figure 27 the fixed-fixed Steel beams backbone curve is plotted against its first natural frequency of 79.02 Hz. The backbone curve shows that the beam has a very strong geometric nonlinearity. When it is subject to a steady state displacement of 0.08 inches, the nonlinear natural frequency of the beam more than doubles from 79 Hz to 165 Hz. This change in the Backbone Curve from a linear to nonlinear analysis is clearly

seen as the nonlinear Backbone Curve is showing a strong hardening affect as it leans to the right. This can be attributed to the increasing contribution that the membrane strain term has in the nonlinear Green Strain equation.

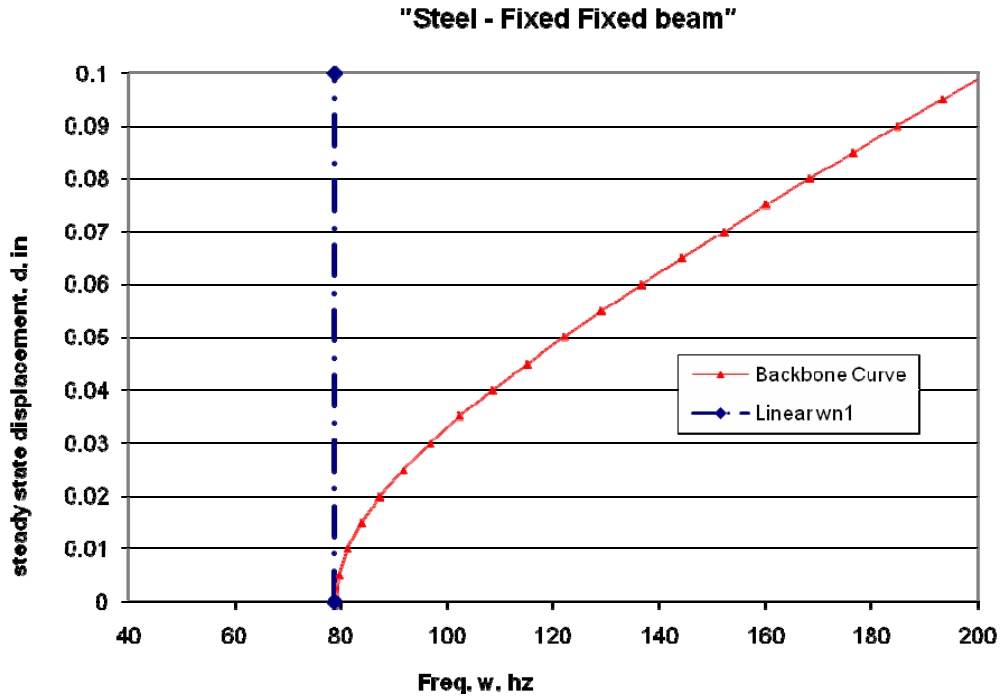


Figure 27. Backbone Curve: Fixed-Fixed Steel

The methods used in this study show close results with previous experiments of Gordon, Holkamp, and Spotswood, and Ernst shown in Table 3.

Table 3. Duffing Equation Results Comparison

Fixed-Fixed Steel Beams	ω_0	β
<i>GHS experimental</i>	79.00	1.80e8
<i>Ernst ABAQUS</i>	79.0047	1.84e8
Current ABAQUS	79.02	1.8140e8

Developing the Frequency Response Function Plots

As mentioned previously, each individual point on the Frequency Response Function is found by applying a force of $P \sin(\omega t)$ at the midspan of the beam. ABAQUS then simulates the beam response for the time length specified. The steady state response of the beam is then measured and recorded. For the Clamped-Clamped Steel beam the following individual points on the Frequency Response Functions were found.

Force: $P = 0.2 \text{ lbf}$: Frequency, $\omega = 60 - 150 \text{ Hz}$

$P = 0.1$: $\omega = 60 - 135 \text{ Hz}$

$P = 0.025$: $\omega = 60 - 105$

The Frequency Response Function points are plotted against the backbone curve for comparison. Below, Figure 28 shows a single data point's ABAQUS run. For Beam 1, each individual data run takes approximately 30 minutes for ABAQUS to simulate.

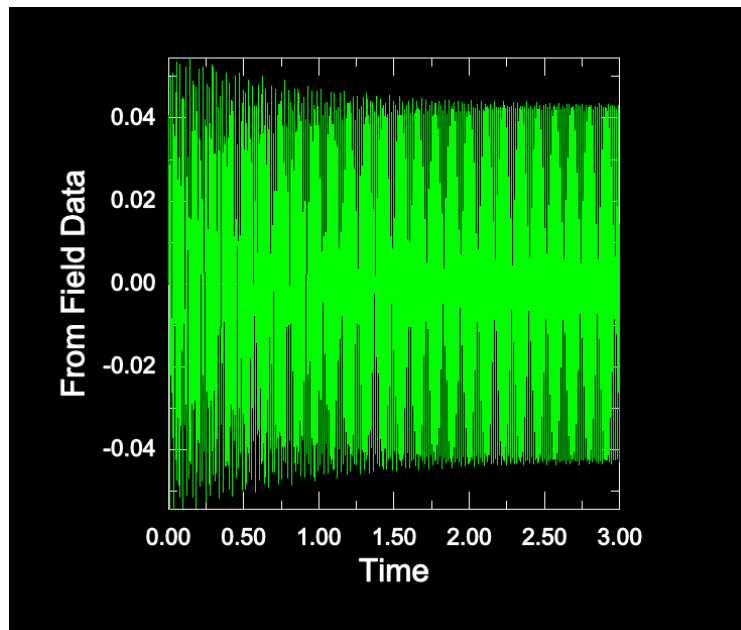
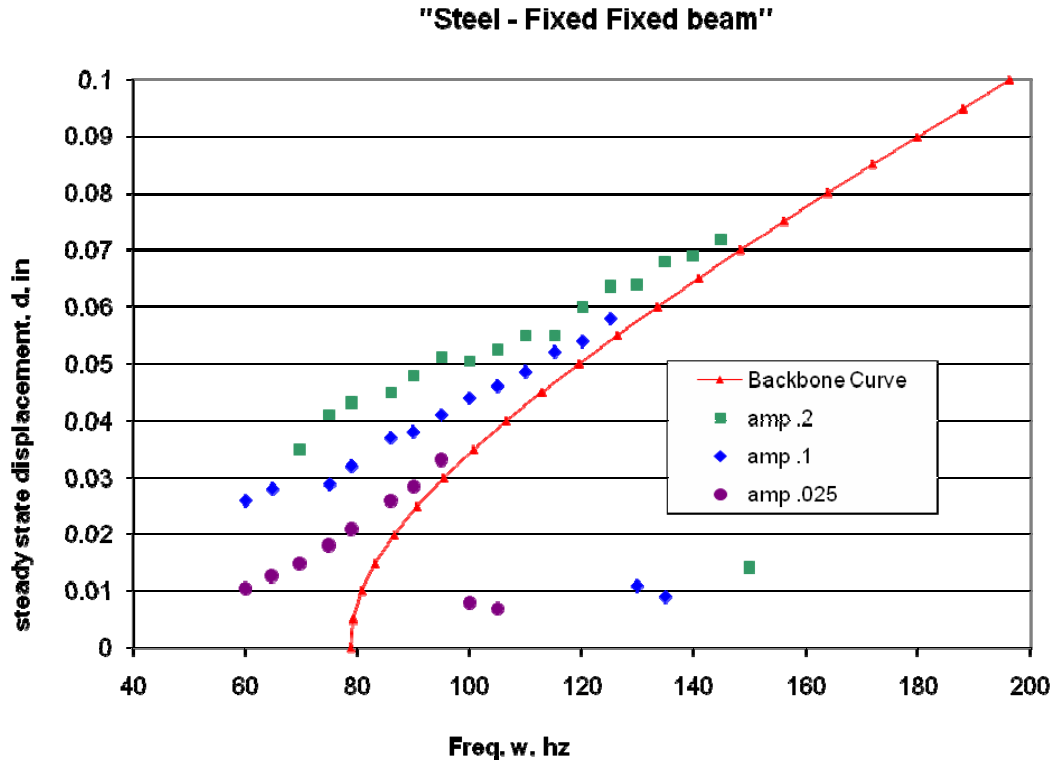


Figure 28. Steady State: Fixed-Fixed Steel

All of these points were plotted together to create three separate Frequency Response Curves. These curves further validate the Backbone Curve data as they follow it asymptotically just as theory predicts.



Clamped-Clamped Aluminum Beam – Beam 2

Next it was desired to look at a more flexible beam of the same dimensions and boundary conditions. The same beam setup as Beam 1 is used while only changing the material properties from Steel to Aluminum. The main values that changed are Young's Modulus, E and material density, ρ . The value of E went from $E_{\text{Steel}} = 29.7 \text{ Mpsi}$ to $E_{\text{Alum}} = 10.6 \text{ Mpsi}$; it became more flexible by a factor of almost 3. The density of the beam

went from $\rho_{\text{Steel}} = .000736$ to $\rho_{\text{Alum}} = .000258$; it became less dense by a factor of almost 3. The specific Modulus of Elasticity, E/ρ only changed slightly from $4.03\text{e}10$ to $4.09\text{e}10$. This beam will show how a more flexible Aluminum beam behaves nonlinearly compared to a stiffer Steel beam. This beam setup will be referred to as Beam 2.

The clamped-clamped model for the Aluminum beam is the same model used for Beam 1, switching appropriate material properties shown in Table 4

Table 4. Section Properties: C-C Aluminum Beam

t, thickness in the 2-direction = 0.031"
w, width in the 3-direction = 0.5"
E, modulus of elasticity = 10.7 Mpsi
ν , poisson's ratio = 0.28
G, Shear Modulus = 4.14 Mpsi
ρ , mass density = $2.588\text{e-}4 \text{ lb}\cdot\text{s}^2\cdot\text{in}^{-4}$

Retrieving the Natural Frequencies

A Frequency Step is applied in ABAQUS to find natural bending frequencies of the beam. The natural frequencies of the Aluminum beam turned out to be just slightly higher than the Steel beam due to the slightly higher specific Modulus.

Table 5. Natural Frequencies: Fixed-Fixed Aluminum Beam

Theoretical results	$\omega_1 = 79.71$	$\omega_2 = 219.56$	$\omega_3 = 430.58$
ABAQUS results	$\omega_1 = 79.60$	$\omega_2 = 219.3$	$\omega_3 = 429.9$
Relative Error	0.13%	0.11%	0.15%

The Rayleigh Damping coefficients, α_1 and α_2 , are solved for using the newly found ω_1 and ω_2 . The Rayleigh Damping coefficient $\alpha_1 = 2.202$, $\alpha_2 = 0$. The coefficients α_1 and α_2 are placed into ABAQUS in the advanced damping section.

Producing the Log Decrement Response

Two 'Explicit, General' steps are setup in ABAQUS. The nonlinear geometry option is turned on. In the first step, a smooth step function load P is applied in the w or 3-direction with a maximum value of 0.5 lbf. This force was chosen to deflect the beam to an initial displacement of 0.07 inches, the same amount as Beam 1 and past experiments. The load is applied for 0.0125 seconds. In the second step, the load is deactivated and the beam is allowed to freely vibrate until the deflections were about 0.01 inches at their maximum. This turned out to be for 1.6 seconds. The fixed-fixed Aluminum beam's free vibration response is below in Figure 30. The beam starts out at a displacement of 0.07 inches and at 1.6 seconds has decayed to a displacement of 0.01 inches. Just like the fixed-fixed Steel beam, the changes in frequencies are visible from the start to finish of the free vibration data. The data saved into a .rpt file and is opened in MATLAB for backbone curve analysis.

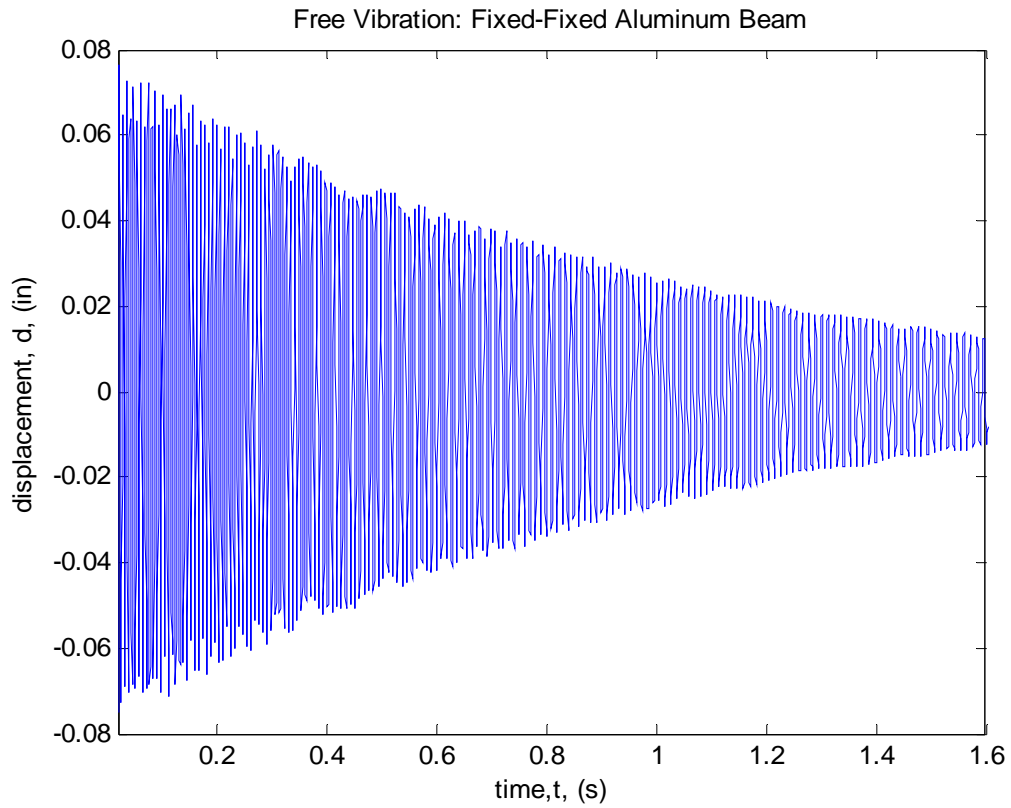


Figure 30. Free Vibration: Fixed-Fixed Aluminum Beam

MATLAB and incorporating the Hilbert transform yield two plots. The Amplitude Envelope is shown in Figure 31. The Instantaneous Frequency versus time is shown in Figure 32.

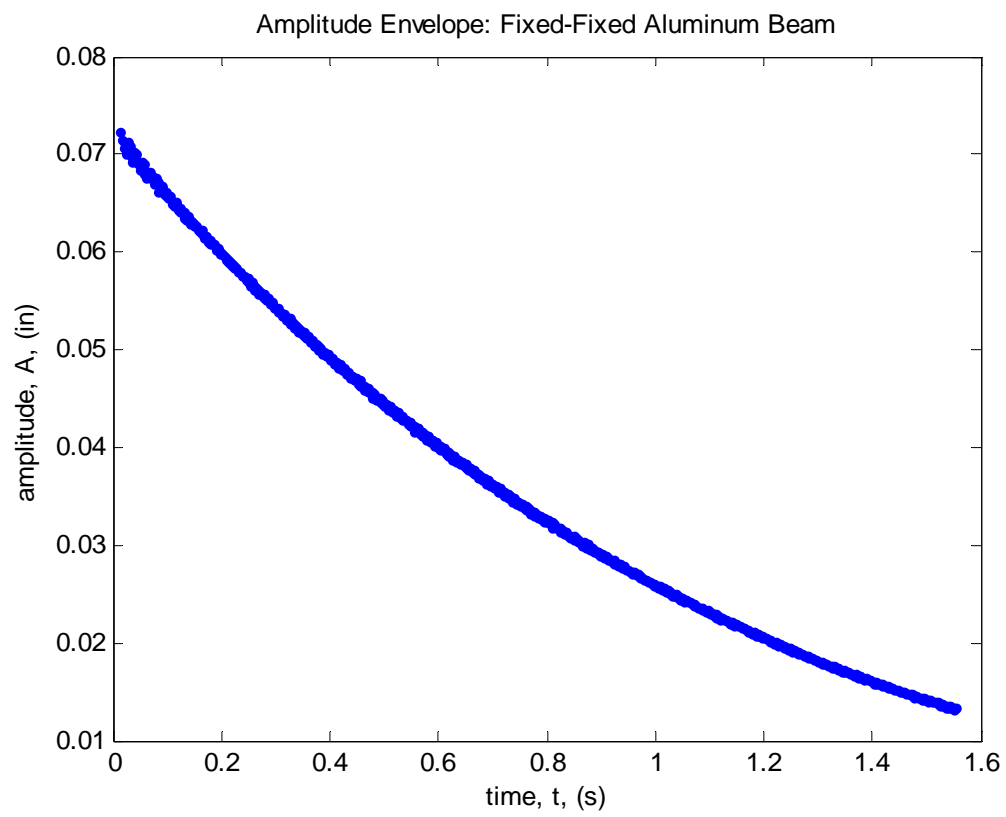


Figure 31. Amplitude Envelope: Fixed-Fixed Aluminum Beam

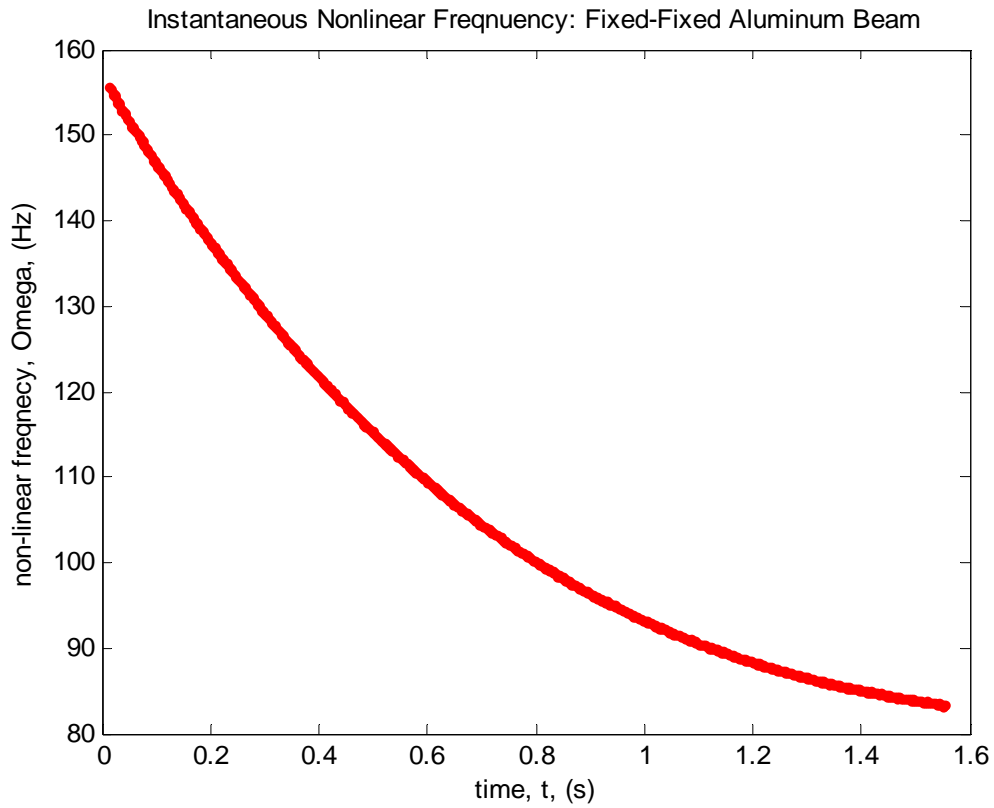


Figure 32. Instantaneous Frequency: Fixed-Fixed Aluminum Beam

These two parts are plotted against one another as in the previous beam in Figure 33 to create a plot of Amplitude versus Nonlinear Frequency. Once again, there are outliers present that are attributed the beginning and ending portions of the ABAQUS data.

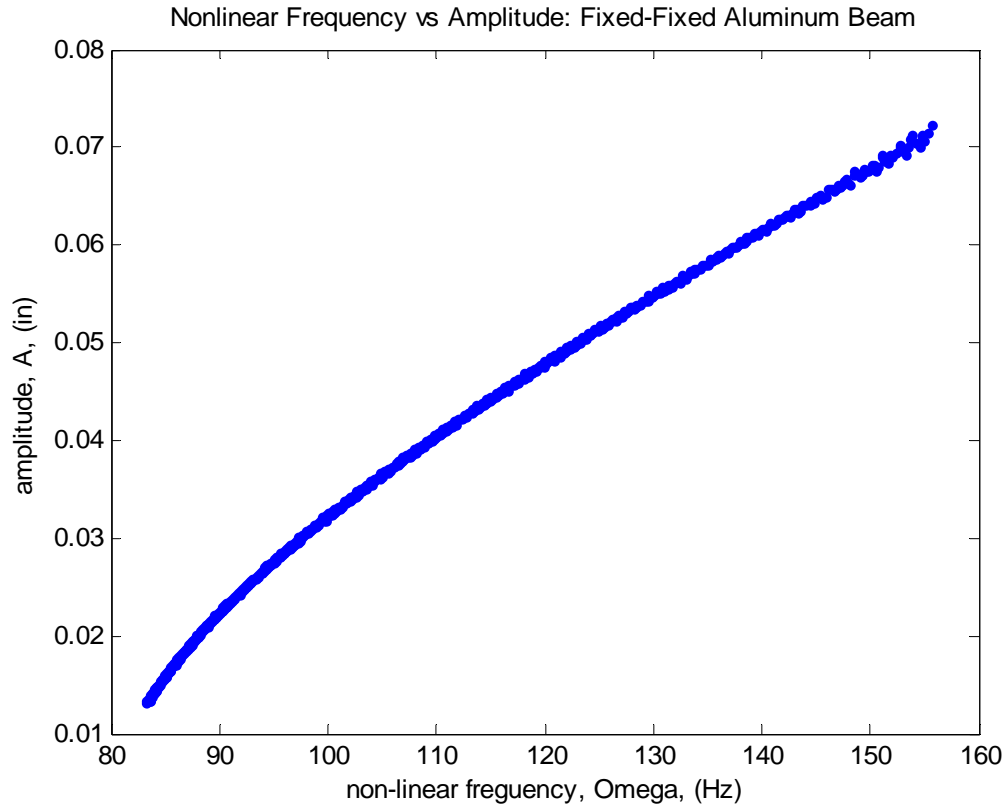


Figure 33. Amplitude vs Nonlinear Frequency: Fixed-Fixed Aluminum

This data is once again used to produce a straight line plot of Amplitude and Nonlinear Frequency values squared as shown in Figure 34. The Estimated Backbone equation (12) is applied to find the values of ω_0 and β .

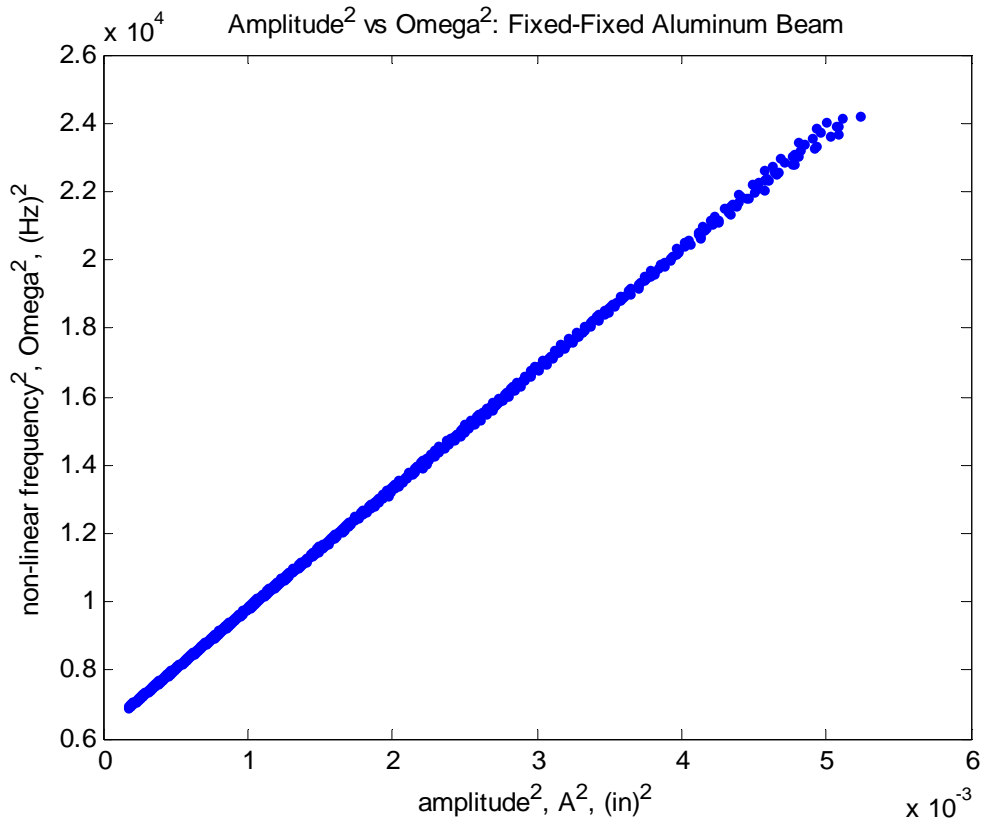


Figure 34. Duffing Equation Plot: Fixed-Fixed Aluminum Beam

The following information was obtained for the first mode Backbone Curve for the Fixed-Fixed Aluminum beam. The linear frequency $\omega_0 = 79.6$ Hz and the coefficient $\beta = 1.84\text{e}8 \text{ in}^{-2} \text{ s}^{-2}$. These values are used in the Estimated Backbone Curve, $\Omega^2 = \omega_0^2 + \frac{3}{4}\beta A^2$. In Figure 35 the fixed-fixed Aluminum beams Backbone Curve is plotted against its first natural frequency of 79.6 Hz. The results are very similar to the fixed-fixed Steel beam.

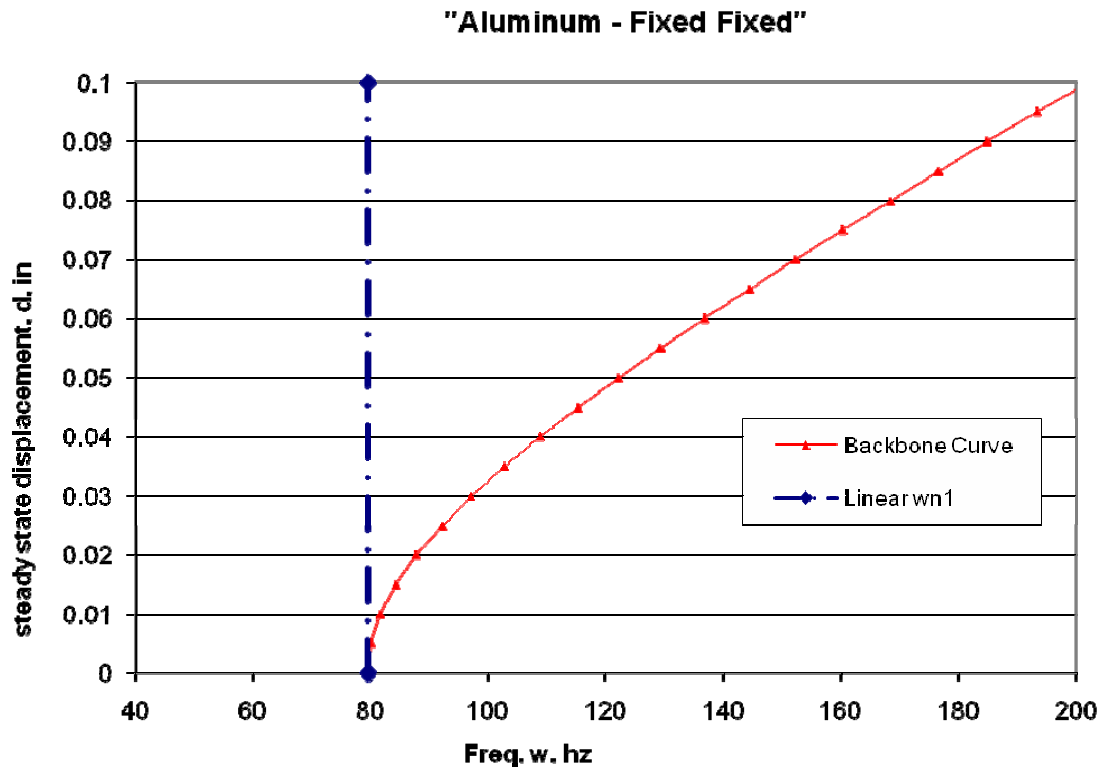


Figure 35. Backbone Curve: Fixed-Fixed Aluminum

To see any real difference between the Backbone Curves, they must be plotted against one another as shown in Figure 36. Both beams show an identical shape however, for a fixed-fixed beam with similar dimensions, it is noticeable that a more flexible beam exhibits less of a nonlinear Backbone Curve. A more flexible beam will be more prone to bending and its strains. This leads to a higher contribution of bending strain in the total strain, a lower contribution of membrane strains, and less of a nonlinear result. This result can also be noticed in the magnitude of the β values in Table 12 where the Aluminum fixed-fixed beam has a lower β value than the Steel fixed-fixed beam.

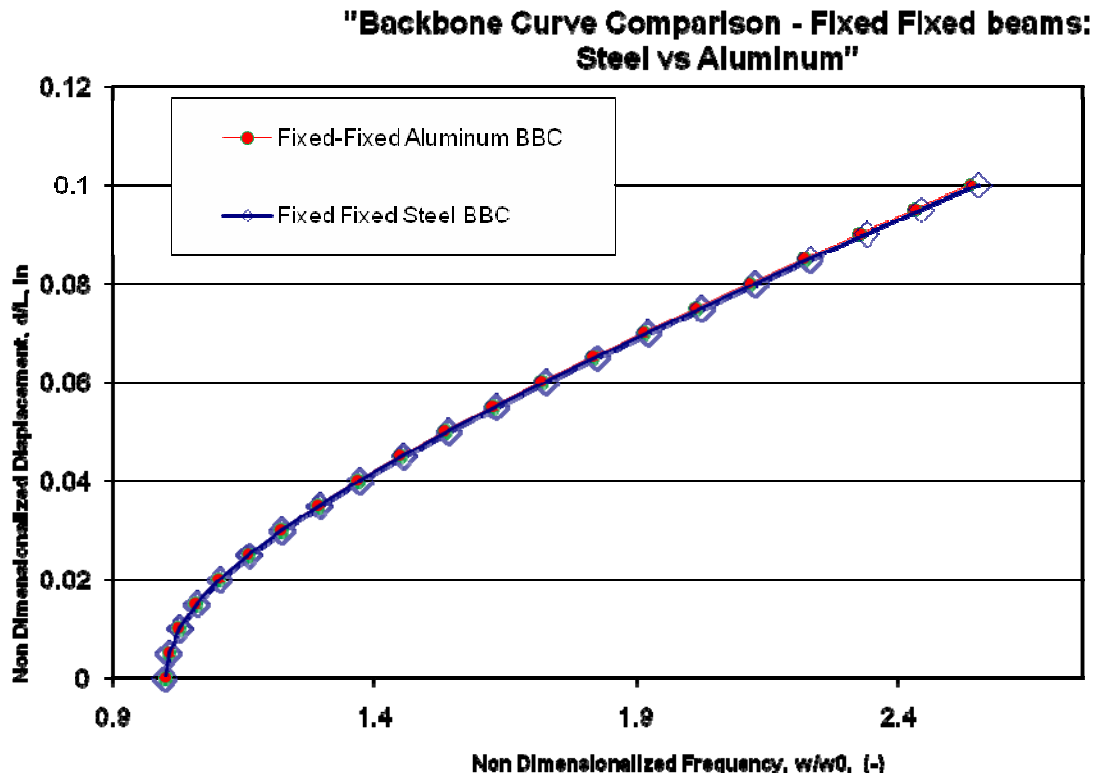


Figure 36. Backbone Comparison: Fixed-Fixed

Clamped- Aluminum Beam – Beam 3

This is the first beam setup that will have a clamped-free boundary condition resembling the setup of a Micro Air Vehicle wing. Keeping the material properties the same as Beam 2, nonlinear characterization can be compared to Beam 2 based on both beam dimensions and beam boundary conditions. This beam has a length of 10.125” and has a thickness $t = 0.0625$, equal to two times the thickness of Beams 1 or 2. This beam will be referred to as Beam 3.

Using ABAQUS/CAE, a finite element model was developed for a Clamped 10.125” long Aluminum beam. Like Beam 1 and 2, this beam is also modeled in 2

dimensional planar modeling space in ABAQUS as a 10.125” deformable wire in the 1-direction. A section is applied to the wireframe with the following Aluminum properties and dimensions:

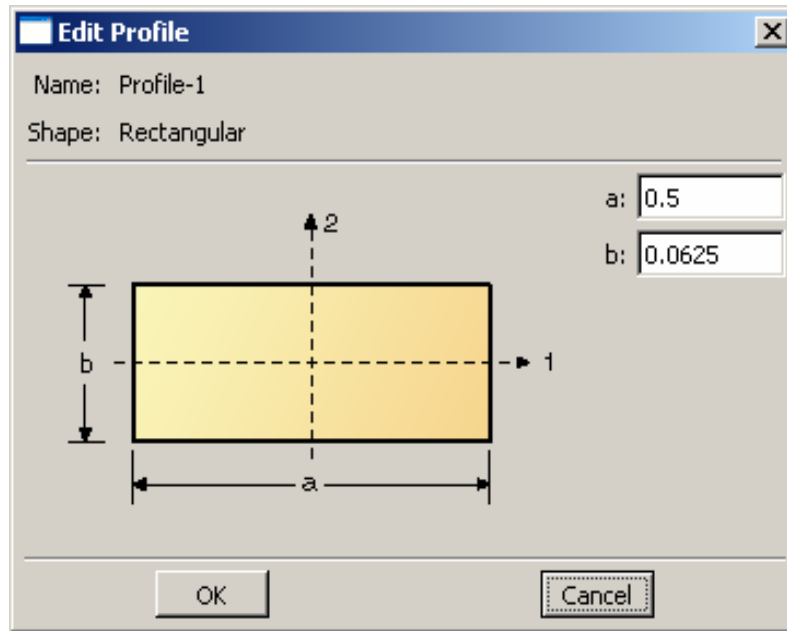


Figure 37. Section Dimensions: Clamped Aluminum

Table 6. Section Properties: C Aluminum

t, thickness in the 2-direction = 0.0625”
w, width in the 3-direction = 0.5”
E, Young’s Modulus of Elasticity = 10.7 Mpsi
ν , Poisson’s ratio = 0.28
G, Shear Modulus = 4.14 Mpsi
ρ , mass density = $2.588\text{e-}4 \text{ lb}\cdot\text{s}^2\cdot\text{in}^{-4}$

A cantilevered boundary condition is applied to one end of the beam, $x = 0$ ” and a load P is applied at $x = 10.125$ ” as shown in Figure 38

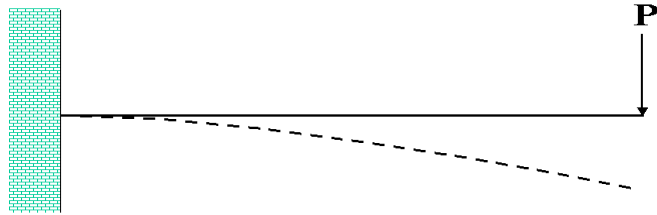


Figure 38. C Aluminum Beam setup

Retrieving the Natural Frequencies

A Frequency Step is applied to find the natural bending frequencies of the beam.



Figure 39. First Mode Eigenvector; $w_1 = 19.911$ Hz



Figure 40. Second Mode Eigenvector; $w_2 = 124.49$ Hz

Table 7. Section Properties: Fixed Aluminum Beam

Theoretical results	$\omega_1 = 19.95$	$\omega_2 = 124.71$
ABAQUS results	$\omega_1 = 19.91$	$\omega_2 = 124.49$
Relative Error	0.2%	0.17%

The Rayleigh Damping coefficients, α_1 and α_2 , are solved for using these new ω_1 and ω_2 values. The Rayleigh Damping coefficient $\alpha_1 = 0.647$ and $\alpha_2 = 0$. The coefficients α_1 and α_2 are placed ABAQUS in the advanced damping section to allow for a damped signal to be simulated.

Producing the Log Decrement Response

Two steps are made to produce a log decrement plot in ABAQUS. As before, both steps are ‘Explicit, General’ steps with the nonlinear geometry option turned on. The first step applies a load to the beam to cause a deflection in the w or 3-direction. In the first step, a smooth step function load P is applied with a maximum value of 0.7 lbf. This leads to a starting deflection of 4.5 inches. The same smooth step type of load from Beam 1 is applied for 0.0125 seconds.

In the second step, the beam is allowed to freely vibrate. The load is deactivated and the beams response is taken for 12 seconds. The time step is longer than the previous two examples due to both the magnitude of the initial deflection of 4.5 inches compared to 0.08 inches for the clamped-clamped Steel beam, and due the lower damping coefficient α_1 estimated by a lower natural frequency of this beam (19.9 Hz) than the previous two (80 Hz).

The fixed-free Aluminum beam's free vibration response is below in Figure 41. The beam starts out at a displacement of 4.5 inches and at 12 seconds has decayed to a displacement of 0.5 inches. The log decrement step was taken out to a time of 12 seconds in order to allow the beam oscillations to decay down to an amplitude less than 1 inch. If the beam has any geometric nonlinearity present then there will be some change in frequency throughout the log decrement step. This change in frequency is not noticeable as it was with the fixed-fixed beams, however the Backbone Curve will provide more information. The data saved as a .rpt file and opened in MATLAB for backbone curve analysis.

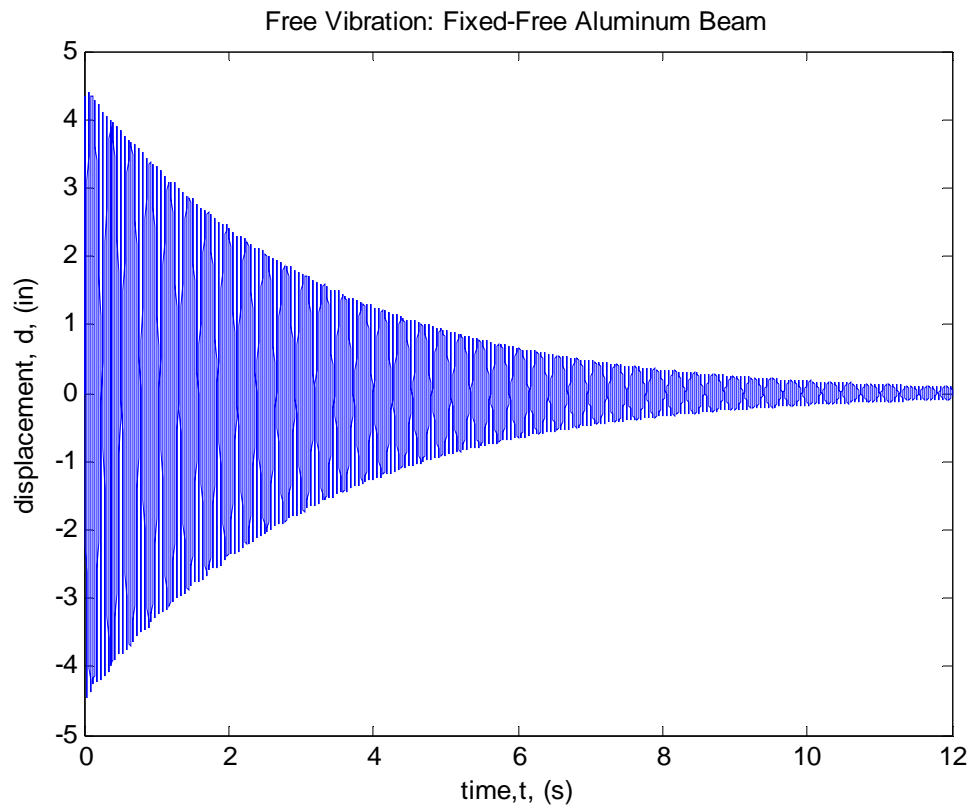


Figure 41. Free Vibration: Fixed-Free Aluminum Beam

Using MATLAB and incorporating the Hilbert transform yields two plots. The Amplitude Envelope is shown in Figure 42. The Instantaneous Frequency versus time is shown in Figure 43.

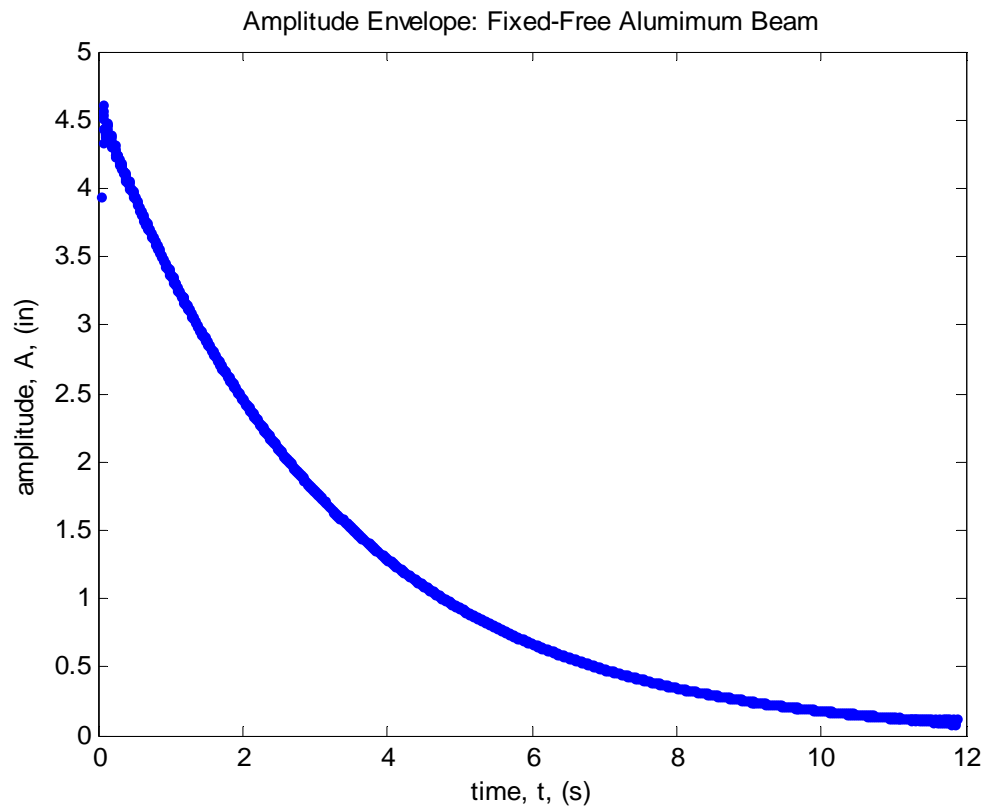


Figure 42. Amplitude Envelope: Fixed-Free Aluminum

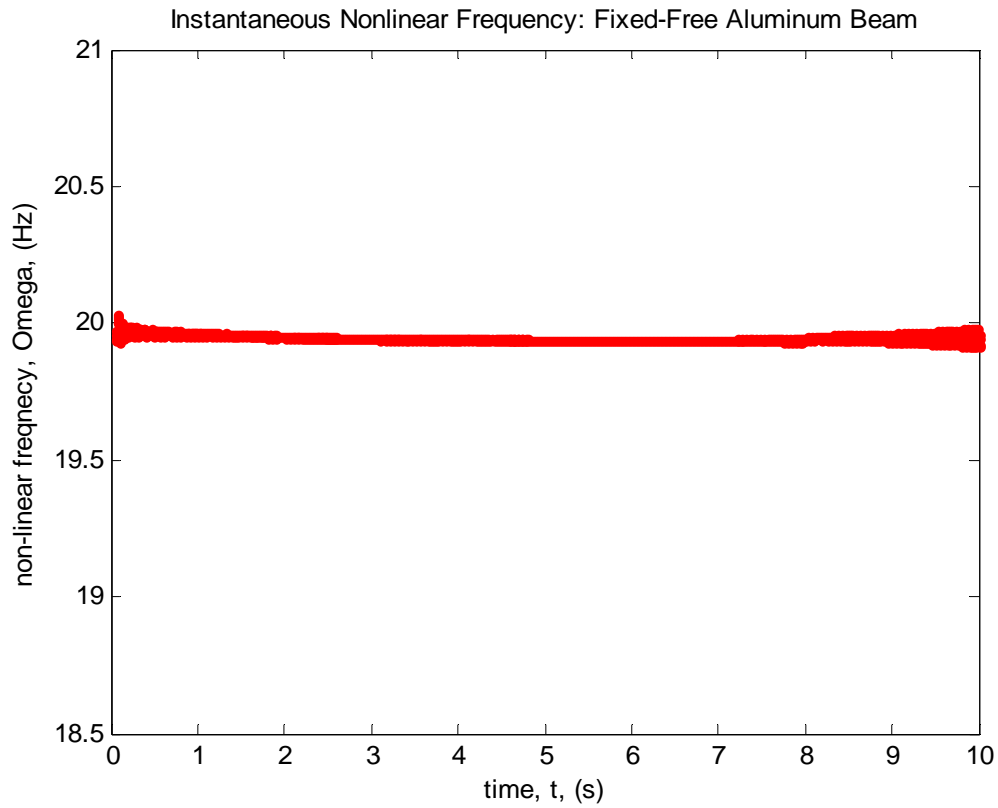


Figure 43. Instantaneous Frequency: Fixed-Free Aluminum

These two parts are plotted against one another in Figure 44 to create a plot of Amplitude versus Nonlinear Frequency. Once again, the outliers present are attributed the beginning and ending portions of the ABAQUS data.

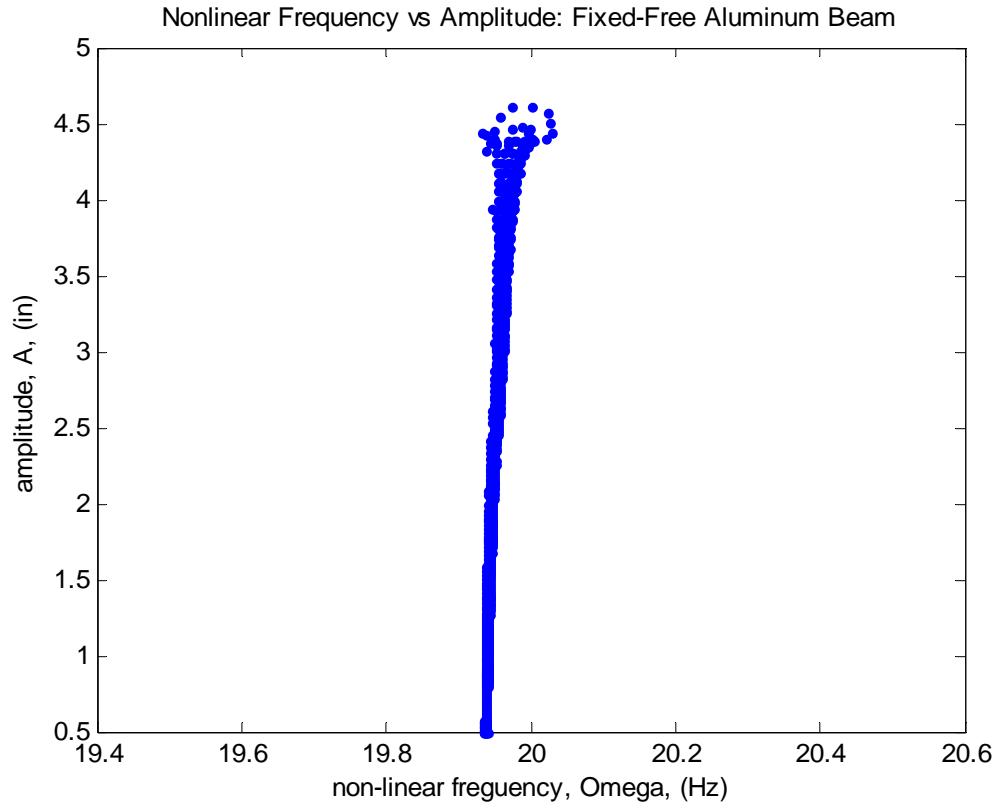


Figure 44. Amplitude vs Nonlinear Frequency: Fixed-Free Aluminum

The Amplitude (A) and Nonlinear Frequency (Ω) values are squared and are plotted against one another in Figure 45. The estimated Backbone Curve equation (12) is utilized in MATLAB to solve for the values of ω_0 and β .

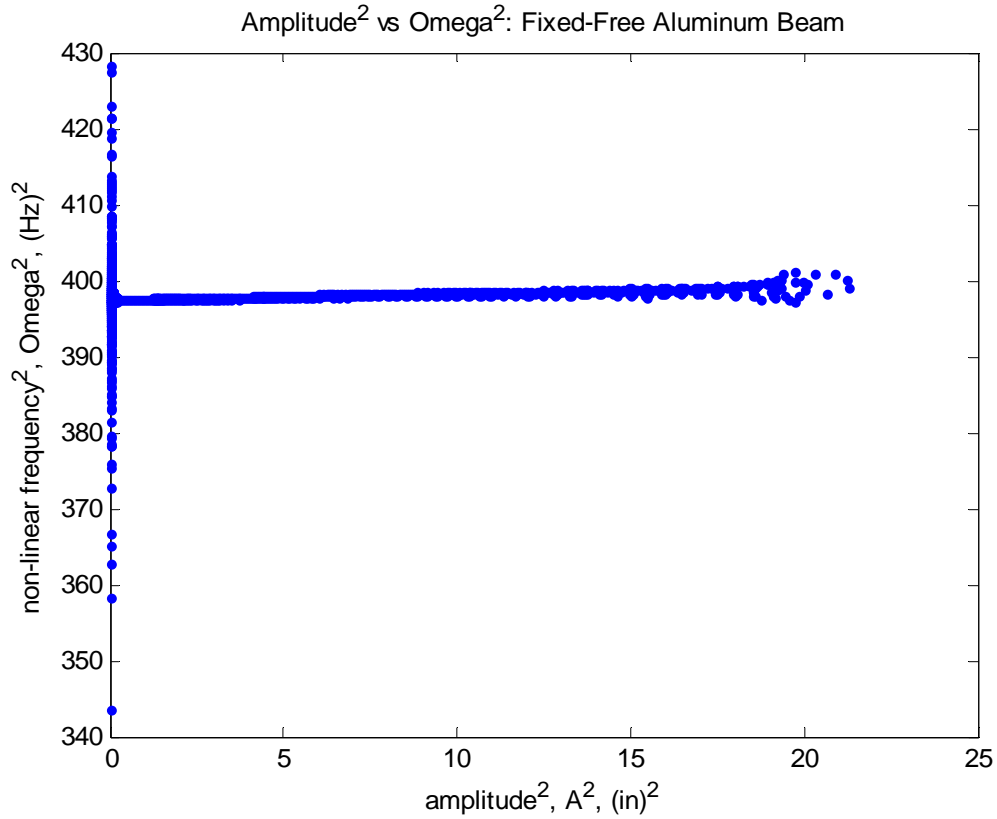


Figure 45. Duffing Equation Plot: Fixed-Free Aluminum

The following information was obtained for the first mode Estimated Backbone Curve, $\Omega^2 = \omega_0^2 + \frac{3}{4} \beta A^2$, for the Fixed-Free Aluminum beam. The linear frequency $\omega_0 = 19.911$ Hz and the cubic stiffness coefficient $\beta = 3.619 \text{ in}^{-2} \text{ s}^{-2}$. This is much lower than the Clamped-Clamped β values of $1.8\text{e}8 \text{ in}^{-2} \text{ s}^{-2}$.

In Figure 46 Beam 3's Backbone Curve is plotted against its first natural frequency of 19.911 Hz. The beam is exhibiting nonlinear hardening as the backbone curve leans to the right of the linear natural frequency. However, the backbone curve is not showing much nonlinearity at all just like the frequency of oscillations didn't seem to be changing noticeably in the log decrement plot for this beam. When the fixed-free

Aluminum beam experiences steady-state displacements greater than 10 times the thickness of the beam, the nonlinear frequency of the beam changed less than 0.1 Hz.

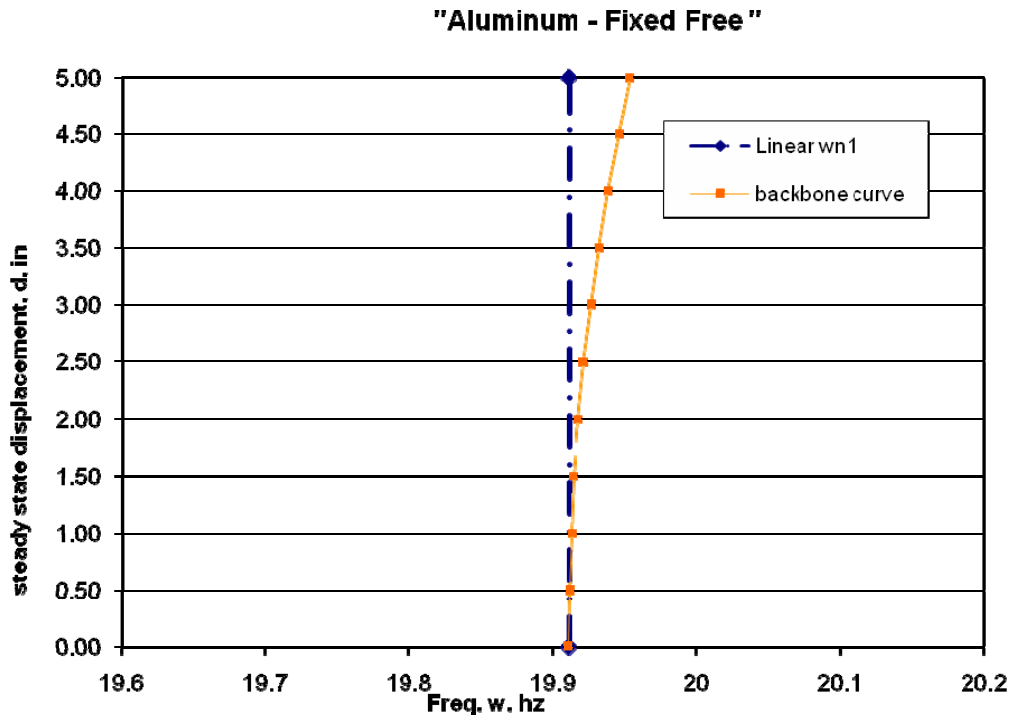


Figure 46. Backbone Curve: Fixed-Free Aluminum

Due to the fact that the Backbone Curves for the clamped-clamped Aluminum beam and the clamped-free Aluminum beam are so drastically different, if they are plotted on the same chart, the clamped-free beam's Backbone Curve will appear to be a vertical line. The fact that the cubic stiffness coefficient (β) value for the clamped-clamped Aluminum beam is about 7 orders of magnitude larger than β for the clamped-free Aluminum beam shows that there is more of a difference in the beams causing the nonlinearity than either their thickness or length. This difference can only be attributed to the fact that one beam is fixed on both ends, while the other is not. As shown in Figure

47 the clamped-clamped beam has two walls pulling on it from each side. As the force P is applied, the walls constrain the beam from deflecting or bending in the w direction. This not only causes an increase in the membrane strain term (du/dx) but also a decrease in any bending strain that would be more obvious in a fixed-free beam. This adds dramatically to the value of the cubic stiffness coefficient β for a fixed-fixed beam.

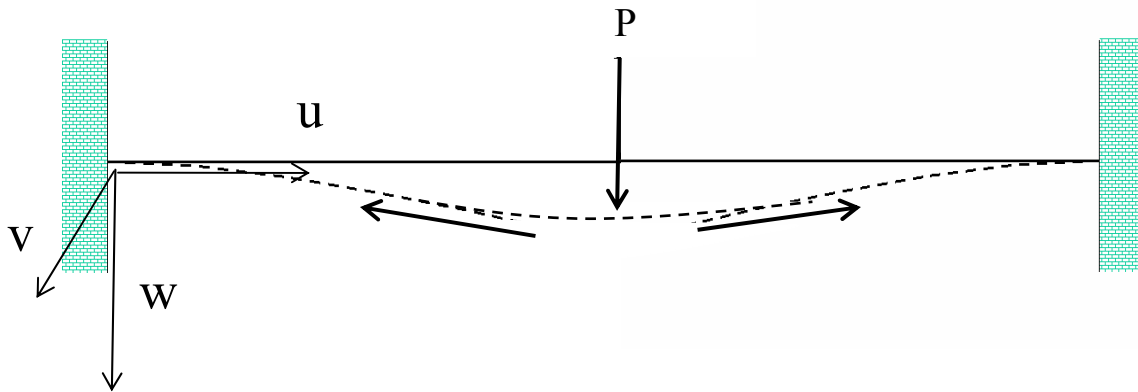


Figure 47. Fixed-Fixed beam setup: Membrane Strain

While the nonlinear effects on the clamped-free Aluminum beam seems small, especially in comparison to Beam 1, other beams of the clamped-free nature will be looked at to bring about further comparison.

Clamped Steel Beam – Beam 4

Next it was desired to look at a less flexible beam of the same dimensions and boundary conditions. The same beam setup as Beam 3 is used while only changing the material properties from Aluminum to Steel. The main values that changed are Young's Modulus, E and material density, ρ . The value of E went from $E_{\text{Alum}} = 10.6 \text{ Mpsi}$ to E_{Steel}

= 29.7 Mpsi; it became less flexible by a factor of almost 3. The density of the beam went from $\rho_{\text{Alum}} = .000258$ to $\rho_{\text{Steel}} = .000736$; it became more dense by a factor of almost 3. The specific Modulus of Elasticity, E/ρ only changed slightly from 4.09×10^6 to 4.03×10^6 . This beam will again show how nonlinear characteristics change for similar a similar Steel and Aluminum beam setup. This beam setup will be referred to as Beam 4.

The clamped Steel beam is the exact model used for Beam 3, only switching the material properties found below.

Table 8. Section Properties: C Steel Beam

t, thickness in the 2-direction = 0.0625"
w, width in the 3-direction = 0.5"
E, modulus of elasticity = 29.7 Mpsi
ν , poisson's ratio = 0.33
G, Shear Modulus = 11.1 Mpsi
ρ , mass density = $7.36 \times 10^{-4} \text{ lb} \cdot \text{s}^2 \cdot \text{in}^{-4}$

Retrieving the Natural Frequencies

A Frequency Step is applied in ABAQUS to find natural in-plane bending frequencies of the beam found in

Table 9.

Table 9. Section Properties: Fixed Steel Beam

Theoretical results	$\omega_1 = 19.80$	$\omega_2 = 123.79$
ABAQUS results	$\omega_1 = 19.76$	$\omega_2 = 123.56$
Relative Error	0.18%	0.18%

The Rayleigh Damping coefficients, α_1 and α_2 are solved for. The Rayleigh Damping coefficient $\alpha_1 = 0.643$ and $\alpha_2 = 0$. The coefficients α_1 and α_2 are placed ABAQUS in the advanced damping section.

Producing the Log Decrement Response

Two ‘Explicit, General’ steps are setup in ABAQUS. The nonlinear geometry option is turned on. In the first step, a smooth step function load P is applied with a maximum value of 1.0 lbf that deflects the tip of the beam to 4.5 inches. The load is applied for 0.0125 seconds. In the second step, the load is deactivated and the beam is allowed to freely vibrate for 12 seconds.

The fixed-free Steel beam’s free vibration response data is almost identical to the fixed-free aluminum beam and is shown below in Figure 48. The main difference is the amount of force it takes to deflect the beam to the same initial perturbation of 4.5 inches. Any frequency change is not seen via visual inspection. The data is saved as a .rpt file and opened with MATLAB to create the Backbone Curve.

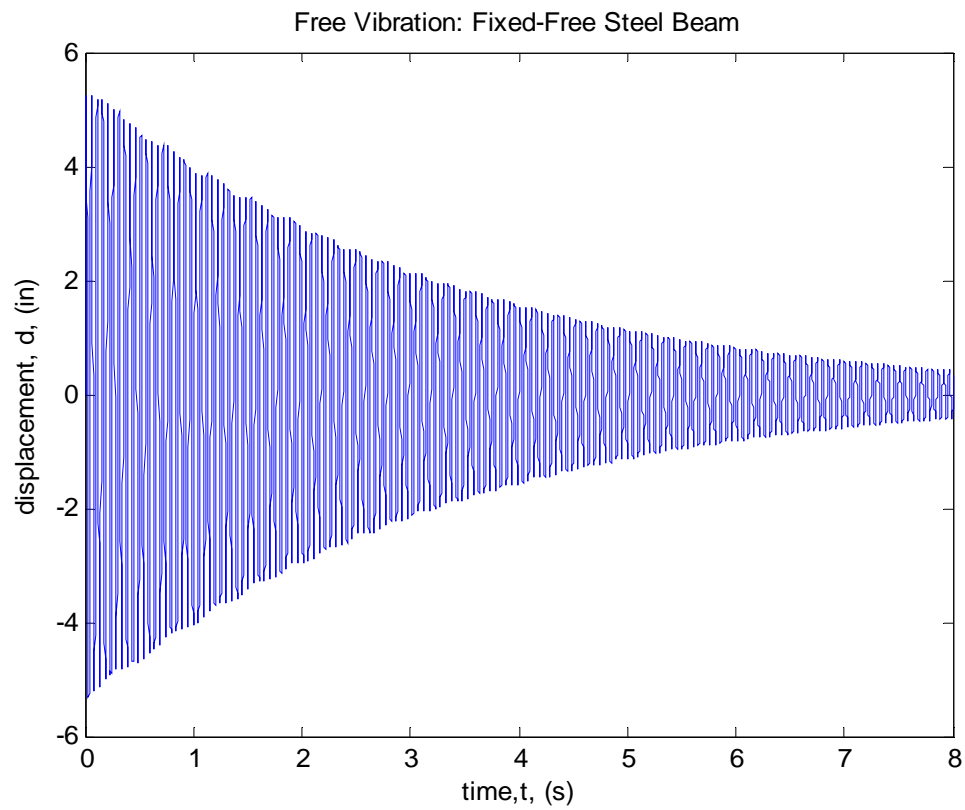


Figure 48. Free Vibration: Fixed-Free Steel Beam

The Amplitude Envelope is shown in Figure 49. The Instantaneous Frequency versus time is shown in Figure 50.

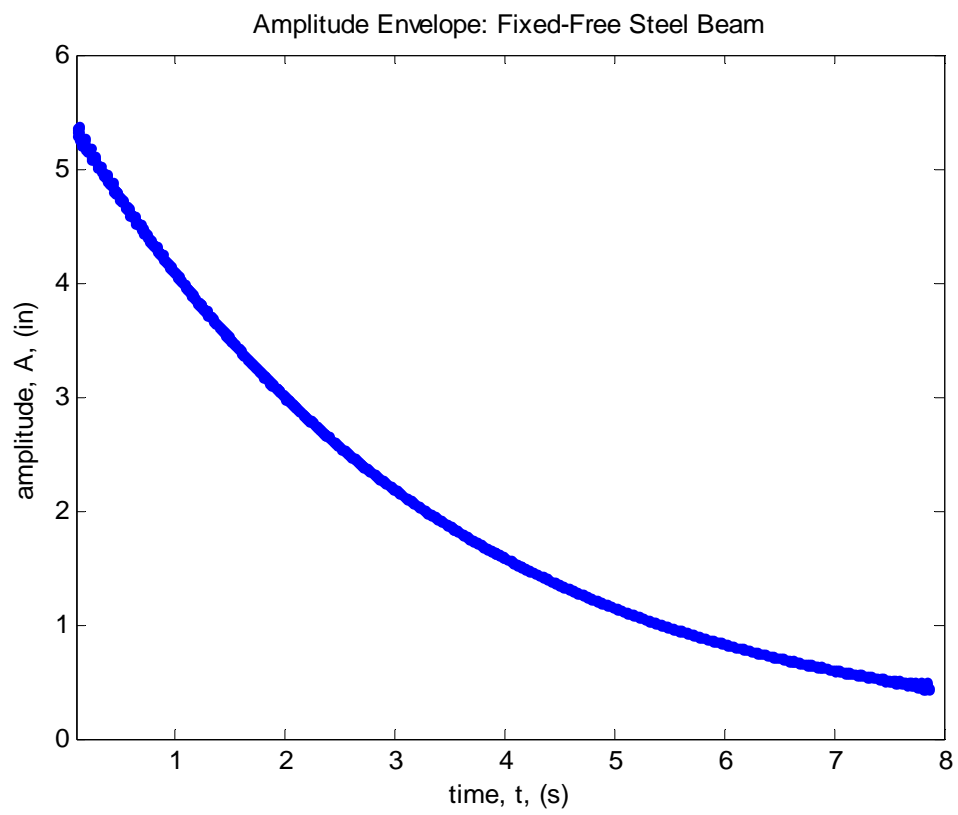


Figure 49. Amplitude Envelope: Fixed-Free Steel

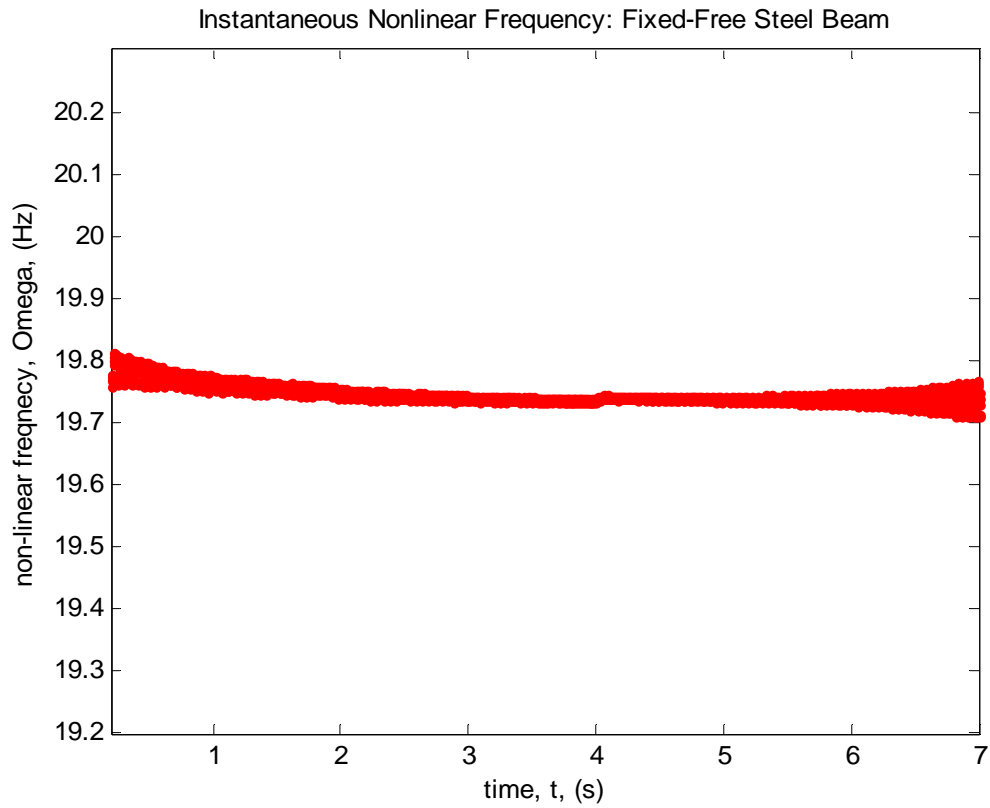


Figure 50. Instantaneous Frequency: Fixed-Free Steel

These two parts are plotted against one another in Figure 51 to create a plot of Amplitude versus Nonlinear Frequency. Once again, the outliers present are attributed the beginning and ending portions of the ABAQUS data.

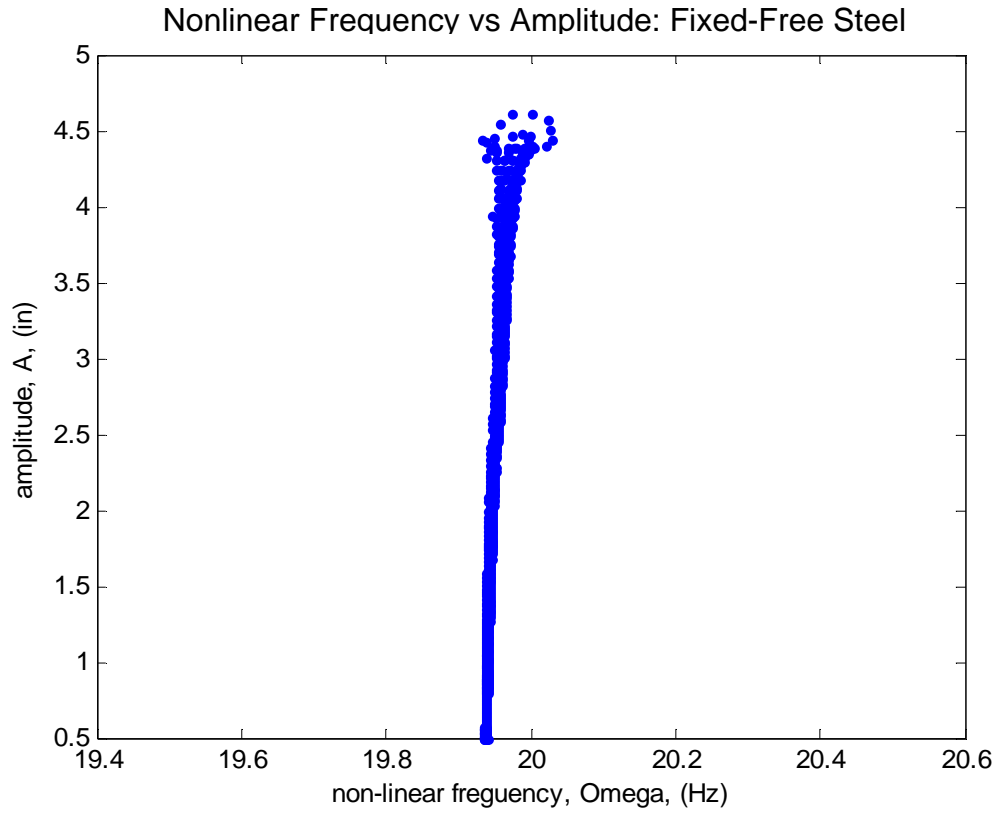


Figure 51. Amplitude vs Nonlinear Frequency: Fixed-Free Steel

The Amplitude (A) and Nonlinear Frequency (Ω) values are squared and are plotted against one another in Figure 52. The Estimated Backbone equation $\Omega^2 = \omega_0^2 + \frac{3}{4}\beta A^2$ is used to find the values of ω_0 and β by fitting it to the data points.

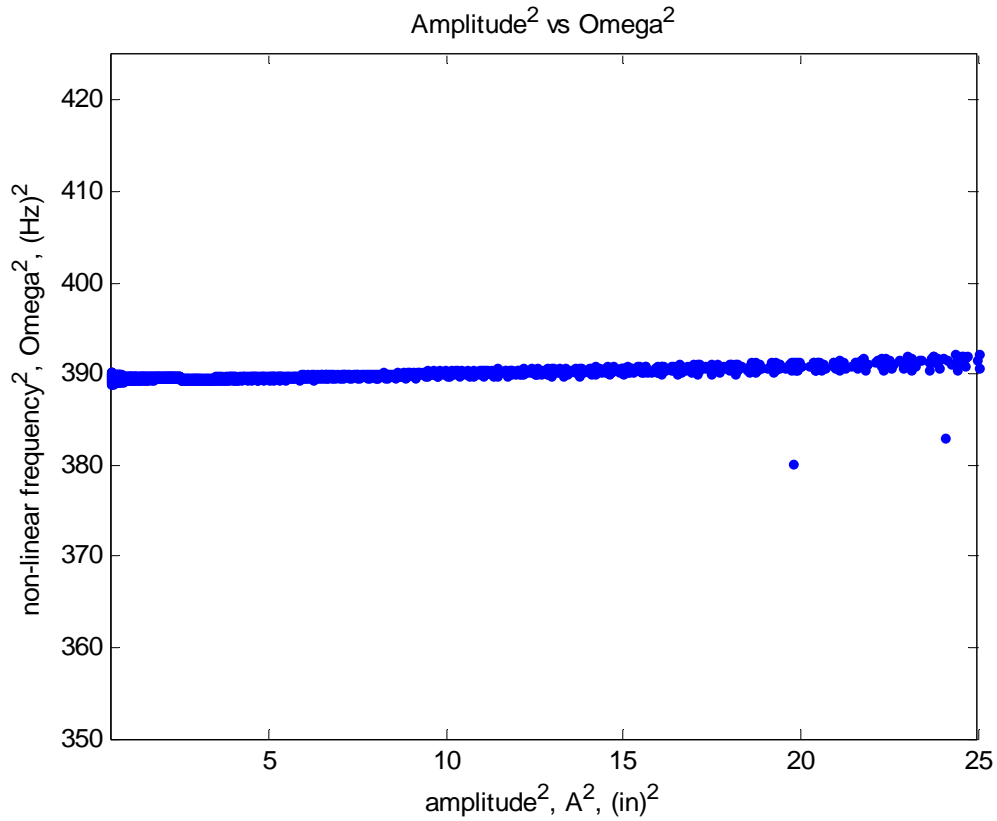


Figure 52. Duffing Equation Plot: Fixed-Free Steel

The following information was obtained for the first mode Backbone Curve for the Fixed-Free Steel beam. The linear frequency $\omega_0 = 19.73$ Hz and the coefficient $\beta = 3.951 \text{ in}^{-2} \text{ s}^{-2}$. In Figure 53 the fixed-free Steel beams backbone curve is plotted against its first natural frequency of 19.73 Hz.

Because the β value for Beam 4 is very similar to the β value found for Beam 3, and because both are at least 7 orders of magnitude smaller than the clamped-clamped beam's β values, it is apparent that clamped-clamped beams exhibit much greater nonlinear tendencies than clamped-free beams. The beam setup had a huge influence on the nonlinear characteristics shown in both the Backbone Curves and the β values. The

boundary condition seems to be the key. A clamped-clamped beam has much more resistance to deflections and bending, cutting down on the bending strain terms. The resistance is caused by the wall boundary conditions pulling on the beam while at the same time causing the membrane strain terms to be a much larger contribution of the total strain.

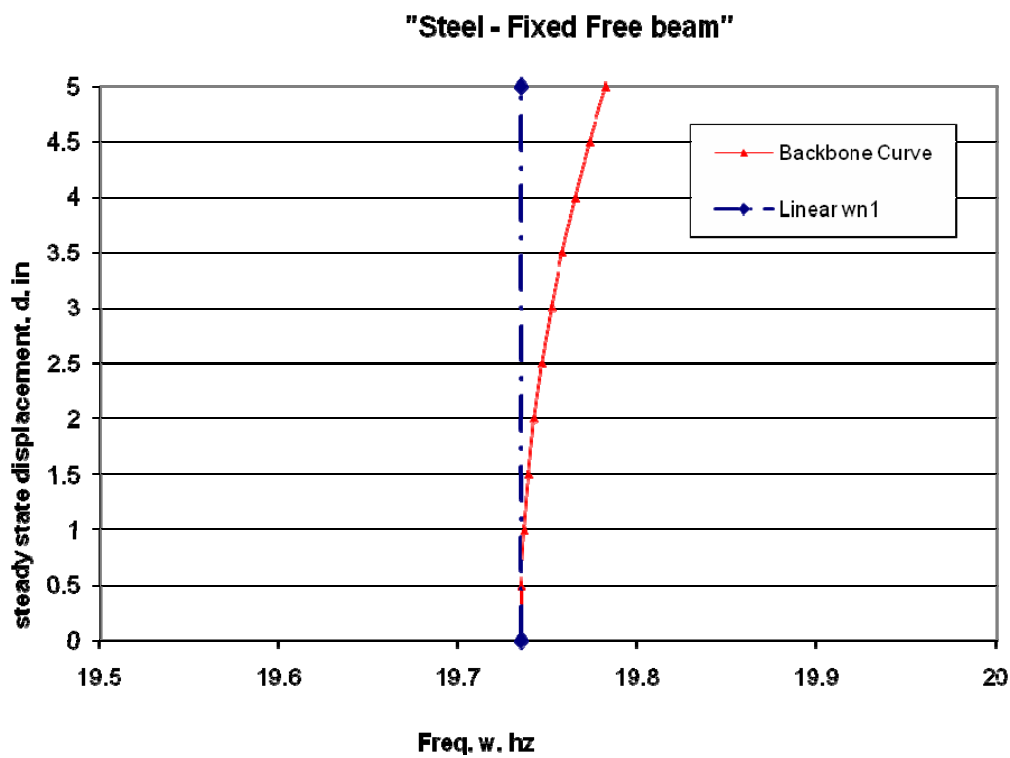


Figure 53. Backbone Curve: Fixed-Free Steel

Like the clamped-clamped data, the results for the fixed-free Steel beam are similar to the fixed-free Aluminum beam. Figure 54 plots the two backbone curves against one another for the two fixed-fixed beams. Both beams are completely identical with the only difference being the difference in material properties between Steel and

Aluminum. Similar to the clamped-clamped results, this plot shows that for a fixed-fixed beam with similar dimensions, a beam made of Steel has a slightly stronger nonlinear hardening effect than a more flexible Aluminum beam. This result can also be noticed in the magnitude of the cubic stiffness coefficient, β values in Table 12. The Aluminum beams both have lower β values than their corresponding Steel beams.

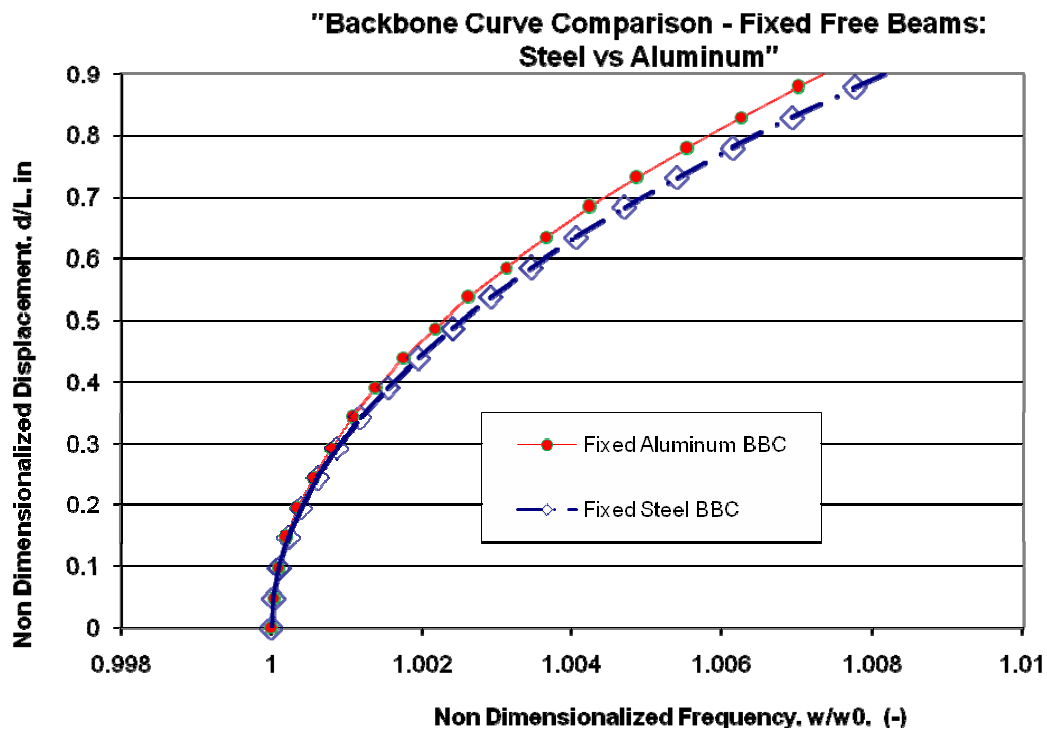


Figure 54. Backbone Comparison: Fixed-Free: Steel vs Aluminum

Clamped Composite Beam – Beam 5

The previous four beams are all isotropic, and while their information is useful in characterizing certain nonlinear effects, Aluminum and Steel may not be likely

candidates to be used as wing material for a future Micro Air Vehicle design. A material more likely to be used would be some sort of Composite layup. Therefore, Beam 5 setup is the same as the clamped-free 6.08 inch Composite beam being studied by Capt Adam Tobias. This beam is the thinnest of all five beams at $t = 0.02''$.

Using ABAQUS/CAE, a finite element model was developed for the Clamped 6.08'' long Composite beam. The beam is a 4-ply $[0/90]_s$ layup as shown in Figure 55.

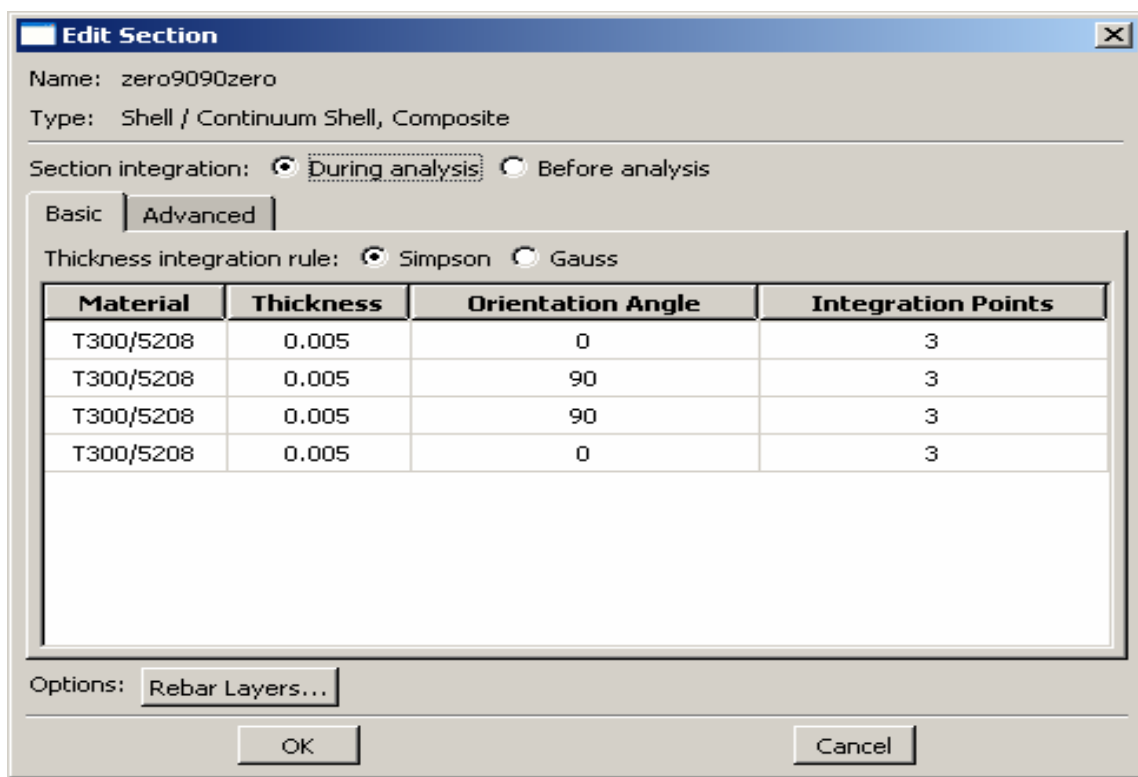


Figure 55. Composite Beam Ply Layup

The composite beam is modeled in 3 dimensional modeling space in ABAQUS as a shell with a total thickness of $.02''$. The shell is divided up into four sections or lamina all of thickness $.005''$. The length of the beam runs parallel with the 1-direction. Each lamina has the same composite properties and dimensions:

Table 10. Section Properties: C Composite Beam

tply, thickness of each ply = .005"
w, width in the 3-direction = 0.5"
E1 = 19.2 Mpsi, E2 = 1.56 Mpsi
V12, poisson's ratio = 0.24
G12 = 8.2e5, G13 = 8.2e5, G23 = 4.9e5
ρ , mass density = .000163 lb·s ² ·in ⁻⁴

A cantilevered boundary condition is applied to one end of the beam, $x = 0$ " and a load P is applied in the 2 or 3-direction at $x = 6.08$ " as shown in Figure 56.

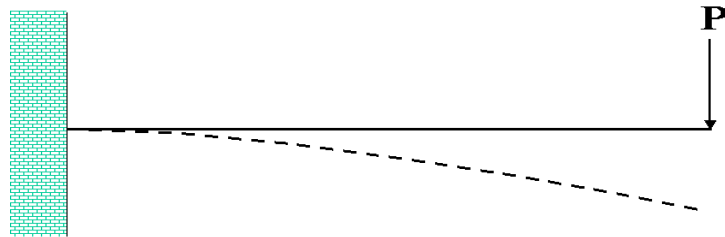


Figure 56. Composite Beam Load

Retrieving the Natural Frequencies

A Frequency Step is applied in ABAQUS to find the in-plane natural bending frequencies of the beam.



Figure 57. First Mode Eigenvector; $\omega_1 = 30.009$ Hz



Figure 58. First Mode Eigenvector; $\omega_1 = 188.48$ Hz

Table 11. Section Properties: Fixed Composite Beam

Theoretical results	$\omega_1 = 30.00$	$\omega_2 = 188.00$
ABAQUS results	$\omega_1 = 30.009$	$\omega_2 = 188.48$
Relative Error	0.03%	0.2%

The Rayleigh Damping coefficients, α_1 and α_2 , are solved for the new ω_1 and ω_2 values. The Rayleigh Damping coefficient $\alpha_1 = 0.976$ and $\alpha_2 = 0$. The α_1 and α_2 values are placed into ABAQUS.

Producing the Log Decrement Response

Two steps are made to produce a log decrement plot in ABAQUS. Both steps are ‘Explicit, General’ steps with the nonlinear geometry option turned on. The first step applies a load to the beam to cause a deflection in the 3-direction. In the first step, a smooth step function load P is applied with a maximum value of .1 lbf. The load is applied for 0.0125 seconds and causes a maximum deflection of 3.7 inches at the tip of the beam.

In the second step, the beam is allowed to freely vibrate. The load is deactivated and the beams response is taken. The load from step 1 is deactivated. Step two is applied for length of time of 1.6 seconds. The fixed-free Composite beam’s free vibration response is below in Figure 59. The beam starts out at a displacement of 3.6 inches and at 4 seconds has decayed to a displacement of 0.5 inches. Like the other fixed-free beams, the geometric nonlinearity of the beam cannot be seen visually from the log decrement plot. The Backbone Curve will once again provide more information. The data is saved as a .rpt file and opened in MATLAB for Backbone Curve analysis.

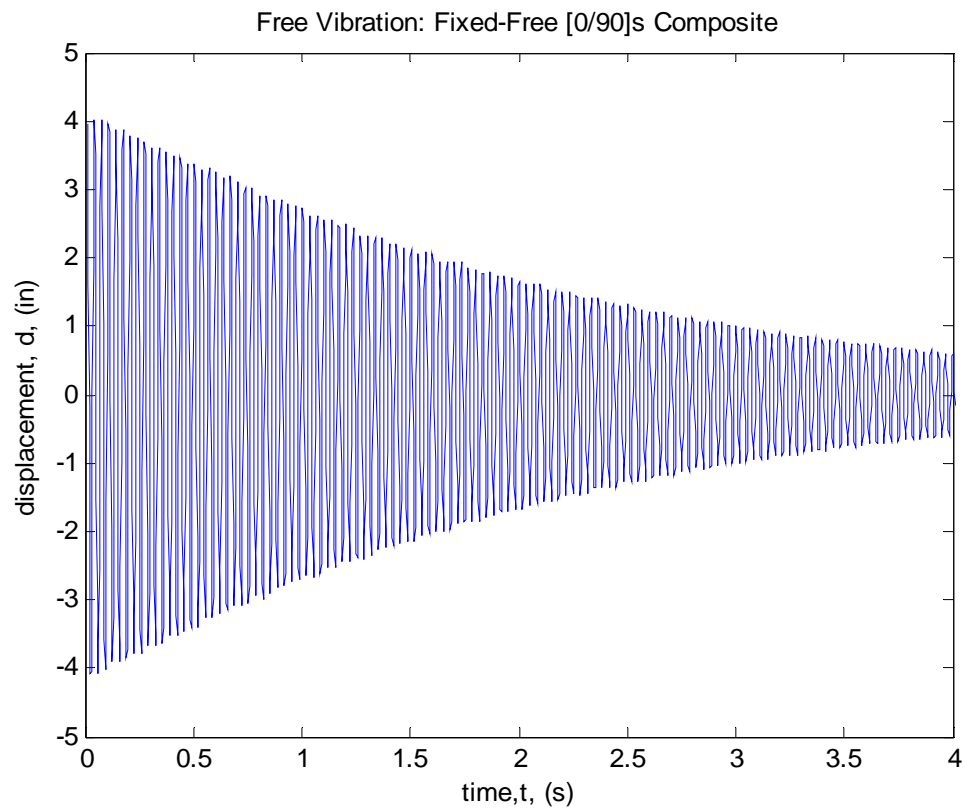


Figure 59. Free Vibration: Fixed-Free Composite Beam

From MATLAB the following two plots were determined. The Amplitude Envelope is shown in Figure 60. The instantaneous frequency versus time is shown in Figure 61.

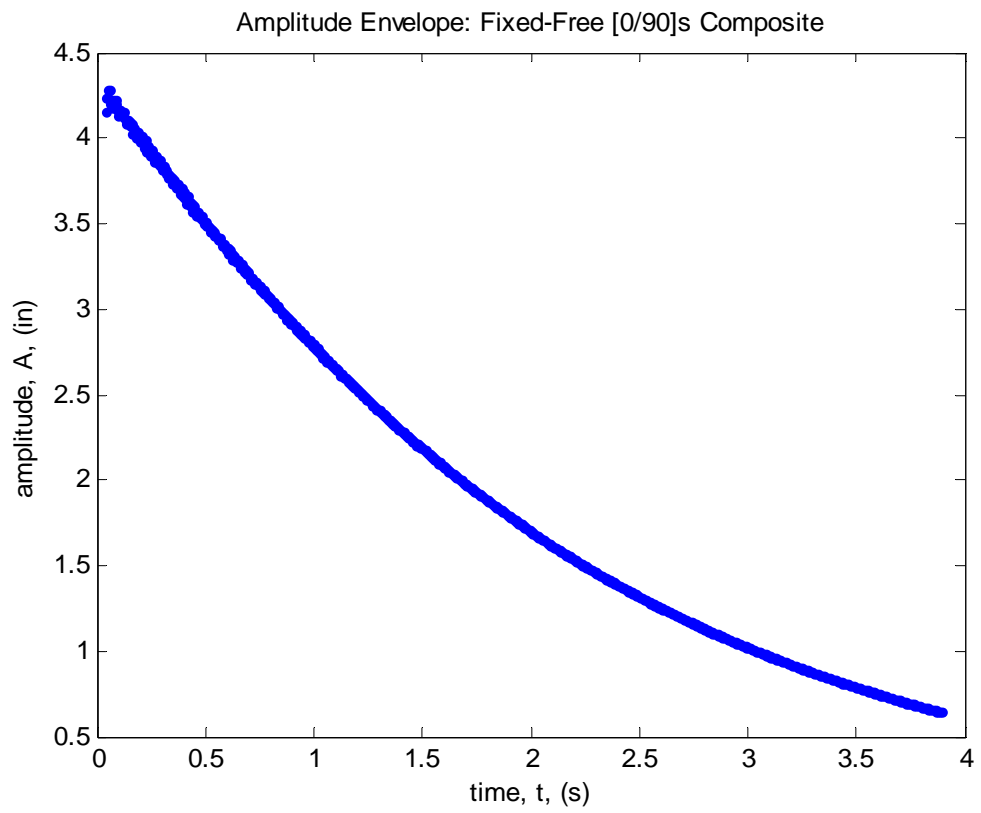


Figure 60. Amplitude Envelope: Fixed-Free Composite

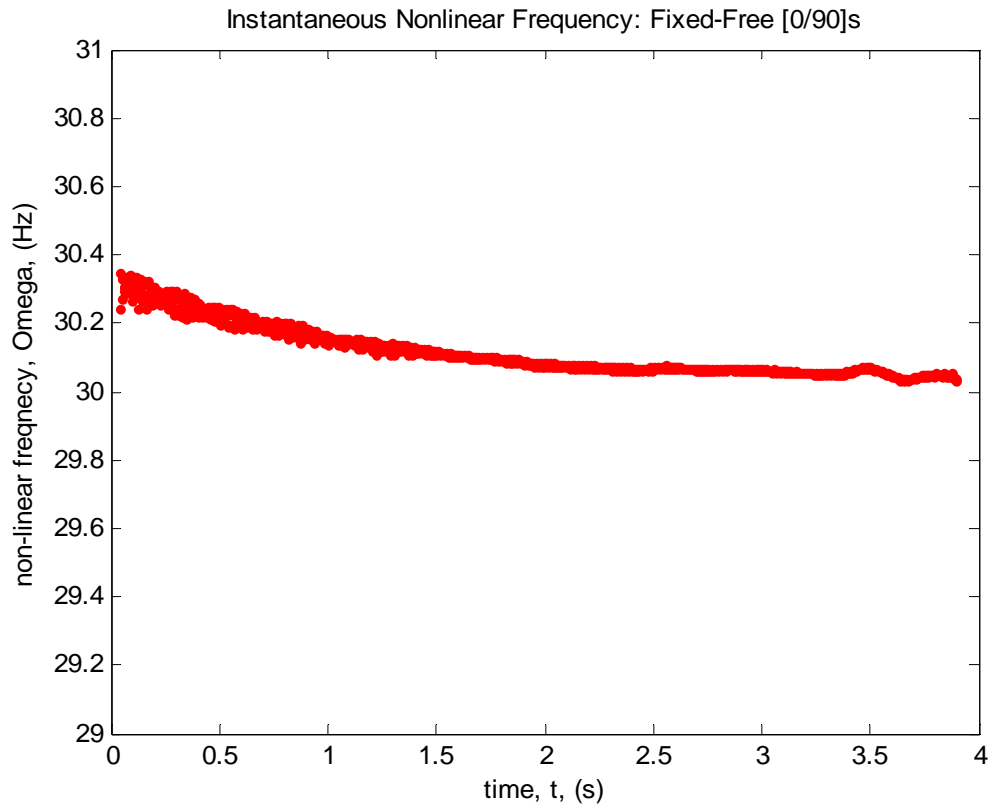


Figure 61. Instantaneous Frequency vs Time: Fixed-Free Composite

These two parts are plotted against one another in Figure 62 to create a plot of amplitude versus nonlinear frequency. These plots look very similar in both their decay and relatively unchanging frequencies to the other fixed free beams.

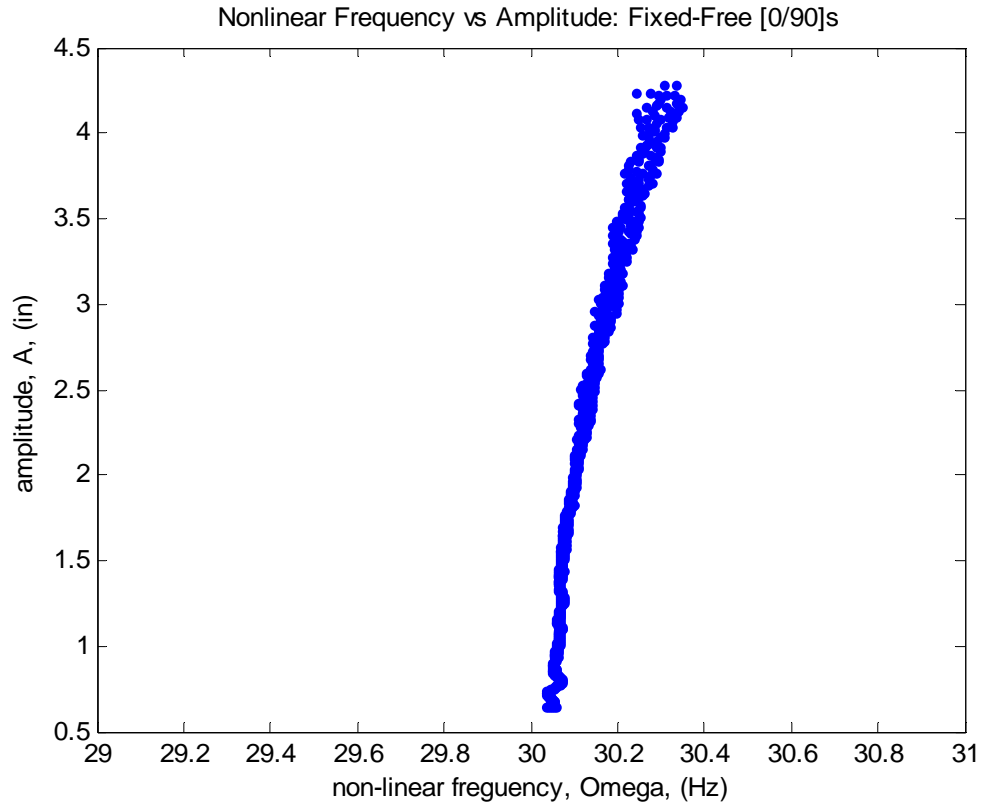


Figure 62. Amplitude vs Nonlinear Frequency: Fixed-Free Composite

The Amplitude (A) and Nonlinear Frequency (Ω) values are squared and are plotted against one another in Figure 63. The values of ω_0 and β are determined using the Estimated Backbone equation $\Omega^2 = \omega_0^2 + \frac{3}{4} \beta A^2$.

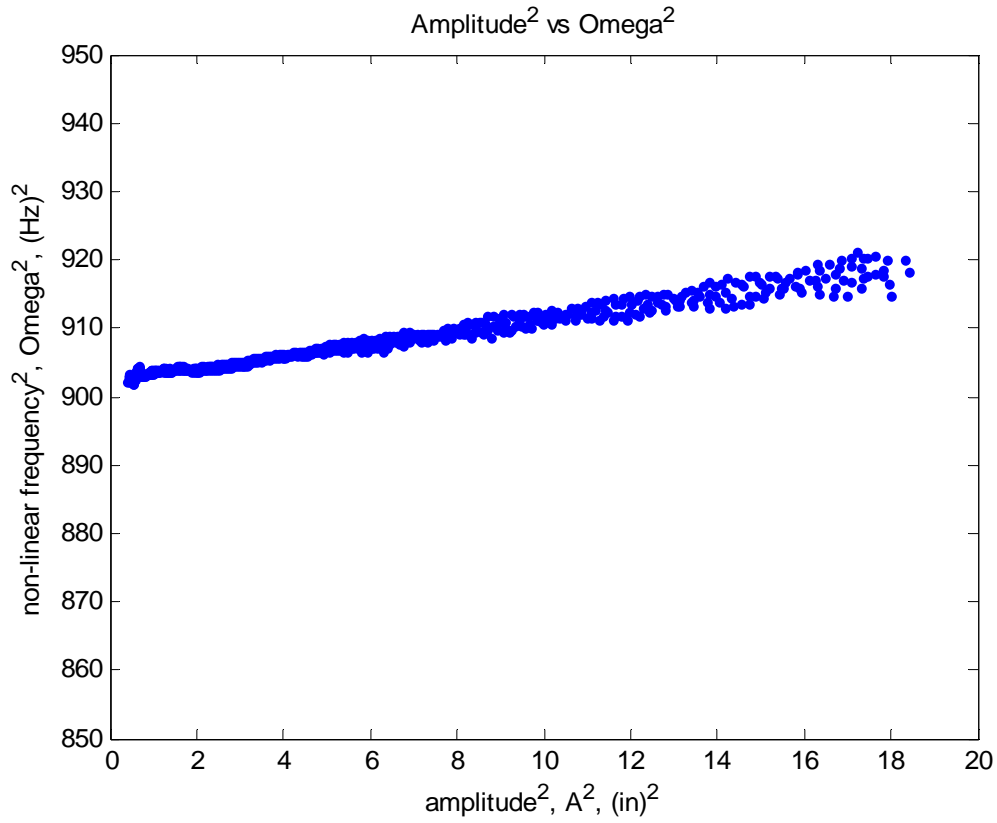


Figure 63. Duffing Equation Plot: Fixed-Free Composite

The following information was obtained for the first mode Backbone Curve for the Fixed-Free Composite beam. The linear frequency $\omega_0 = 30.05$ Hz and the coefficient $\beta = 47.45 \text{ in}^{-2} \text{ s}^{-2}$. In Figure 64 the fixed-free Composite beams Backbone Curve is plotted against its first natural frequency of 30.00 Hz. The plot shows that just like all of the other beams, the Composite beam is undergoing nonlinear hardening.

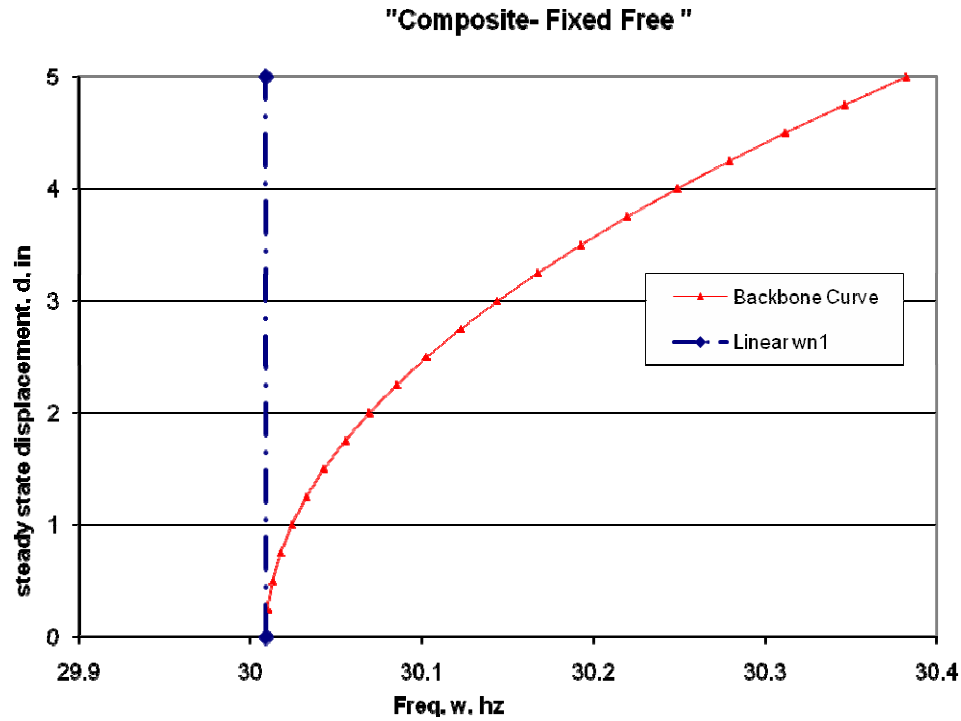


Figure 64. Backbone Curve: Fixed-Free Composite

Figure 65 shows the fixed-free Steel and Aluminum Backbone Curves against the fixed free Composite curve. All backbone curves are non-dimensionalized. The displacements are divided by each beams length while the nonlinear frequencies are divided by each beams linear natural frequency. This plot shows that in the first mode a Composite beam experiences a higher nonlinear hardening effect than either an isotropic Steel or Aluminum beam of similar dimensions. This shows that composite beams of [0/90]_s layups are more affected by membrane strain than the isotropic beams. All three clamped-free beam materials show very weak Backbone Curves compared to the clamped-clamped beams. When the clamped-free beams are compared to one another, the isotropic beams Backbone Curve appears even weaker than it was before. For

displacements greater than 20 times the thickness for isotropic fixed-free beams, the nonlinear characteristics in the 1st mode are almost negligible. The composite beam of similar dimensions shows a 12 times larger contribution of the membrane strain terms, $\frac{1}{2}(dw/dx)^2$ and (du/dx) . This result can also be noticed in the magnitude of the β values in Table 12. A higher positive β value attributes to a stronger effect of nonlinear hardening.

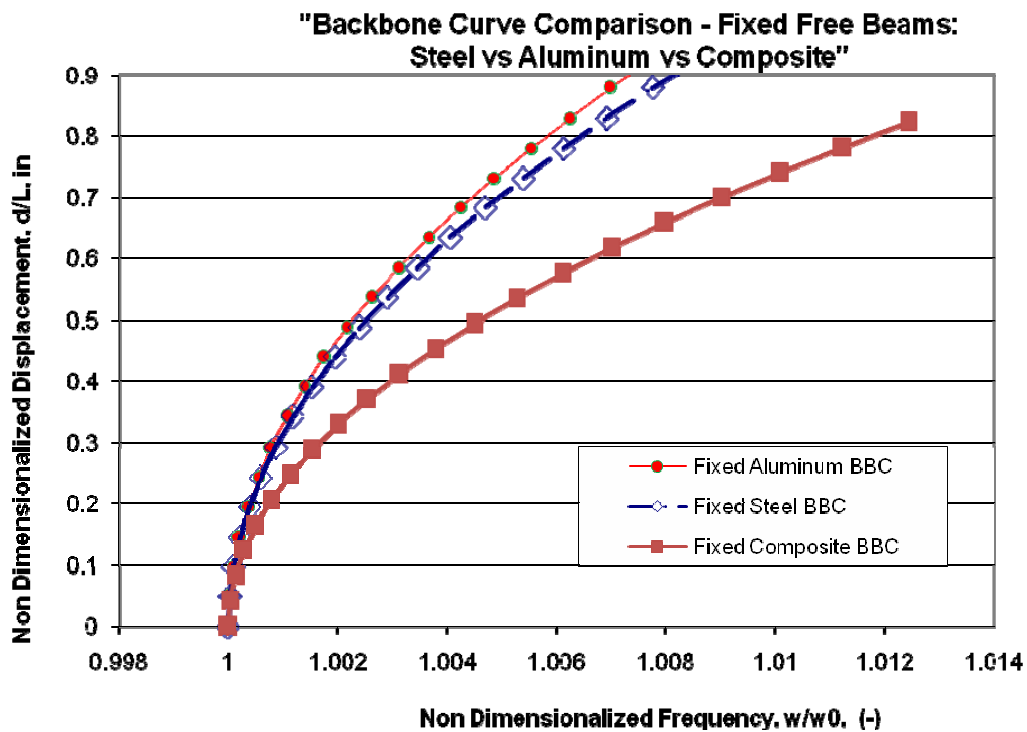


Figure 65. Backbone Comparison: Fixed-Free: Isotropic vs Composite

It is not just the composite material that increases the nonlinearity of the beam. The same composite beam dimensions are applied to a composite beam with a [0/0]_s layup. The Backbone Curve is plotted against both the isotropic Beam 3 and 4 Backbone Curves as well as the Backbone Curve for Beam 5's [0/90]_s layup. This is shown in

Figure 66 and shows that the actual layup of the Composite beam increases the nonlinearity effects more than the actual values of Modulus of Elasticity and Density changing. The two stronger 0 degree layers being stacked on the outside of the beam allow the membrane strain to be more of a contributing factor than in the [0/0]s beam.

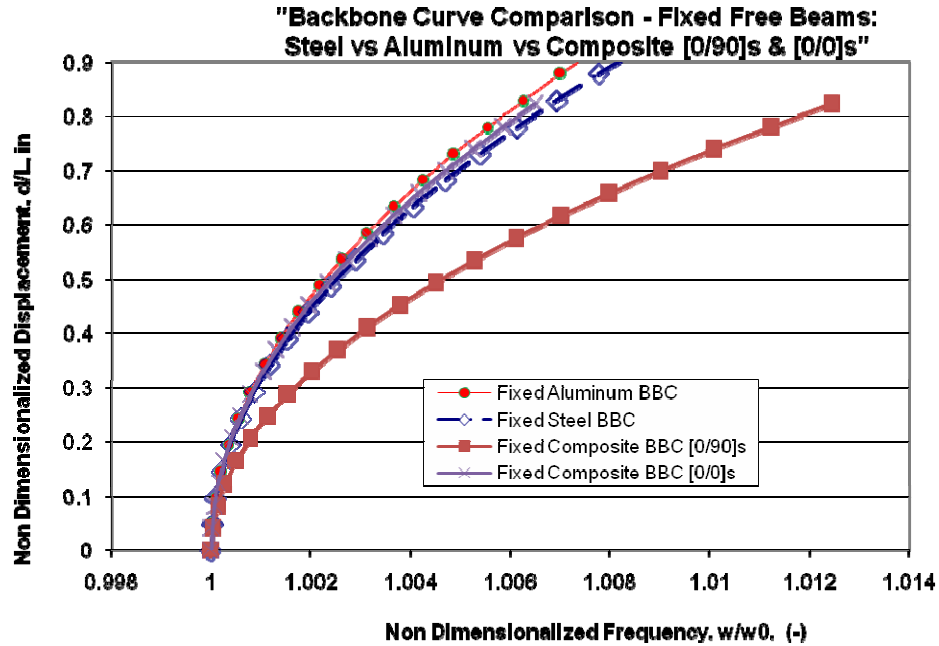


Figure 66. Backbone Comparison: Fixed-Free: All

Figure 67 compares the [0/90]s Composite with a density = 0.000144 to the same [0/90]s beam with a slightly higher density = 0.000163. The [0/0]s beam is also compared. This shows as density is decreased, the membrane strain term becomes more of a contributing factor, and the nonlinear effects are increased. However, it is not as big of an effect as changing the ply layup.

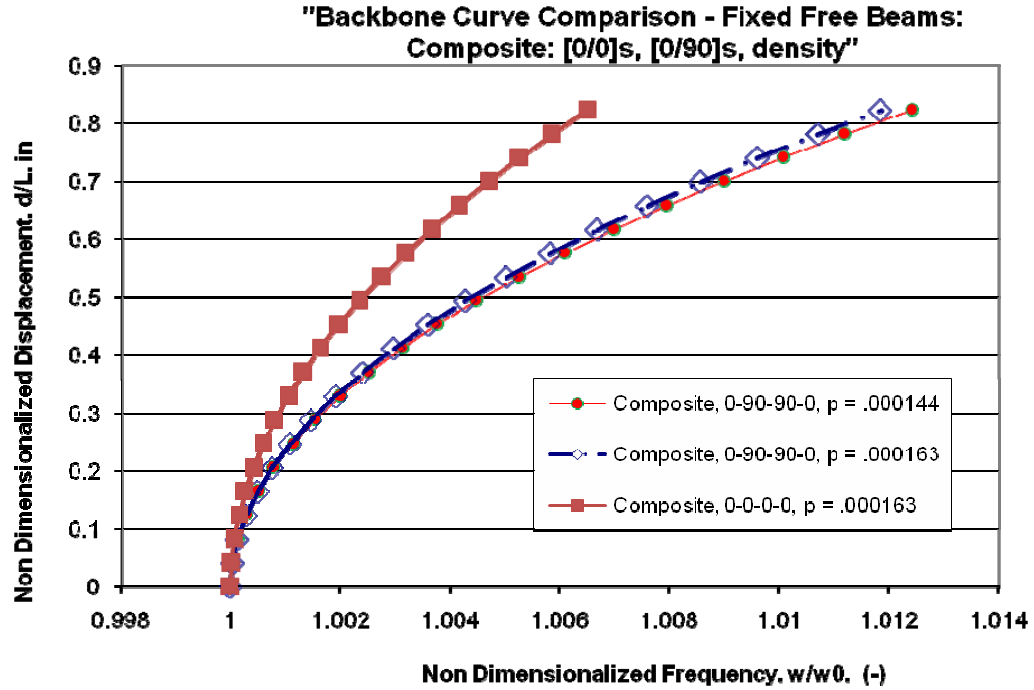


Figure 67. Backbone Comparison: Fixed-Free Composite Beams

We already saw in a previous comparison that the clamped-clamped beams experiences a much stronger effect of nonlinear hardening in their Backbone Curves than any of the clamped-free beams. This can be seen in both the β values both in Table 12 and visually in the above plots. This was attributed to the two walls in the clamped-clamped system pulling on the beam and adding to the membrane strain effects. A separate Backbone Curve was generated for three different nodes on the [0/90]s Composite beam to see if the wall pulling on the beam has the same effect in a clamped-free system. The results are shown in Figure 68.

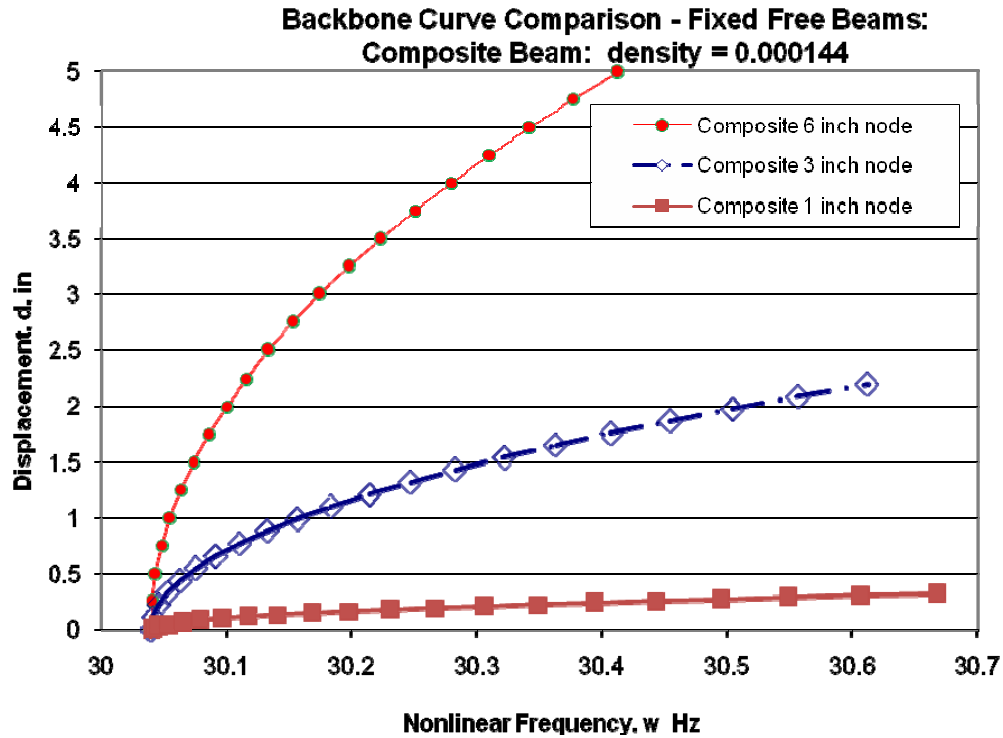


Figure 68. Backbone Comparison: Fixed-Free Composite: 3 Nodes

Shown in Figure 69, the closer the point on the beam is to the clamped end the less of an effect of curvature there is. This corresponds to less of a contribution there is of the bending strain term ($z (d^2w/dx^2)$). This increase in the membrane strain contribution . Likewise the point on the free end of the beam has the largest curvature and the largest contribution of bending strain terms. For this reason, the cubic stiffness β value is always going to increase as a point on a fixed-free beam becomes closer to the fixed end.

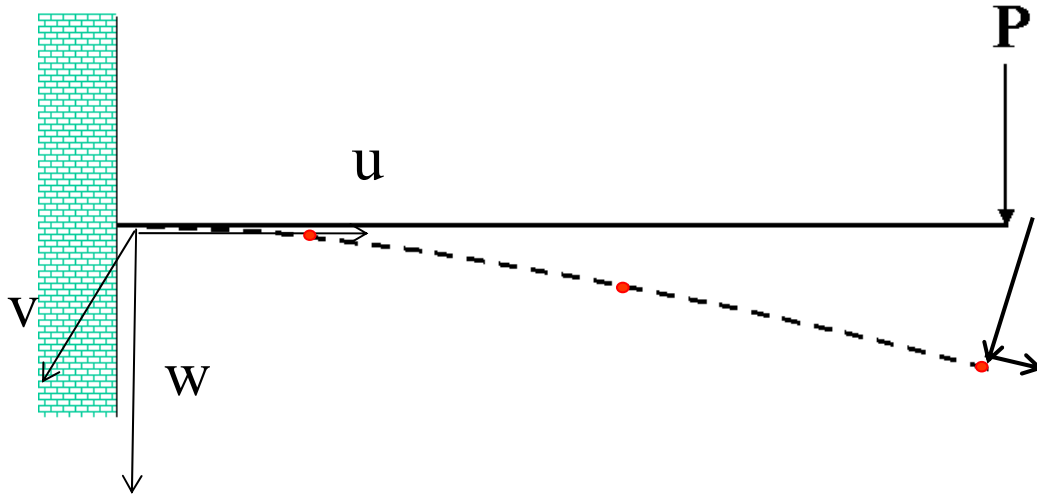


Figure 69. Node Placement on Composite Beam: 1", 3" and 6.08" from fixed end

Chapter Summary:

The five beams setups show how both boundary conditions, material properties, and beam location affect the nonlinear characteristics of the Backbone Curve. Table 12 lists all of the Estimated Backbone Curve values for Beams 1-5 from the equation $\Omega^2 = \omega_0^2 + \frac{3}{4} \beta A^2$. The cubic stiffness coefficient values β are a direct relationship to the strength of the nonlinear strength of each beam.

Table 12. Estimated Backbone Curve Values

Fixed-Fixed Beams	ω_0 - Hz	$\beta - \text{in}^{-2} \text{s}^{-2}$
<i>Steel Beam 1</i>	79.09	1.8140e8
<i>Aluminum Beam 2</i>	80.07	1.8105e8
Fixed-Free Beams	ω_0 - Hz	$\beta - \text{in}^{-2} \text{s}^{-2}$
<i>Aluminum Beam 3</i>	19.91	3.619
<i>Steel Beam 4</i>	19.73	3.951
<i>Composite [0/90]s low ρ</i>	30.00	47.45
<i>Composite [0/90]s high ρ</i>	28.28	40.13
<i>Composite [0/0]s high ρ</i>	30.01	24.69

In fixed-fixed beams, the vertical load P is quickly translated into an axial force as the boundary conditions constrain the bending of the beam. This leads to a huge β value

In fixed-free beams, the vertical load P is not translated into an axial force as quickly as in a fixed-fixed beam. It takes large displacements and rotations in the beam to translate the P force into an force in the axial direction of the beam. However, once this begins to happen, the nonlinearity of the fixed-free beams can be seen in the Backbone Curves.

The less flexible Steel beams, Beam 1 and Beam 4, show less of a contribution of bending than the more flexible Aluminum beams, Beam 2 and Beam 3. This leads to

more of a contribution of membrane strain, and a slightly stronger nonlinear Backbone Curve and slightly higher β values.

The [0/90]_s composite beams Backbone Curve leans away from the linear solution even more so as the β value is 12 times higher than the isotropic beams. The stronger 0 degree plies on the outside of the beam allow for a higher contribution of membrane strain, and thus a more nonlinear effect.

Just as the wall boundary condition affected the fixed-fixed beams nonlinearity greatly, as a point on a fixed-free beam becomes closer to its fixed end, its Backbone Curve also shows a much higher nonlinear characteristic with much higher β values.

IV. Conclusions and Recommendations

Chapter Overview

This chapter summarizes the important findings from results and discussion. The methods used in finding the Backbone Curve using ABAQUS/CAE are verified. The trends between the nonlinear characteristics and the following are reiterated:

Beam Setup

- Clamped-Clamped vs Clamped-Free

- Clamped-Free beams Backbone Curve for different points on beam

- Each point has a new Backbone Curve

Beam Material

- Changes in Density, ρ

- Changes in Stiffness, E

- Changes in Composite Beam layup

- Changes in Thickness, t

Final thoughts on how this affects the flapping Micro Air Vehicle study are made.

Methods Verified

The methods used in this study showed close results with previous experiments of Gordon, Holkamp, and Spotswood, and showed a slightly better result than the previous ABAQUS experiment by Ernst as shown in the table below.

Table 13. Past and present Backbone Curve parameter comparison

Fixed-Fixed Steel Beams	ω_0	β
<i>GHS experimental</i>	79.00	1.80e8
<i>Ernst ABAQUS</i>	79.0047	1.84e8
Current ABAQUS	79.09	1.8140e8

Nonlinear Characteristics Summarized

Clamped-Clamped beams exhibit much greater nonlinear tendencies than Clamped-Free beams. The beam setup had a huge influence on the nonlinear characteristics shown in the Backbone curves. The cubic stiffness coefficient values, β show this best in Table 12. The clamped-clamped beams both have β values in the 1.8e8 range, while the beta values for the clamped-free beams range from around 3 to 48. The boundary condition seems to be the key. A clamped-clamped beam has much more resistance to deflections, and the membrane strain term is a bigger player because of the resisting force placed on the beam from both wall boundary conditions.

The closer a point on a Clamped-Free beam is to the wall support, the greater its nonlinear tendencies. This is shown in Figure 68 and displays that membrane strain contributions are highest when a beam has a wall pulling on it. The Backbone curve for the free end node is the least nonlinear as it has less resistance or pull on it axially from the wall.

A more flexible beam exhibits less of a nonlinear Backbone Curve. Steel beams, Beams 1 and 4, show slightly higher nonlinear characteristics effects than Aluminum beams, Beams 2 and 3.

As thickness of a beam decreases, the membrane strain contribution increases and nonlinearity increases. Nonlinear theory mentions that the thin beams experience more contribution through their membrane than thicker beams. No studies were done to verify this, however the composite beam was 3 times thinner than the isotropic beams, and experienced a higher contribution from the membrane strain. This increase in nonlinearity was due to both the thickness of the beams and the composite material layup.

For composite beams, a [0/90]_s layup is more affected by nonlinearity than a [0/0]_s layup. This is shown in Figure 67. It shows that a composite beam aligned in somewhat isotropic manner of [0/0]_s produces a similar effect as an isotropic material of Aluminum or Steel. The [0/90]_s layup has produced a higher contribution of membrane strain leading to a Backbone Curve that falls further away from the linear solution.

Composite beams are more affected by membrane strain and the nonlinear tendencies that come with it than beams made of isotropic materials. This is shown in Figure 65. All three clamped-free beam materials show very weak Backbone Curves compared to the clamped-clamped beams. When the clamped-free beams are compared to one another, the isotropic beams Backbone Curve looks even weaker. There doesn't seem to be nearly as much membrane strain present in the Aluminum and Steel beams. That being said, for displacements greater than 20 times the thickness for isotropic fixed-free beams, the nonlinear characteristics in the 1st mode are negligible. They might

become a little less negligible in even thinner beams, however the composite beam of the same thickness would still show a larger contribution of the membrane strain terms, $\frac{1}{2}(dw/dx)^2$ and (du/dx) .

Thoughts on Future Research

The methods prescribed in this study are valuable in that they allow us to find certain nonlinear characteristics of a beam setup in a timely manner without the use of laboratory or experimental setup.

While the clamped-clamped beams exhibit extremely high nonlinear effects, they are not practical models when representing a flapping wing Micro Air Vehicle. When looking at the first mode of isotropic clamped-free beams, their nonlinearity is almost if not completely negligible. The first mode nonlinearity for a Composite clamped-free beam was almost 7 times as noticeable. Because future flapping wing MAVs are more likely to be made from composite materials, the nonlinearity must be considered. With wing designs that will certainly have a much smaller thickness and density, the membrane stress term will become a larger contributor, increasing the nonlinearity. Future studies will be needed to see if these nonlinear characteristics will be a factor.

Appendix

Convergence: Number of Elements in each FEM

The accuracy of the results in ABAQUS/CAE relies on the number of elements in each finite element model. The more elements there are in the model, the more accurate the analysis will be. However, with the increase in elements comes an increase in computational expense. For each model, a convergence test was done to find the least number of elements necessary for ABAQUS to find w_1 and w_2 within .1% of their actual values. Each model's true natural frequencies were found using at least $n=1000$ elements. The 1st and 2nd natural bending frequencies were then found for the models using $n = 1$ element, increasing n until the values converged to 0.3%. This allows the ABAQUS model to keep its accuracy while cutting down on the computational time of later tests. The Aspect Ratio of each element is also taken into consideration. Each element is preferred to have an Aspect Ratio of 1 to 1. The number of elements chosen in each Finite Element Model was chosen to also keep the AR close to a 1 to 1 ratio.

Clamped-Clamped Steel Finite Element Model

ABAQUS shows that the Finite Element Model only needs 5 elements to keep accuracy greater than 0.3% for predicting the 1st and 3rd natural bending frequencies. Five elements on a 4.5” beam section would produce 5 elements with an Aspect Ratio of almost 2 and a dimension of 0.9” x 0.5”. Therefore the beam was seeded in ABAQUS to have 9 elements and a dimension of 0.5” x 0.5”

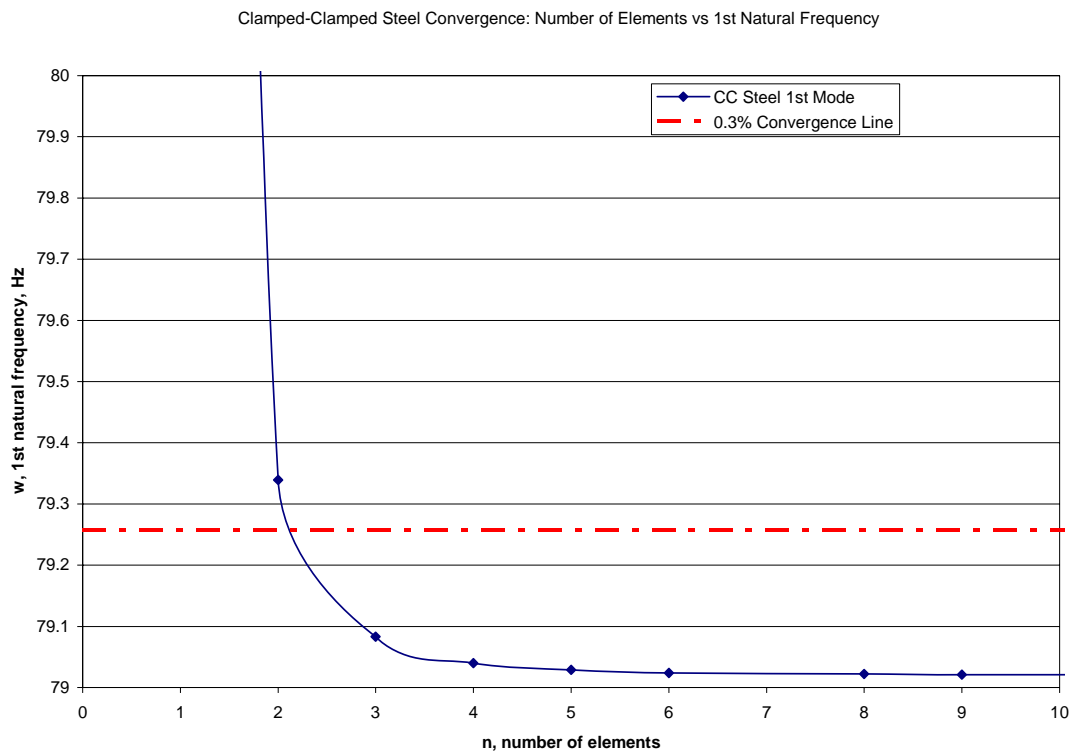


Figure 70. Convergence plots C-C Steel

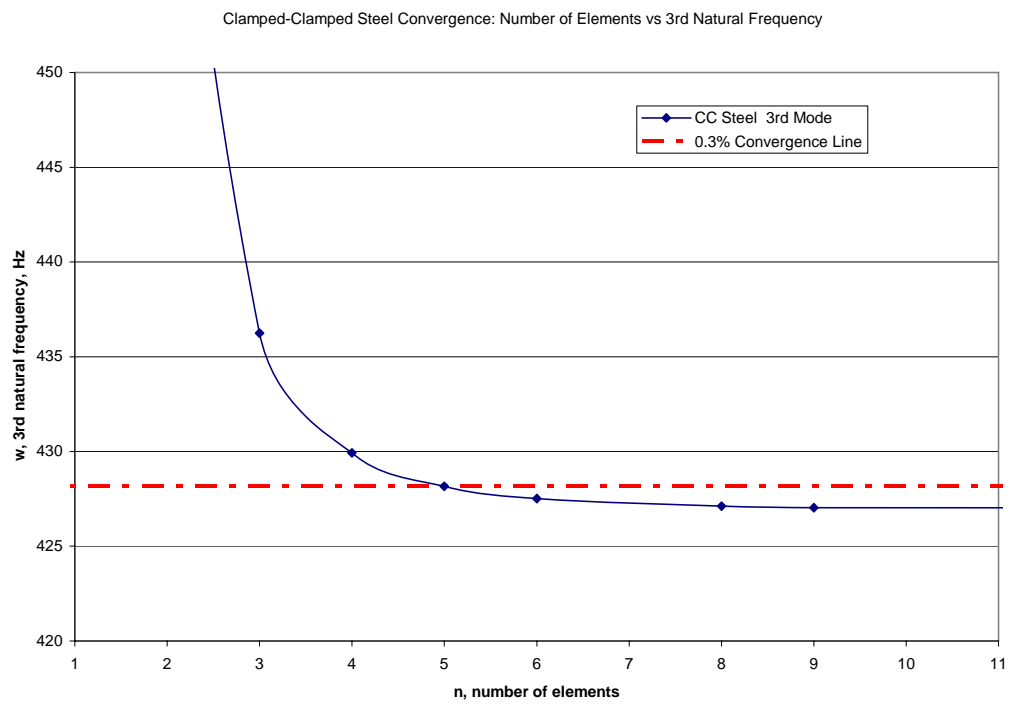


Figure 71. Convergence plots C-C Steel

Clamped Aluminum Finite Element Model

ABAQUS shows that the Finite Element Model only needs in between 20 elements to keep accuracy greater than 0.3% for predicting the 1st and 2nd natural bending frequencies. Twenty elements on a 10.125” beam section would produce 20 elements with an Aspect Ratio of 1.0125 and a dimension of 0.50625” x 0.5”. Therefore the beam was seeded in ABAQUS to have 20 elements.

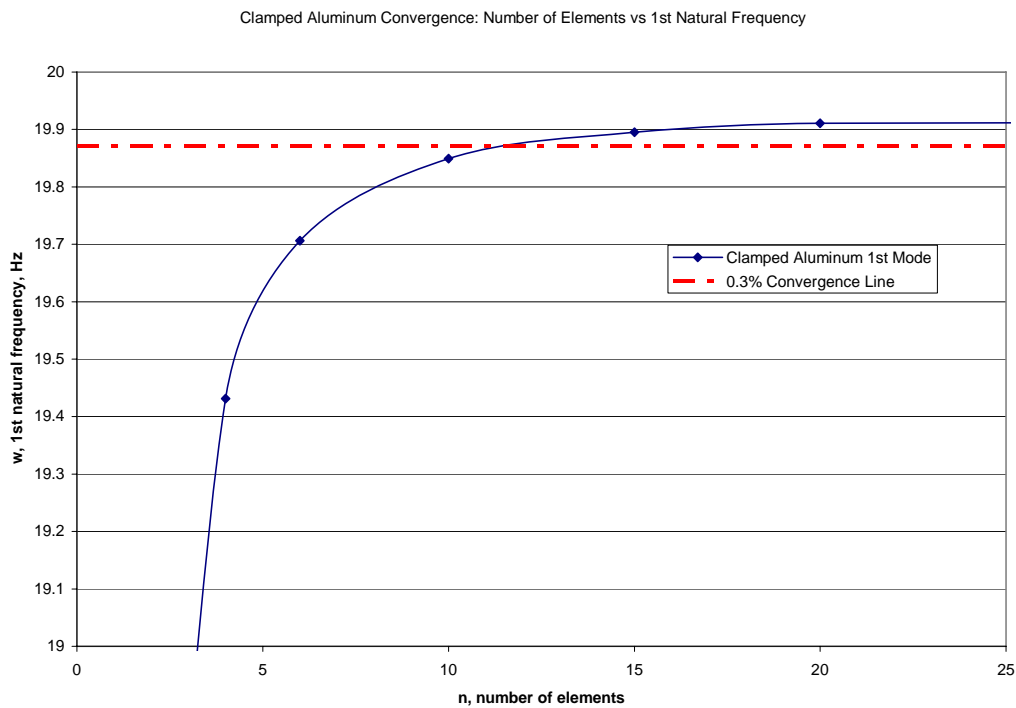


Figure 72. Convergence plots C-C Aluminum

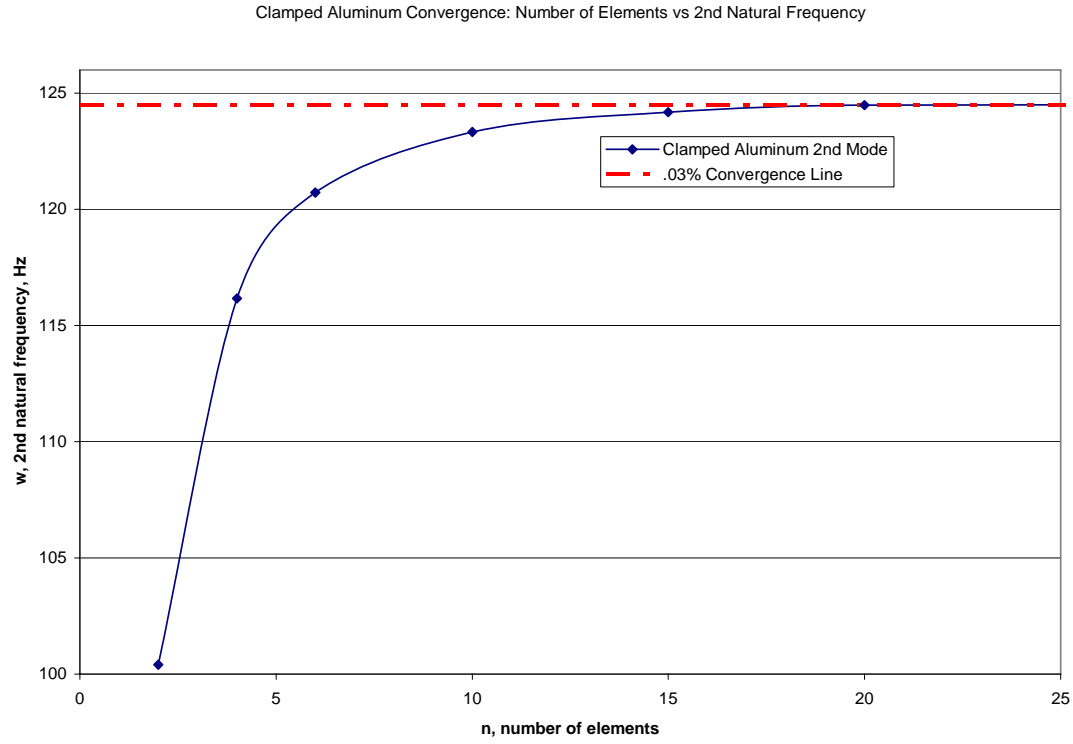


Figure 73. Convergence plots C Aluminum

Clamped Composite Finite Element Model

ABAQUS shows that the Finite Element Model only needs around 80 elements to keep accuracy greater than 0.3% for predicting the 1st and 2nd natural bending frequencies.

Ninety elements on a 0.5" x 6" beam would produce 90 elements in a 3 x 30 grid with an Aspect Ratio of 1.2 and a dimension of 0.2" x 0.166". The beam was seeded in ABAQUS to have 90 elements.

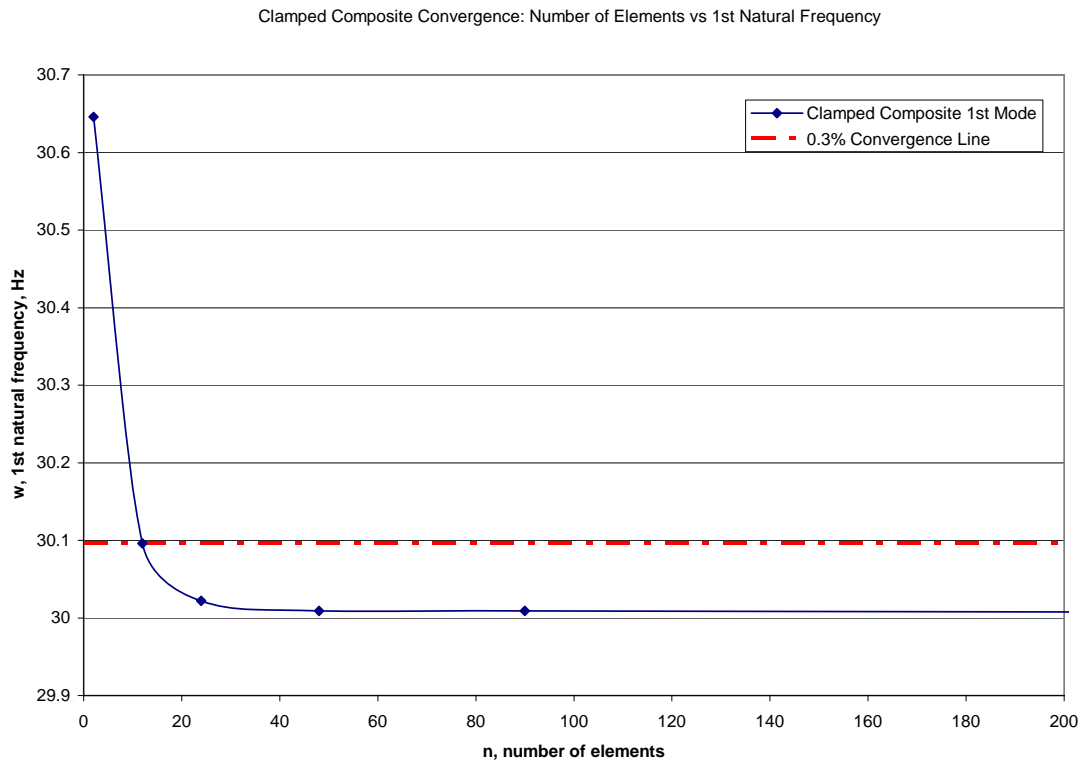


Figure 74. Convergence plots C Composite

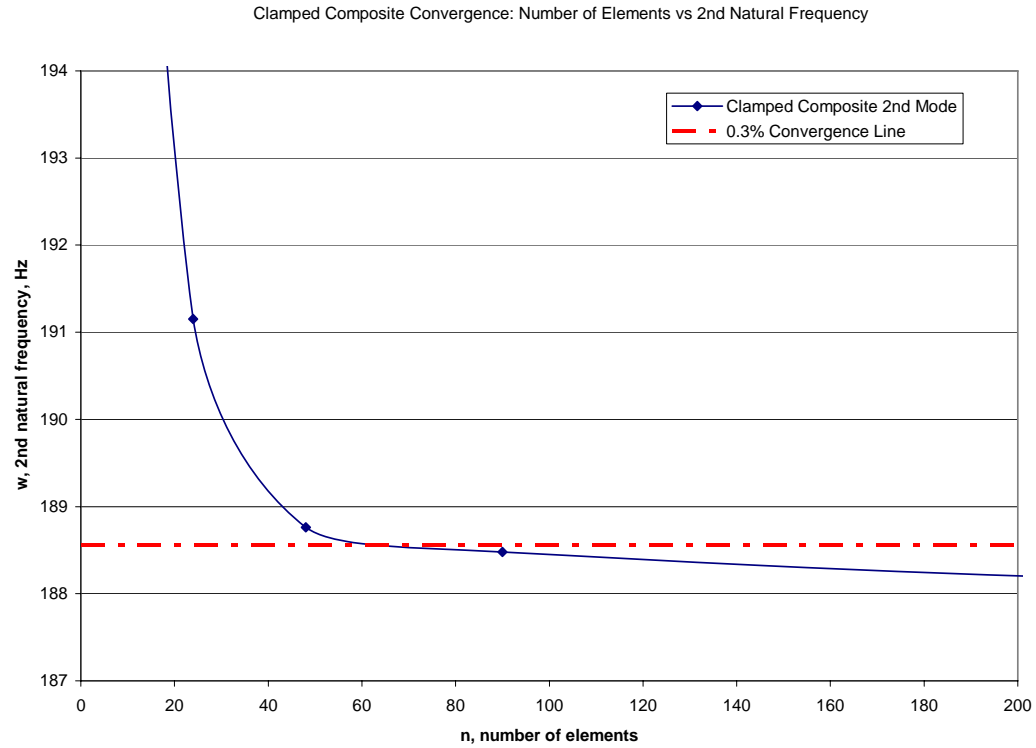


Figure 75. Convergence plots C Composite

Clamped-Clamped Aluminum Finite Element Model

Like the Clamped-Clamped Steel beam, ABAQUS shows that the Finite Element Model only needs 5 elements to keep accuracy greater than 0.3% for predicting the 1st and 3rd natural bending frequencies. Five elements on a 4.5” beam section would produce 5 elements with an Aspect Ratio of almost 2 and a dimension of 0.9” x 0.5”. Therefore the beam was seeded in ABAQUS to have 9 elements and a dimension of 0.5” x 0.5”

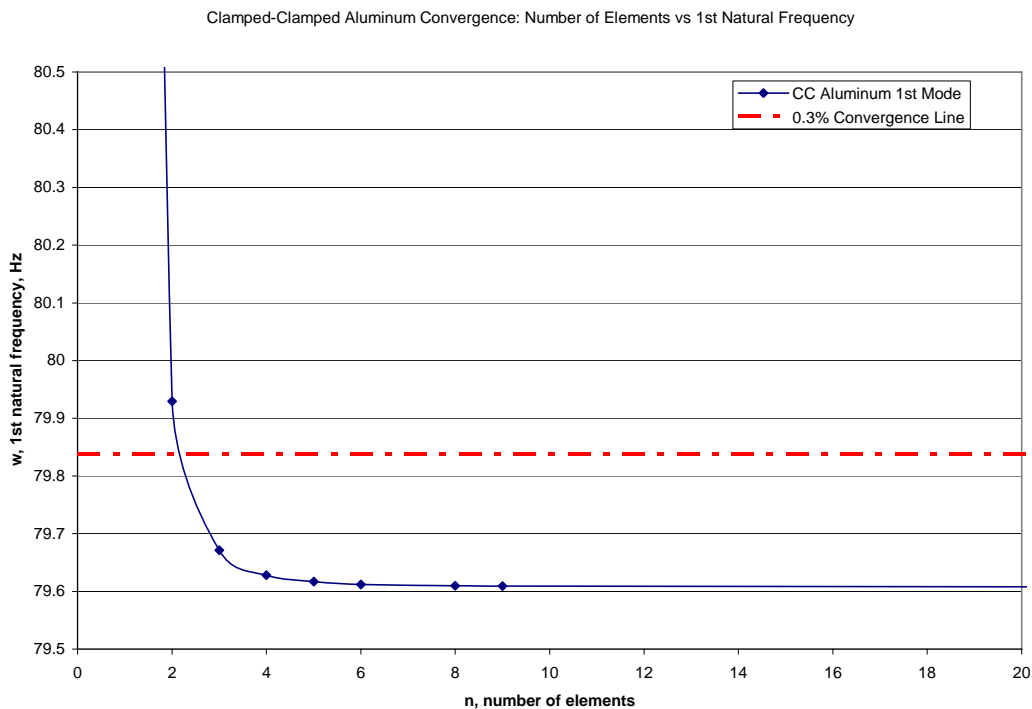


Figure 76. Convergence plots C C Aluminum

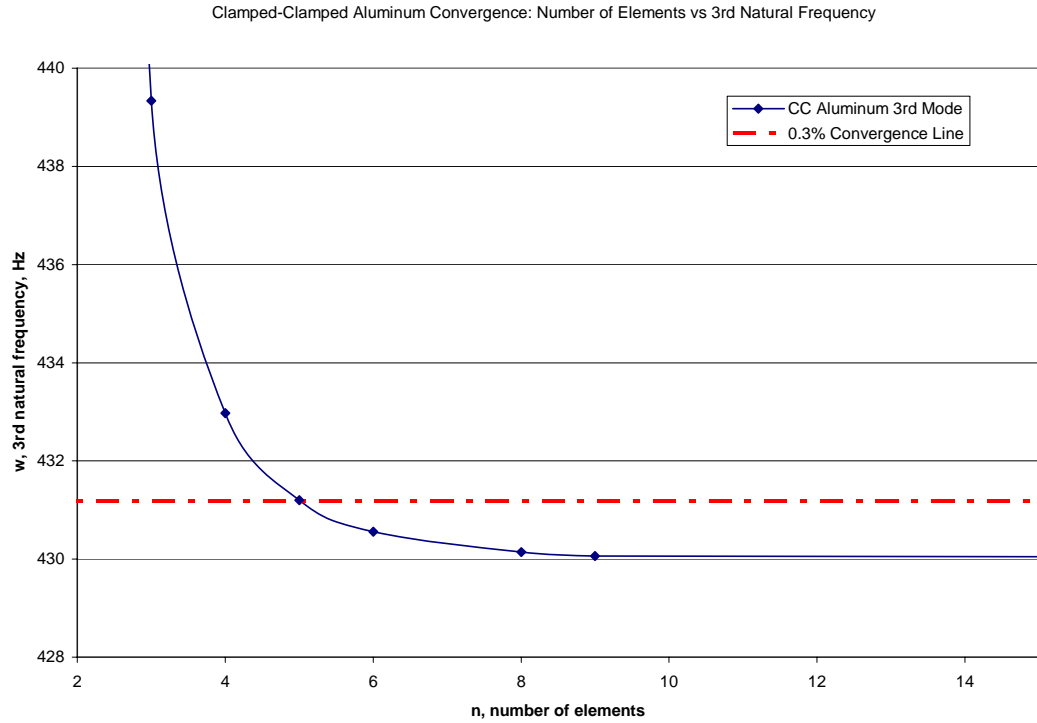


Figure 77. Convergence plots C-C Aluminum

Clamped Steel Finite Element Model

Like the Clamped Aluminum beam, ABAQUS shows that the Finite Element Model only needs in between 20 elements to keep accuracy greater than 0.3% for predicting the 1st and 2nd natural bending frequencies. Twenty elements on a 10.125” beam section would produce 20 elements with an Aspect Ratio of 1.0125 and a dimension of 0.50625” x 0.5”. Therefore the beam was seeded in ABAQUS to have 20 elements.

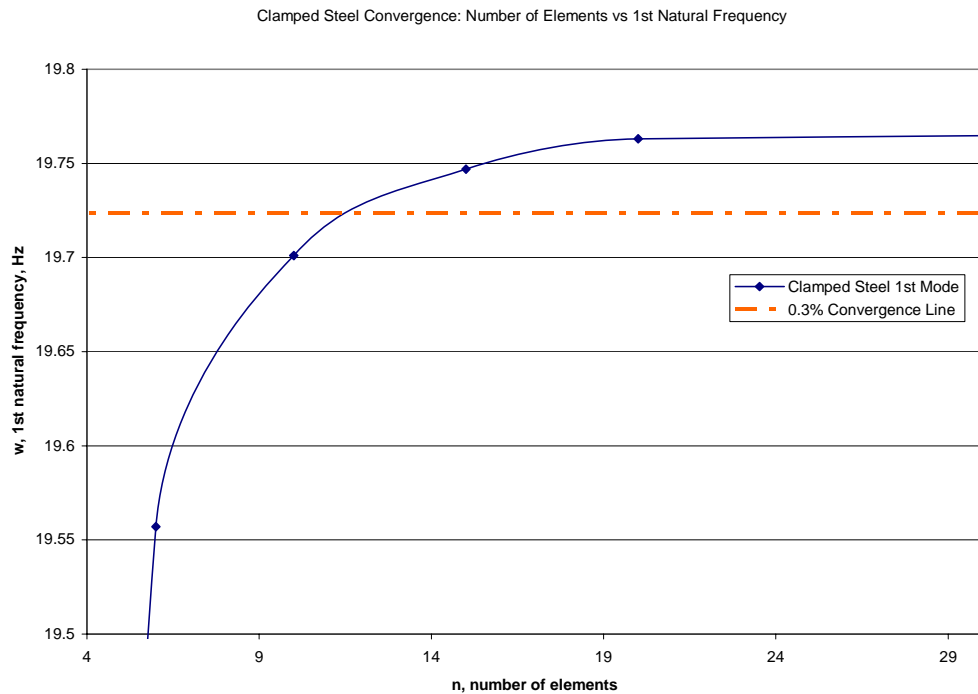


Figure 78. Convergence plots C Steel

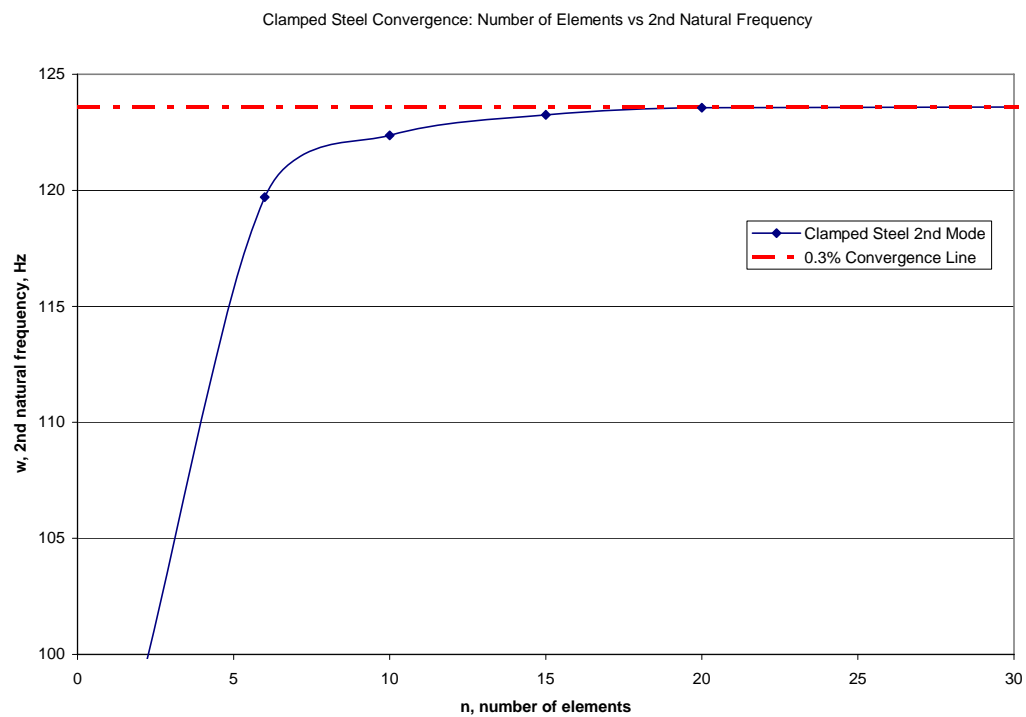


Figure 79. Convergence plots C Steel

MATLAB CODE for Backbone Curve Estimation

```
%BackboneCurveEstimation
%Robert Walker
%original code provided by Dr Anthony Palazottl and Matthew Ersnt.
clear all;
clc;

%Block 1 DATA

%Xe1: Clamped-Clamped Steel beam: (.5 x .031 x 9) 1.4 sec, w = 79.0 Hz
%EalumX: Clmpd-Clmpd Alum beam: (.5 x .031 x 9) 1.6 sec, w = 79.73 Hz

%X12BA2: Clmpd-Free Alum beam (.5 x .0625 x 10.125) 12 sec, w = 19.91 Hz
%CSSteelX: Clmpd-Free Steel beam (.5 x .0625 x 10.125) 12 sec, w = 19.76 Hz

%XC442: Clmp-Free Comp [0/0]s beam (.5 x .02 x 6.08) 4 sec, w = 30.0 Hz
%C090X1 C090X2 and C090X3: [0/90]s den = 0.166, 4 sec, w = 28 Hz
%Cden090X1 Cden090X2 and Cden090X3: [0/90]s with den = 0.1445, 4 sec, w = 30 Hz

load '(place.rpt file here)'
X = (place.rpt file here)

omega1 = 30; %place natural frequency of beam here

%Block 2

[L W] = size(X);
interval = round(2*L/X(L,1)/omega1); %sets up individual increments

%interval = 51

%Block 3
skip = 2; % sets up the overlapping of the data in each increment

%Block 4
time = X(L,1) - X(1,1);

%Block 5
Z = hilbert(X(:,2));

%Block 6
i = 0
for h=1:skip:(L-2*interval);

    i = i+1;
    rotation = 0;
```

```

%Block 7
    for j=1:interval;
        Za(j) = Z(h+j);
%Block 8
        absZa(j) = abs(Za(j));
%Block 9
        Zangleclean(j) = angle(Za(j));
%Block 10
        Zangle(j) = angle(Za(j));
        if j==1;
            Zangle(j);
        elseif Zangle(j)<=0 & Zangleclean(j-1)>0
            rotation = rotation+2*pi;
            Zangle(j) = Zangle(j) +rotation;
        else
            Zangle(j) = Zangle(j)+ rotation;
        end
    end
    b = (0:1:interval-1)./(L/time);
%Block 11
    P1 = polyfit(b,log(absZa),1);
    %if h==5*skip+1
    %figure(6)
    %axis tight
    %plot(b,log(absZa),'*-')
    %end
%Block 12
    A(i) = exp(P1(2));
%Block 13
    P2 = polyfit(b,Zangle,1);
    %if h==5*skip+1
    %figure(7)
    %axis tight
    %plot(b,Zangle)
    %end
%Block 14
    omega(i) = P2(1)/2/pi;
end

tinc = time/L*interval/2+time/L*skip*(1:i);

%Block 15
figure(1)
plot(X(:,1),X(:,2))
xlabel('time,t, (s)')
ylabel('displacement, d, (in)')

%Block 16
figure(2)
%subplot(2,2,1)
plot(tinc,omega,'r.')
xlabel('time, t, (s)')
ylabel('non-linear freqnecy, Omega, (Hz)')

```

```

%Block 17
figure(3)
%subplot(2,2,2)
plot(tinc,A, '.')
xlabel('time, t, (s)')
ylabel('amplitude, A, (in)')

%Block 18
figure(4)
%subplot(2,2,3)
plot(omega,A, '.')
ylabel('amplitude, A, (in)')
xlabel('non-linear frequency, Omega, (Hz)')

%Block 19
figure(5)
%subplot(2,2,4)
plot(A.^2,omega.^2, '.')
xlabel('amplitude^2, A^2, (in)^2')
ylabel('non-linear frequency^2, Omega^2, (Hz)^2')

%Block 20
P3 = polyfit(A.^2,omega.^2,1);

%Block 21
w0 = sqrt(P3(2))

%Block 22
Beta = 4/3*P3(1)*(2*pi)^2

```

Bibliography

1. Bajaj, A., Krousgrill, C.M. “Nonlinear System Resonance Phenomena.” Academic Press, 2001.
2. Cisneros, N. “The UF Micro Air Vehicle Team is on a Roll.” May 24th 2006.
http://www.eng.ufl.edu/elinks/news/detail_article.php?id=779
3. Cook, R.D., Malkus, D.S., Plesha, M.E., and Witt, R.J. Concepts and Applications of Finite Element Analysis. John Wiley & Sons Publishing, New York. 2002
4. Crisfield, M.A. Non-linear Finite Element Analysis of Solids and Structures –Volume 1. John Wiley & Sons Publishing, New York. 2001.
5. Daniel, I.M., Ishai, O. Engineering Mechanics of Composite Materials. Oxford University Press, New York. 2006.
6. Ernst, M.R, Palazotto, A.N. “Analysis of the Nonlinear Free-Response of a Thin Plate Using Finite Elements.” Communicated.
7. Feldman, M. “Hilbert Transforms.” Academic Press, 2001.
8. Feldman, M. “Non-linear free vibration identification via the Hilbert transform.” *Journal of Sound and Vibration*, 1997, 208(3), 475-489.

9. Gordon, R.W., Hollkamp, J.J. and Spottswood, S.M., “Nonlinear Response of a Clamped-Clamped Beam to Random base Excitation”, Proc. Of the 8th International Conference on Recent Advances in Structural Dynamics, University of south Hampton, July 2003.
10. Meirovitch, L. Fundamentals of Vibrations. McGraw-Hill, New York. 2001.
11. Nayfeh, A and Mook D. Nonlinear Oscillations, John Wiley & Sons Publishing , New York. 1979.
12. Nayfeh, A.H. and Pai, P.F. Linear and Nonlinear Structural Mechanics. John Wiley & Sons Publishing, New York. 2004.
13. Pramod, M. “Nonlinear Vibrations of Cantilever Beams and Plates”. Blacksburg, VA. July, 2003.
14. Stiles, E. “World's Smallest Ornithopter Wins at Micro Air Vehicle Competition.” July 2006. <http://uanews.org/cgi-bin/webobjects/uanews.woa/7/wa/engrstorydetails?articleID=-12905>
15. Tobias, A. “Experimental Methods to Characterize Nonlinear Vibration for us with Flapping Wing Micro Air Vehicles” Communicated, 2007.

16. Yamaki, N. and Mora, A., "Non-linear vibrations of a clamped beam with initial deflection and initial axial displacement, Part II: Experiment." *Journal of Sound and Vibration*, 1980, 71(3), 333-346.
17. ----. "DARPA Selects Micro Air Vehicle Contractor." Defense Advanced Research projects Agency. Decmeber 12th 1997
<http://www.defenselink.mil/Releases/Release.aspx?ReleaseID=1538>.
18. ----. "Micro Air Vehicles Provide Soldiers a Birds-Eye View." Defense Advanced Research projects Agency. Decmeber 8th 2005.
<http://www.darpa.mil/body/news/2005/mav.pdf>
19. ----. "Ornithopter." Wikipedia .Free Software Foundation, Inc. 2002
<http://en.wikipedia.org/wiki/Ornithopter>
20. ----. <http://www.flytechonline.com/about.html>

Vita

Robert Walker was born in Columbus, Ohio and graduated from Mount Vernon High School, in Mt Vernon, Ohio in 1999. He went on to earn a Bachelors degree in Aeronautical Engineering from the United States Air Force Academy in Colorado Springs, Colorado from 1999 - 2003. Following graduation, he was commissioned as an Officer in the United States Air Force and was stationed in Warner Robins, Georgia. In the Fall of 2005, he began attending the Air Force Institute of Technology at Wright Patterson Air Force Base, Ohio for completion of his Masters Degree in Aeronautical Engineering-Structures. After graduation in Spring 2007, he will continue working at WPAFB in the Air Force Research Laboratories Air Vehicles Directorate.

REPORT DOCUMENTATION PAGE				Form Approved OMB No. 074-0188	
<p>The public reporting burden for this collection of information is estimated to average 1 hour per response, including the time for reviewing instructions, searching existing data sources, gathering and maintaining the data needed, and completing and reviewing the collection of information. Send comments regarding this burden estimate or any other aspect of the collection of information, including suggestions for reducing this burden to Department of Defense, Washington Headquarters Services, Directorate for Information Operations and Reports (0704-0188), 1215 Jefferson Davis Highway, Suite 1204, Arlington, VA 22202-4302. Respondents should be aware that notwithstanding any other provision of law, no person shall be subject to a penalty for failing to comply with a collection of information if it does not display a currently valid OMB control number.</p> <p>PLEASE DO NOT RETURN YOUR FORM TO THE ABOVE ADDRESS.</p>					
1. REPORT DATE (DD-MM-YYYY) 22-03-2007		2. REPORT TYPE Master's Thesis		3. DATES COVERED (From – To) 26-06-2006 – 22-03-2007	
4. TITLE AND SUBTITLE FINITE ELEMENT SOLUTION: NONLINEAR FLAPPING BEAMS FOR USE WITH MICRO AIR VEHICLE DESIGN				5a. CONTRACT NUMBER	
				5b. GRANT NUMBER	
				5c. PROGRAM ELEMENT NUMBER	
6. AUTHOR(S) Walker, Robert L., 1 st Lieutenant USAF				5d. PROJECT NUMBER	
				5e. TASK NUMBER	
				5f. WORK UNIT NUMBER	
7. PERFORMING ORGANIZATION NAMES(S) AND ADDRESS(S) Air Force Institute of Technology Graduate School of Engineering and Management (AFIT/EN) 2950 Hobson Way, Building 640 WPAFB OH 45433-8865				8. PERFORMING ORGANIZATION REPORT NUMBER AFIT/GAE/ENY/07-M26	
9. SPONSORING/MONITORING AGENCY NAME(S) AND ADDRESS(ES) AFRL/VASD Attn: Dr. Philip S. Beran Bldg 146, 2210 8th St WPAFB OH 45433 DSN: 785-6645				10. SPONSOR/MONITOR'S ACRONYM(S)	
				11. SPONSOR/MONITOR'S REPORT NUMBER(S)	
12. DISTRIBUTION/AVAILABILITY STATEMENT APPROVED FOR PUBLIC RELEASE; DISTRIBUTION UNLIMITED.					
13. SUPPLEMENTARY NOTES					
14. ABSTRACT <p>The development and use of Micro Air Vehicles is becoming more and more important to the military. Size, weight, maneuverability, stealth, and fuel consumption are just some of the constraints on a future Micro Air Vehicle. Perfect blueprints for a small scale flying machine are both insects and humming birds. Medium sized hummingbirds are found to have wings-beats at a frequency of 18-28 Hz. There is a vast amount of complexity to just how these creatures can create lift; however, this study looks at different beams made of common materials with 1st natural bending frequencies in this range. This study documents and evaluates the use of analytical tools to solve for nonlinear characteristics of a system. A function called the backbone curve is incorporated into a MATLAB program. The Hilbert transform characterized by the nonlinear decrement approach captures all of the necessary coefficients for this function. ABAQUS/CAE is relied upon. The numerical finite element results are compared to experiments. This work gives a better understanding of how materials and geometry perform when used in Micro Air Vehicle design considering large displacements.</p>					
15. SUBJECT TERMS <p>Nonlinear, Vibration, Beam, Micro Air Vehicle, Flapping, ABAQUS, Hilbert transform, ornithopter, natural frequency, clamped-clamped, clamped-free,</p>					
16. SECURITY CLASSIFICATION OF:			17. LIMITATION OF ABSTRACT UU	18. NUMBER OF PAGES 122	19a. NAME OF RESPONSIBLE PERSON Palazotto, Anthony, Dr., AFIT/ENY
a. REPORT U	b. ABSTRACT U	c. THIS PAGE U			19b. TELEPHONE NUMBER (Include area code) 937-255-3636 x4599 (anthony.palazotto@afit.edu)